Food Structure

Volume 9 | Number 2 Article 1

1990

Food Microstructure

Follow this and additional works at: https://digitalcommons.usu.edu/foodmicrostructure

Recommended Citation
(1990) "Food Microstructure," *Food Structure*: Vol. 9 : No. 2 , Article 1.
Available at: https://digitalcommons.usu.edu/foodmicrostructure/vol9/iss2/1

This Article is brought to you for free and open access by the Western Dairy Center at DigitalCommons@USU. It has been accepted for inclusion in Food Structure by an authorized administrator of DigitalCommons@USU. For more information, please contact digitalcommons@usu.edu.

UtahStateUniversity
MERRILL-CAZIER LIBRARY

FOOD STRUCTURE

(FORMERLY FOOD MICROSTRUCTURE)

ISSN 1046-705X CODEN - FSTUE2 Vol. 9, No. 2, 1990

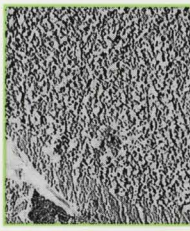

Published by **Scanning Microscopy International**

FOOD STRUCTURE

(Formerly FOOD MICROSTRUCTURE)

International journal on the structure of foods and feeds with special emphasis on relation between processing, molecular properties, microstructure and behavior.

EDITORS

M. Kalab, Food Research Institute, Agriculture Canada, Ottawa, Ontario, Canada K1A 0C6 (Phone 613-995-3722 x 7707, FAX 613-995-3845)

S.H. Cohen, Science and Advanced Technol. Lab., U.S. Army Natick R&D Ctr., Natick, MA, 01760 USA (Phone 508-651-4578, FAX 508-651-5104)

E.A. Davis, Dept. of Food Science & Nutrition, Univ. of Minnesota, St. Paul, MN 55108 USA (Phone 612-624-1758, FAX 612-625-5272)

D.N. Holcomb, Kraft General Foods Tech. Ctr., 801 Waukegan Rd., Glenview, IL 60025 USA (Phone 708-998-3724, FAX 708-998-3864)

W.J. Wolf, USDA Northern Regional Res. Ctr., Peoria, IL 61604 USA (Phone 309-685-4011 x350, FAX 309-671-7814)

***I. Heertje**, Unilever Research Lab., P.B. 114, 3130 AC Vlaardingen, Netherlands (Phone 31-10-4605513, FAX 31-10-4605671)

*European address for submission of papers, Letters of Intent, and inquiries.

MANAGING EDITOR

Om Johari (Phone 708-529-6677, FAX 708-980-6698), Scanning Microscopy International (see below)

EDITORIAL BOARD

B. Brooker, AFRC Inst. Food, Research, Reading, U.K.

M. Caric, Univ. Novi Sad, Yugoslavia

R.G. Cassens, Univ. Wisconsin, Madison

V.E. Colombo, F. Hoffman-La Roche, Switzerland

J.M. deMan, Univ. Guelph, Ontario, Canada

J.M. Faubion, Kansas State Univ., Manhattan

D.J. Gallant, Ministry Agriculture, Nantes, France

A.M. Hermansson, Swedish Food Inst., Goteborg, Sweden

E. Kovacs, Central Food Res. Inst., Budapest, Hungary

C.M. Lee, Univ. Rhode Island, Kingston

D.F. Lewis, British Food Manufact. Res. Assoc., Leatherhead, U.K.

P. Resmini, Univ., Milano, Italy

K. Sato, Hiroshima Univ., Japan

B. G. Swanson, Washington State Univ., Pullman

H.J. Swatland, Univ. Guelph, Ont. Canada

M.A. Tung, Tech. Univ. Nova Scotia, Halifax, Canada

J.G. Vaughan, King's College, Univ. London, U.K.

P.D. Velinov, Inst. Meat Industry, Sofia, Bulgaria

S.H. Yiu, Agriculture Canada, Ottawa, Canada

Annual Subscription Rates (including postage and handling):

1982 to 1988 U.S. $50 (U.S. delivery); U.S. $55 (elsewhere)
1989 & 1990 U.S. $65 (U.S. delivery); U.S. $70 (elsewhere)

Business Communications:

Address all communications regarding subscriptions, change of address, etc. to Dr. Om Johari. (See below)

Editorial Correspondence and Inquiries:

Submit papers (see Instructions for Authors), news items, books for review, etc. to one of the editors or to:
Dr. Om Johari, Scanning Microscopy International (SMI)
P.O. Box 66507, Chicago (AMF O'Hare), IL 60666, U.S.A.

Copyright © 1990 Scanning Microscopy International, except for contributions in the public domain. All rights reserved.

Where necessary, permission is granted by the copyright owner for libraries and others registered with Copyright Clearance Center (CCC) to photocopy, provided that the base fee of $3.00 per copy of the article, plus .00 per page is paid directly to CCC, 27 Congress Street, Salem, MA 01907. Copying done for other than personal or internal reference use, without the expressed permission of the SMI is prohibited. Those articles without a fee-code are not included in the CCC service. Serial fee code: 1046-705X/90$3.00 +.00.

Permission is granted to quote from this volume in scientific works with the customary acknowledgement of the source. To print a table, figure, micrograph or other excerpt requires, in addition, the consent of one of the original authors and notification to SMI. Republication or systematic or multiple reproduction of any material in this volume (including the abstracts) is permitted only after obtaining written approval from SMI, and in addition, permission should also be obtained from one of the original authors. Every effort has been made to trace the ownership of all copyrighted material in this volume and to obtain permission for its use.

Printed in U.S.A.

Food Structure, Vol. 9, Number 2, June 1990
Scanning Microscopy International, Chicago (AMF O'Hare), IL 60666-0507, USA

Table of Contents

Food Structure, Vol. 9, Number 2, June 1990
Scanning Microscopy International, Chicago (AMF O'Hare), IL 60666-0507, USA

LIST of REVIEWERS

The editors gratefully thank the following reviewers for their help with the papers included in this issue (**please note**: the names of editors and editorial board members listed on the inside cover page are not included in this list).

Blaurock, A.E.	Kraft Technology Center, Glenview, IL
Bolin, H.R.	USDA Western Reg.Res.Ctr., Albany, CA
Boulter, D.	University of Durham, U.K.
Bourne, M.C.	Cornell University, NY
Cavalieri, R.P.	Washington State University, Pullman,
Comer, F.W.	The Griffith Laboratories, Scarborough, Canada
Flint, F.O.	University of Leeds, U.K.
Gordon, J.	University of Minnesota, Saint Paul
Grider, J.	University of Minnesota, Saint Paul
Hoseney, R.C.	Kansas State University, Manhattan
Hunter, J.E.	Procter & Gamble Technical Center, Cincinnati, OH
Krog, N.	Grindsted Products A/S, Brabrand, Denmark
Martin, Jr., R.W.	Kraft Technology Center, Glenview, IL
Offer, G.	AFRC Institute Food Res., Bristol, U.K.
Parker, W.	Seabrook Blanching Corp., Edenton, NC
Regenstein, J.M.	Cornell University, Ithaca, NY
Schellhaass, S.M.	General Mills Technical Center, Minneapolis, MN
Schmidt, G.R.	Colorado State University, Fort Collins
Stanley, D.W.	University of Guelph, Ont., Canada
Tamime, A.Y.	W. Scotland College Agri., Ayr, Scotland
Theno, D.M.	Foster Farms, Livingston, CA
Uebersax, M.A.	Michigan State University, East Lansing

Announcement:

FOOD STRUCTURE 1991 Meeting

Following its best and the largest meeting in Bethesda this May; Food Structure will also hold its 1991 meeting at the Hyatt Regency Hotel in Bethesda from May 4 to 9. General SEM tutorials on May 4 will be followed by general scanning microscopy and food tutorials on Sunday May 5; the scientific program will be on May 6-9. At the time this issue going to press, the following programs have been formulated (the names of editors / editorial board members who agreed to be organizers is given below also).

Tutorials:	S.H. Yiu and C.M. Lee
Food Biotechnology:	S.H. Cohen and B.E. Brooker
Image Processing:	D. Gallant and J. M. Faubion
Radiation Effects:	E. Kovacs and A. Keresztes (Hungary)
Rheology:	D.N. Holcomb and M.A. Tung
Surface Properties and Food Emulsions	I. Heertje
Packaging/Contamination	J.E. Charbonneau, Natl. Food Process. Assn., WDC
Muscle Foods:	S. Barbut (U. Guelph) and M.B. Solomon (USDA, MD)

We seek your contributions and suggestions for potential contributors (in any area covered by the scope of our journal, see subtitle on the inside front cover), as well as other possible organizers. Programs will also be planned on different food types (as in the past).

For a Letter of Intent Form, Registration Form, Hotel Form, or additional information please either contact Om Johari (at Scanning Microscopy International, P.O. Box 66507, AMF O'Hare, IL 60666, USA; Phone: 708 529 6677 or FAX 708 980 6698); or Milos Kalab or Isaac Heertje (see addresses on the inside front cover).

FOOD STRUCTURE, Vol. 9 (1990), pp. 77-90
Scanning Microscopy International, Chicago (AMF O'Hare), IL 60666 USA

1046-705X/90$3.00+.00

THE ROLE OF THE INTERFACIAL PROTEIN FILM IN MEAT BATTER STABILIZATION

A. Gordon and S. Barbut

Animal and Poultry Science Department, University of Guelph, Guelph, Ontario, Canada, N1G 2W1.

Abstract

The microstructure of meat batters made with equal ionic strengths of NaCl, $MgCl_2$, $CaCl_2$ and KCl (IS=0.43) and a reduced-NaCl batter (IS=0.26) were examined by scanning and transmission electron microscopy. Micrographs revealed that fat globules with smooth and rough protein coats were present in all treatments. The roughly-coated globules were prevalent in the unstable batters. Pores were observed in the interfacial protein film (IPF) surrounding the globules and were more prevalent in the globules with rough protein coats. Fat was seen to exude from the pores in both types of globules. Fat globules were shown to be immobilized by the physical binding of their IPF to the protein matrix. Thread-like protein strands appeared to play a role in binding the smaller fat globules to the protein matrix. The IPF had a complex, multi-layered structure. Some of the larger globules had internal protein structures which were connected to the IPF and which partitioned and further stabilized the fat. The results indicate that fat emulsification and the interfacial film are important in preventing fat separation in meat batters.

Initial paper received January 30, 1990
Manuscript received June 11, 1990
Direct inquiries to S. Barbut
Telephone number: 519 824 4120 ext. 3669

Key Words: Meat batter, microstructure, interfacial protein film (IPF), chloride salts, fat exudation, physical binding, emulsification.

Introduction

The solubilization of the salt soluble myofibrillar proteins in comminuted meat products is of great importance in preventing fat separation. These proteins are the major structural components of the comminuted meat matrix (Fukazawa et al., 1961a,b) and have also been shown to form an interfacial protein film (IPF) around fat globules (Swift et al., 1961; Galluzzo and Regenstein, 1978a; Jones and Mandigo, 1982). Finely comminuted meat products are a complex mixture of muscle tissue, fat particles, water, spices and solubilized proteins which are held together by a variety of attractive forces (Jones, 1984). These components are combined to form what has been referred to as either a meat emulsion (Theno and Schmidt, 1978) or a non-emulsion meat batter (Lee, 1985; Regenstein, 1988). A classical emulsion consists of two immiscible liquid phases, one of which is dispersed in the other in the form of a colloidal suspension (Kramlisch, 1977). In meat batters, fat globules constitute the dispersed phase (Swasdee et al., 1982) but are sometimes larger than the size required to form a true emulsion. Hence, there are currently two theories for explaining the stabilization of meat batters: a) the emulsion theory and b) the physical entrapment theory (Lee, 1985).

The emulsion theory suggests that the salt soluble proteins are drawn to, and concentrated at, fat globule surfaces thus forming a stabilizing membrane in the raw emulsion (Hansen, 1960). Jones (1984) proposed that undenatured myosin first forms a monomolecular layer around fat globules in uncooked emulsions to which other proteins are then bound by protein-protein interactions. This is possible because of the thin layer of melted fat which is believed to be formed on the surface of the fat globules as a result of localized frictional forces during comminution. The myosin molecule is believed to be oriented at the interface such that the heavy meromyosin (HMM) head is facing the hydrophobic phase and the light meromyosin (LMM) tail is towards the aqueous phase (Jones, 1984). This theory is supported by the relatively high surface hydrophobicity of the HMM S1 fragment of myosin (Borejdo, 1983). Galluzzo and Regenstein (1978a,b,c) and Schut (1978) have used model systems to show that myosin is adsorbed

to form a film during emulsification. Hence, it appears that myosin may act as an emulsifier even in its native state and form an interfacial film of defined viscoelastic and mechanical properties at the oil-in-water interface. These properties determine the stability of emulsions (Asghar et al., 1985). Consequently, the emulsifying action of myosin may be vital to the stabilization of the uncooked meat batter.

Borchert et al. (1967) showed the presence of the interfacial protein film (IPF) in cooked meat batters and suggested that it may play a role in stabilizing the product during cooking. Their study also revealed drastic changes in the microstructure of the protein matrix on cooking and the existence of small holes or 'pores' in the protein films around fat globules in the cooked product. Jones and Mandigo (1982) focused on these pores in their study of the mechanism of meat emulsion stabilization. They found numerous pores in the protein envelope surrounding larger fat globules as well as several small fat droplets in the vicinity of these pores. They therefore proposed that the pores play the role of a "pressure release" valve which allows the thermal expansion of fat during cooking without a collapse of the stabilizing IPF. They concluded that batter stability was related to the thickness of the IPF as well as the integrity and density of the protein matrix.

The physical entrapment theory of meat batter stability proposes that the fat phase is stabilized by physical entrapment within a gelled protein-water matrix. The myofibrillar proteins in the matrix of the uncooked batter are thought to exist in a sol form (Acton and Dick, 1984). Cooking causes the aggregation of the proteins to form a three-dimensional gel which physically traps the fat particles (Lee et al., 1981). This theory suggests that large amounts of undisrupted fat cells remain after the batter is made and therefore help to stabilize the raw batter. The theory was supported by the finding that non-protein emulsifiers decrease rather than increase meat batter stability (Meyer et al., 1964). The chemical and physical properties of fat as well as the size and distribution of fat particles have been shown to affect fat stabilization (Townsend et al., 1968; Smith et al., 1983; Lee, 1985). These findings suggest that the emulsification of fat by the myofibrillar proteins is incidental to fat stabilization by other mechanisms.

Deng et al. (1981) and Lee (1985) have reported that fat channel formation resulting from the melting of fat at high chopping temperatures was caused by the discontinuity of the protein matrix in unstable batters and led to fat and water loss. However, Deng et al. (1981) also noted that large amounts of broken interfacial film were found in unstable batters. Gordon and Barbut (1989) indicated that fat channel formation in $CaCl_2$ and $MgCl_2$ (ionic strength (IS)=0.43) destabilized batters was due to the formation of a weak interfacial film combined with the aggregation of the protein matrix. Fat and water lost from unstable batters were also found to be closely related (r=0.95). Hence, although the formation of a coherent protein matrix is important in the preparation of a stable meat batter, interactions between the encapsulated fat droplets, matrix proteins and water influence the stability of the system.

The results reported here are the second part of a study in which several chloride salts were used to produce stable and unstable meat batters (Gordon and Barbut, 1989). The specific objectives of this study were to investigate the microstructure of the IPF and explore its role in the stabilization of fat in meat batters.

Materials and Methods

Batter Preparation

Five mechanically deboned chicken meat (MDCM) batters were produced in three separate trials as previously described (Gordon and Barbut, 1989). Four different chloride salts (NaCl (2.5%), $MgCl_2$, $CaCl_2$, KCl) were used so as to give an ionic strength (IS) of 0.43. In addition, a reduced-NaCl batter (1.5%, IS=0.26) was also prepared. The 2.5% NaCl represents the most widely used level for comminuted products. The MDCM was obtained from a local processing plant and used to make 0.5 kg batches. The meat was frozen (-18°C) for one month prior to use. Proximate analysis of the raw meat as determined in duplicate (AOAC, 1980) was: 66.7% moisture, 16.1% fat, 14.3% protein and 1.1% ash. The batters contained 6.0% added water and the chloride salts (Fisher Co., Ont.), which were added (as solids) at the initial stages of comminution, varied between treatments. Batters were chopped for 4 min in a non-vacuum bowl cutter (Hobart, Model 84142, Troy, OH) at high speed; end point temperatures did not exceed 8°C. Small air bubbles were removed from the batters by tumbling in a pre-cooled table top vacuum tumbler (Lyco, Columbus, WI) for 30s at a pressure of 0.15 atm. Batters (34g) were weighed into 50ml plastic test tubes, centrifuged (Fisher Centrific, Fisher, Ont.) at low speed (600 G) for 5 min to remove air bubbles trapped during hand stuffing and cooked in a water bath at 0.66°C/min using a programmable controller (Haake PG20, Haake, Berlin, W. Germany) to an internal temperature of 69°C.

Electron Microscopy

For SEM 3 mm cubes were cut from the centre of cooked batters from each treatment and were broken such that the broken side would be used for SEM. The specimens were fixed in 2% glutaraldehyde/ 1% paraformaldehyde in 0.1M HEPES buffer, pH 6.0 (Sigma Chemical Co., St. Louis) for 2 hr, rinsed with buffer, post-fixed with 1% OsO_4 for 4 hr, rinsed, dehydrated through a graded series of ethanols, critical point dried, mounted on aluminum stubs with silver paint, sputter-coated with palladium/gold in a Hummer VII unit (Anatech Ltd., VA), and examined at 10 kV (Hitachi S-570 SEM, Tokyo, Japan) as described by Gordon and Barbut (1989). For TEM, alcohol dehydrated samples were infiltrated with Spurr's resin and cured (16 hr) in capsules at 60°C. Sections were cut, picked up on grids and stained for 10 min with uranyl acetate and 5 min with lead citrate and viewed at 60 kV on a JEOL JEM 100CX TEM.

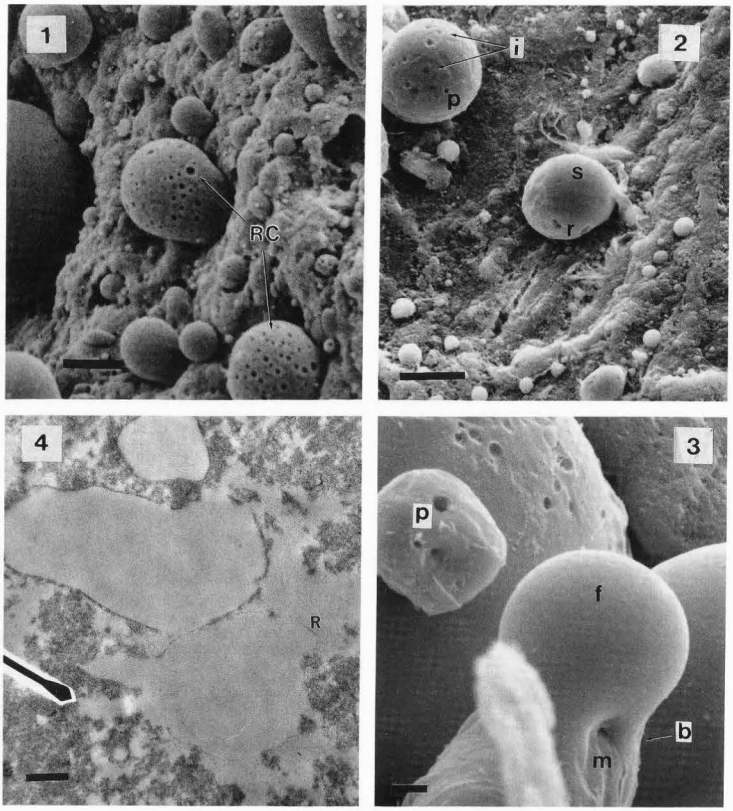

Figure 1. SEM of $CaCl_2$ treatment showing rough-coated (RC) globules with large pores (Bar=10μm).

Figure 2. SEM of KCl treatment showing small globules with smooth (s) and rough (r) protein coats. Note pores (p) concentrated in rough sections of coat and the indentations (i) (Bar=4μm).

Figure 3. SEM of smooth and rough coated globules from the 2.5% NaCl treatment. Pores only visible in the rough coat. p - pore, F - fat globule, m - matrix, b -point of physical binding of fat globule to matrix (Bar=1μm).

Figure 4. TEM of relatively stable, membrane enclosed globules adjacent to unstable globule with disrupted membrane ($CaCl_2$ treatment). Note thick coat which is continuous with the matrix around extended 'fingers'; r - protein film residue (Bar=0.5μm).

Results and Discussion

Fat Globule Morphology

The first part of this study was designed to examine the surface morphology of fat globules in both stable and unstable batters produced by using monovalent and divalent chloride salts respectively. A microscopical study of the five treatments revealed that two basic types of fat globules, smooth and rough, existed in meat batters

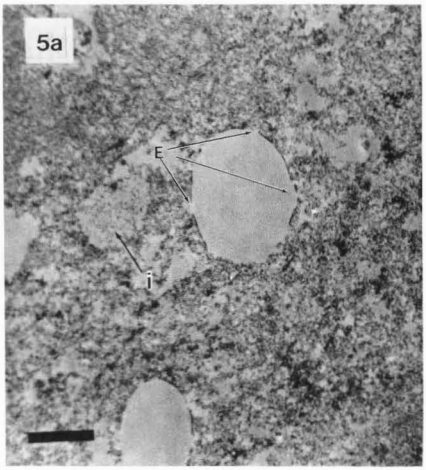

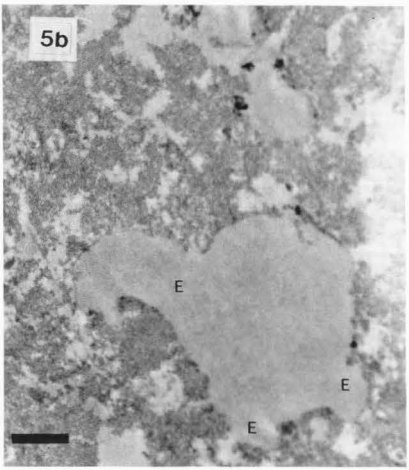

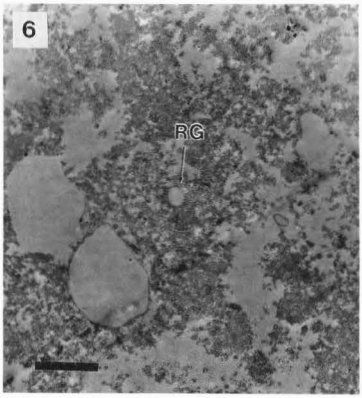

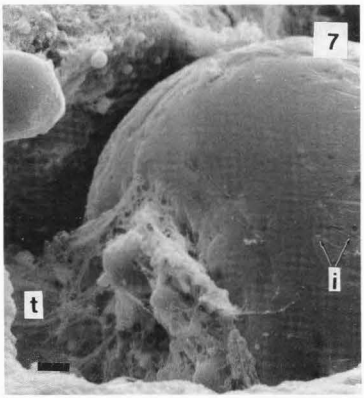

Figure 5. TEM of a) stable fat globules from the 1.5% NaCl treatment with relatively thick coats and evenly distributed pores; b) a globule ($MgCl_2$ treatment) with a thin protein coat in an unstable matrix showing multiple exudation of fat; I - internal structure; "E" - exudation (Bar=1μm).

Figure 6. TEM micrograph of a general field from the $CaCl_2$ treatment showing fat channels interconnected throughout the matrix. RG - round, stable globules (Bar=2μm)

Figure 7. SEM micrograph (2.5% NaCl treatment) of thread-like protein strands (t) bound to large fat globule and entrapping smaller globules. (Bar=2μm).

as was also described by Jones and Mandigo (1982). These two types were found in all treatments; however, the globules with rough surfaces were more prevalent in the unstable meat batters such as the

$CaCl_2$ treatment (Fig. 1). Pores were always present in the protein film of rough globules and were often relatively large in size. The rough area of the protein envelope was often not evenly distributed around the fat globule and there were globules in all treatments with both smooth and rough coats; the pores appeared to be concentrated in the rougher sections of the proteins coats (Figs. 2 and 3). The rough coat appeared to be due to thick, dense protein deposited unevenly around the globule. These deposits were continuous with the protein matrix as can be seen in a TEM cross-section (Fig. 4). Barbut (1988) also showed the presence of "rough" surfaces in batters prepared with different polyphosphates and NaCl. He suggested that the rough (wrinkled) appearance of the IPF was due to excessive fat loss from the globules during cooking. In this study, even globules which lost some of their fat retained their round shape (Figs. 1 and 4).

The smooth fat globules were prevalent in the more stable batters such as the 2.5% NaCl treatment. Basically, the smooth globules could be divided into two sub-groups. The first group was comprised of smooth globules which were relatively thickly coated with a few evenly distributed, tiny pores ranging from 0.01-0.1μm (Figs. 3 and 5a). The second group had globules with thin protein envelopes and larger pores (Fig. 5b). Generally, for smooth globules in all treatments, it appeared that the smaller, round globules had a relatively thick protein coat with few or no pores while larger round globules were thinly coated and had several pores. The irregular-shaped large globules tended to be thickly coated and had a rough protein envelope (Fig. 4). Lin and Zayas (1987) have also reported that large, irregular-shaped globules were thickly coated in frankfurters prepared with pre-emulsified fat. In the less stable batters ($MgCl_2$, Fig 4), protein envelopes ranged from fairly thick (>0.05μm) to almost indiscernible (<0.005μm).

In a previous study, it was found that batter stability was affected by the type of chloride salt used; monovalent salts produced stable batters while $MgCl_2$ and $CaCl_2$ resulted in batter instability (Gordon and Barbut, 1989). In that paper it was suggested that the differences observed may have been due to differences in the quantity and type of protein extracted and we have recently found that protein extraction influences the morphology of fat globules in meat batters (Gordon and Barbut; in preparation). It therefore appears that the external morphology of fat globules is dependent on the type and amount of protein forming the IPF. The external morphology of fat globules is also affected by IPF thickness (Jones and Mandigo, 1982; Lin and Zayas, 1987). Jones and Mandigo (1982) have indicated that IPF thickness affects batter stability. Deng et al. (1981) also observed that IPF thickness was related to batter stability. Hence it appears that fat globule morphology in meat batters is a major determinant of batter stability.

Fat Stabilization

The thermal gelation properties of the protein matrix and the resulting physical entrapment of fat have been proposed as the major contributors to batter stability (Lee, 1985; Comer and Allan-Wojtas, 1988; Regenstein, 1988). However, while coalescence may be prevented by the physical restriction of fat by the protein sol in the uncooked state, it is difficult to see how fat not localized within a membrane could be stabilized by this entrapment mechanism during cooking. In the temperature range of 35-50°C, the fat would be liquid (Townsend et al., 1968) while most of the matrix proteins would not yet have begun to gel. Further, in the range of 50-70°C, the majority of the matrix proteins would have undergone thermal gelation (Acton and Dick, 1984) while the fat would still be in a molten state (Townsend et al., 1968). In both cases, the unlocalized large pools of fat should therefore spread freely throughout the aggregated matrix during cooking (unless they are confined by a cohesive matrix) resulting in the formation of a microstructure similar to that observed in the $CaCl_2$ treatment (Fig. 6). However, this is not the case in stable batters (Fig. 5a) and, even in unstable treatments ($CaCl_2$, Fig. 6), fat globules surrounded by a protein membrane remain stable during cooking. These observations support the idea of the importance of the IPF in fat stabilization during cooking.

In this study it was observed that many fat globules were physically restricted by being bound to the protein matrix. This may have resulted from protein-protein interactions between the IPF and the matrix proteins. TEM micrographs revealed that globules of various types and sizes showed continuity between their protein coats and the matrix at several points on their circumference (Figs. 5a and b). Theno and Schmidt (1978) and Gordon and Barbut (1990) have shown that physical binding of fat globules to the protein matrix does take place. Katsaras and Stenzel (1984) have also published micrographs which possibly show this phenomenon and Hermansson (1986) suggested that the proteins of the IPF may be part of the total protein network. It is therefore logical to assume that protein aggregation during cooking increases the immobilization of protein-coated fat globules by binding them to the matrix, thereby further stabilizing these globules and preventing coalescence. Thread-like protein strands were seen connecting the protein matrix and some fat globules, especially the smaller globules (Fig. 7). Hence, it is likely that the lacy structures often seen on the surface of fat globules in SEM micrographs (Theno and Schmidt, 1978; Jones and Mandigo, 1982; Gordon and Barbut, 1990) are remnants of this thread-like matrix protein bound to the IPF.

Jones and Mandigo (1982) proposed that fat was exuded through pores which developed at weak points in the protein envelope during cooking in response to internal pressure build-up. The present study provides some evidence of the existence of such a mechanism. Fat exudation was evident in all treatments. Exudation was observed with all types of globules but depended on fat globule size since very small globules (<1.0μm) which did not have pores did not show the phenomenon. Figure 8 shows exudation occurring in rough and smooth globules. Figure 8b shows multiple exudation which was occasionally observed, where even newly exuded globules themselves seemed to be in the process of fat release. No pores were visible on the surface of the exuding globule in

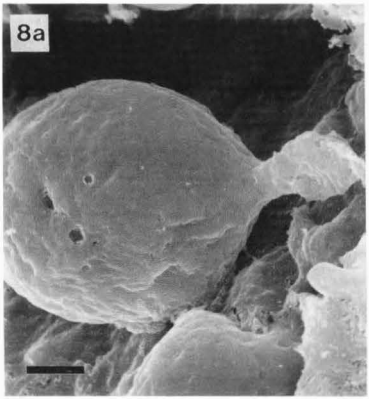
8a

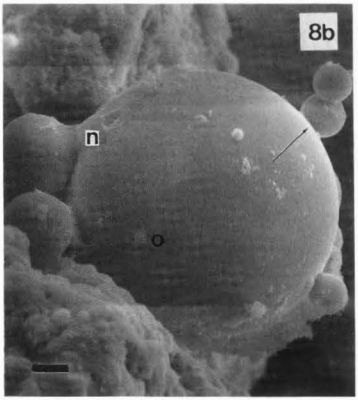
8b
n
o

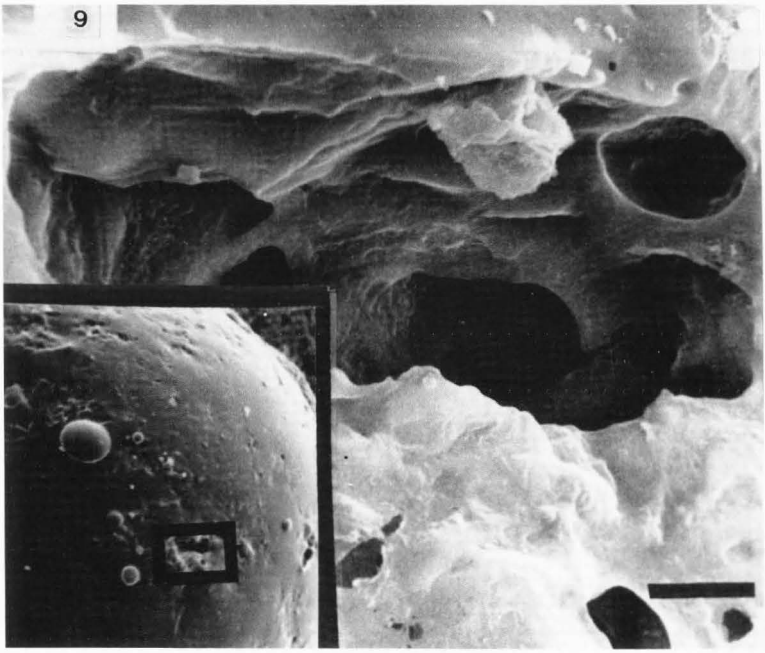
9

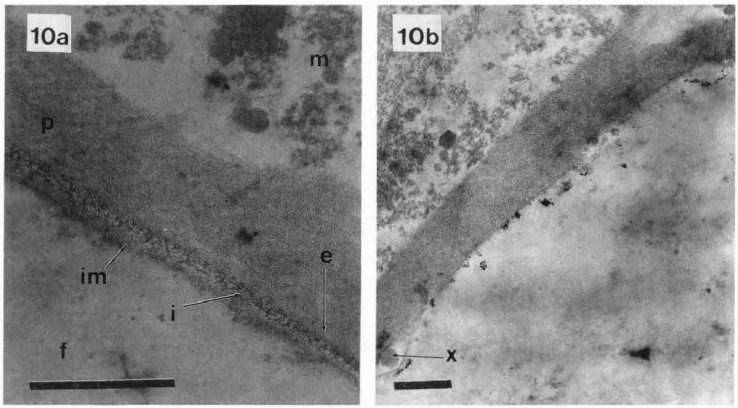

Figure 10. TEM of a) a thickly coated fat globule; b) a lower magnification of the IPF, both from the KCl treatment. m - matrix; p - thick, diffuse protein coat; e - external membrane; i - interconnecting diffuse region; im - internal membrane; f -internal fat; X - unidentified particle (Bar=1μm).

Fig. 8b. The protein coat around the exuded fat was continuous with that of the 'parent' globules (Figs. 5b and 8b). However, 'bumps' which may represent the early stages of exudation were evident in the protein coat of the fat globule (Fig. 8b).

A possible mechanism for exudation and pore formation could be that during cooking, expanding fat pushes out the protein film at points of weakness to form round, stable appendages. These break off to form smaller round globules with the same type of protein envelope as the 'parent' globule (Fig. 8). This break leaves insufficient protein to properly seal the gap left in the parent globule, hence the formation of pores or indentations (Figs. 2 and 7). This phenomenon continues until smaller, more stable globules are formed or all the matrix and interfacial film proteins of the system gel as a result of cooking. The exuded fat associated with the formation of these pores or indentations was not always seen by SEM since it was probably retained as part of the fracture face on the other half of the specimen during fracturing for SEM preparation. However, these pockets of fat or globules are clearly evident in TEM preparations (Figs. 4 and 5b). It may be argued that the process described above represents fat coalescence and not exudation. However, while the more stable batters had globules which exhibited several small, uniform pockets of exuding fat (Fig. 5a), unstable emulsions contained globules which showed large exudations at weak points in their protein coats (Figs. 4 and 5b). These were more likely to form fat channels and facilitate coalescence (Gordon and Barbut, 1989). Fat coalescence can be distinguished from the exudation phenomenon in TEM by the lack of a defined spherical shape of the fat within the matrix (Koolmees et al., 1989), the existence of incomplete protein film residues within the fat (Comer and Allan-Wojtas, 1988; Gordon and Barbut, 1989) and the numerous inter-connections between fat pockets as can be seen in Fig. 6. The micrographic evidence presented here gives credence to the role of the IPF and the mechanism of exudation in meat batter stabilization.

Structure of the Interfacial Protein Film and Interior of Fat Globules

While the protein envelope which surrounds thinly coated fat globules is probably formed by the adsorption of a monomolecular layer of myosin (Jones, 1984), the protein film of more thickly coated fat globules appears to be more complex. The internal structure of a pore in a thickly coated fat globule appeared to consist of a complex, convoluted series of tunnels which seemed to extend into the globule (Fig. 9; showing the enlargement of the inset). Jones and Mandigo (1982) observed similar internal structures which they believed were internal pores within the main

Figure 8. SEM micrograph of a) a rough globule from the 2.5% NaCl treatment with large pores in the process of exudation; b) a fat globule showing multiple exudation ($MgCl_2$ treatment). Note interconnecting 'neck'(n) of coat between parent and daughter globule. O - out-pushing ('bumps'); arrow - continuing process of exudation. (Bar=2μm).

Figure 9. SEM micrograph from $MgCl_2$ treatment showing close up of large pore in the surface of a rough globule (inset). (Bar=2μm).

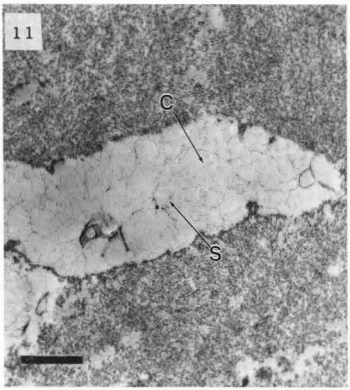

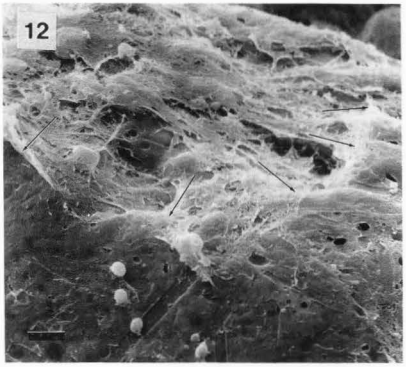

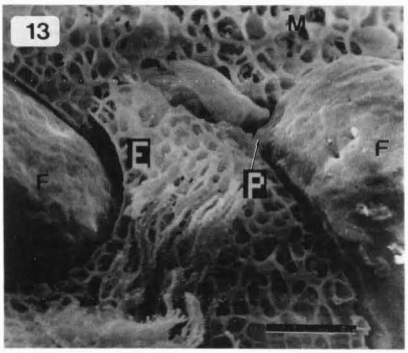

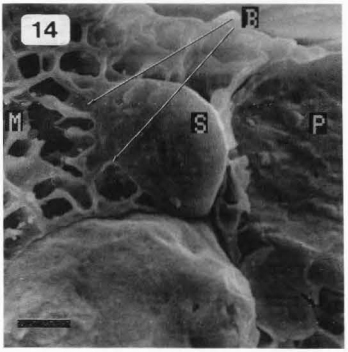

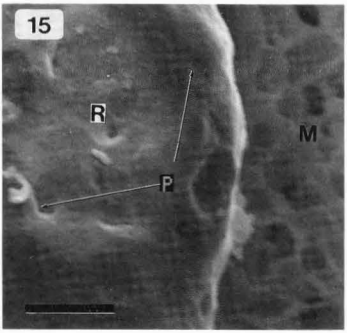

Figure 11. TEM of the compartmentalized internal structure of a membrane-bound fat globule (1.5% NaCl treatment). S - internal interconnected strands, C - compartment (Bar=1μm).

Figure 12. SEM micrograph of a fractured globule showing what appears to be lobes of protein coated fat further entrapped by mesh-like network of fibres ($CaCl_2$ treatment). Arrows-junction between protein envelope and fibres. (Bar=2μm).

Figure 13. Cold stage SEM (cryo SEM) micrograph of chicken meat batter made with 2.5% NaCl. E- physical entrapment within matrix, P- physical binding of fat to matrix, F- fat; M- matrix (Bar = 2 μm).

Figure 14. Cold stage SEM micrograph of chicken meat batter made with 2.5% NaCl. S- small fat globule, P- pore, M- matrix, B- physical binding (Bar = 2 μm).

Figure 15. Cryo SEM micrograph of chicken meat batter. R- rough coat, P- pore, M- matrix (Bar = 2 μm).

pores. They suggested that this could indicate the existence of an inner protein membrane and therefore that the IPF had a more complex structure than was previously thought to exist. We observed that the protein coat around thickly coated globules was multi-layered in nature (Fig. 10a). In this case, the IPF appeared to consist of four distinct layers. A thin internal layer coated the surface of the fat and was bound through a diffuse region to another layer of similar density. This in turn was bound to a very thick, relatively diffuse protein coat. The three internal layers of the protein coat seemed to form what may be a thermodynamically favoured lipid bilayer-type structure. Jones and Mandigo (1982) have proposed a similar structure for the IPF as is shown here. The two internal layers were shown to be separated by the interjunction of an unidentified particle (possibly bone from the MDCM) between them (Fig. 10b). The structure and formation of this membrane merits further investigation.

Some of the larger fat globules appeared to have a more complex internal structure than was originally thought. While small globules appeared to contain only fat, some of the larger globules contained internal structures of different densities and arrangements (Figs. 5a and 11). These might be the result of protein which coats internal fat, increasing the stability of the globule. This definitely appears to be the case in the compartmentalized structure evident in Figure 11. Lin and Zayas (1987) have also found internal structures assumed to be protein within large fat globules in frankfurters made with pre-emulsified fat. The internal appearance of a fractured fat globule from the $CaCl_2$ treatment revealed that its internal fat was partially separated into lobes but was essentially continuous throughout the globule (Fig. 12). The fat appeared to be enveloped in a fairly cohesive protein coat. The internal protein appears to be interlinked and this could possibly explain the convoluted sub-structure of the pore seen in Fig. 9. This protein may be the source of the internal channels within the pores which possibly form a route out of the globule for thermally expanding fat thereby facilitating exudation. A transverse section of the globule in Figure 12 would probably produce a structure similar to that shown if Figure 11. While the origins of these different levels of internal organization is unclear, the continuity of the IPF with the internal structure is clearly seen in Figures 5a and 12.

Conclusion

The dominant surface morphology of fat globules was found to be different between stable and unstable batters made with four chloride salts. These differences may be due to variations in the amount and type of protein forming the IPF. Fat was shown to exude through pores in the interfacial protein film in all treatments and was further stabilized by the binding of the IPF of fat globules to the protein matrix, thereby physically restricting the fat and preventing its coalescence in stable batters. The number and size of pores in the interfacial film appeared to depend on IPF thickness. The interfacial film has a complex, multi-layered structure which gives it stability and strength. The indications are that fat within some globules may be further stabilized by internal protein which interacts with the IPF. Further work is needed to more fully explore the functional significance of some of these observations. These findings indicate that fat emulsification and the interfacial protein film play a role in the production of stable meat batters.

References

Acton JC and Dick RL (1984). Protein-protein interactions in processed meats. Recip. Meat Conf. Proc. 37: 36-43.

AOAC. (1980). "Official Methods of Analysis", 13th ed. Association of Official Analytical Chemists, Wash., D.C.

Asghar A, Samejima K, Yasui T. (1985). Functionality of muscle proteins in gelation mechanisms of structured meat products. CRC Crit. Rev. Food Sci. Nutrit. 22(1): 27-106.

Barbut, S. (1988). Microstructure of reduced salt meat batters as affected by polyphosphates and chopping time. J. Food Sci. 53, 1300-1304.

Borejdo J. (1983). Mapping of hydrophobic sites on the surface of myosin and its fragments. Biochem. 22: 1182-1187.

Borchert LL, Greaser ML, Bard JC, Cassens RG, Briskey EJ. (1967). Electron microscopy of a meat emulsion. J. Food Sci. 32: 419-421.

Comer FW, Allan-Wojtas P. (1988). Functional and microstructural effects of fillers in comminuted meat products. Food Microstr. 7: 25-46.

Deng JC, Toledo RT, Lillard DA. (1981). Protein-protein interactions and fat and water binding in comminuted flesh products. J. Food Sci. 46: 1117-1121.

Fukazawa T, Hashimoto Y, Yasui T. (1961a). Effect of some proteins on the binding quality of an experimental sausage. J. Food Sci. 26: 541-549.

Fukazawa T, Hashimoto Y, Yasui T. (1961b). The relationship between the components of myofibrillar proteins and the effect of various phosphates that influence the binding quality of sausage. J. Food Sci. 26: 550-555.

Galluzzo SJ, Regenstein JM. (1978a). Emulsion capacity and timed emulsification of chicken breast muscle myosin. J. Food Sci. 43: 1757-1760.

Galluzzo SJ, Regenstein JM. (1978b). Role of chicken breast muscle protein in meat emulsion formation: myosin, actin and synthetic actomyosin. J. Food Sci. 43: 1761-1765.

Galluzzo SJ, Regenstein JM. (1978c). Role of chicken breast muscle protein in meat emulsion formation: natural actomyosin, contracted and uncontracted myofibrils. J. Food Sci. 43: 1766-1770.

Gordon A, Barbut S. (1989). The effect of chloride salts on the texture, microstructure and stability of meat batters. Food Microstr. 8: 271-283.

Gordon A, Barbut S. (1990). Use of cold stage scanning microscopy to study meat batters. J. Food Sci. 55 (in press).

Hansen LJ. (1960). Emulsion formation in finely comminuted sausage. Food Technol. 14: 565-569.

Hermansson AM. (1986). Water- and fat-holding. In "Functional Properties of Food Macromolecules," Mitchell JR and Ledward DA (eds.), p273. Elsevier Appl. Sci. Pub., New York.

Jones KW, Mandigo RW. (1982). Effect of chopping temperature on the microstructure of meat emulsions. J. Food Sci. 47: 1930-1935.

Jones KW. (1984). Protein-lipid interactions in processed meats. Recip. Meat Conf. Proc. 37: 52-57.

Katsaras K, Stenzel R. (1984). The microstructure of frankfurter-type sausages as observed under the scanning and the transmission microscope. Fleischwirtschaft. 64: 951-952.

Koolmees PA, Moerman PC, Zijderveld, MHG. (1989). Image analysis of the fat dispersion in a comminuted meat system. Food Microstr. 8: 81-90.

Kramlisch WE. (1977). Sausage products. In "The Science of Meats and Meat Products", Price JF and Schweigert BS (eds.), p484. W.H. Freeman & Co., San Francisco.

Lee CM, Carroll RJ, Abdollahi A. (1981). A microscopical study of the structure of meat emulsions and its relationship to thermal stability. J. Food Sci. 46: 1789-1793.

Lee CM. (1985). Microstructure of meat emulsions in relation to fat stabilization. Food Microstructure. 4: 63-72.

Lin CS, Zayas JF. (1987). Microstructural comparisons of meat emulsions prepared with corn protein emulsified and unemulsified fat. J. Food Sci. 52: 267-270.

Meyer JA, Brown WL, Giltner ME, Grinn JR. (1964). Effect of emulsifiers on the stability of sausage emulsions. Food Technol. 18: 1796-1798.

Regenstein JM. (1988). Meat batters: Why it is not an emulsion. Recipr. Meat Conf. Proc. 41: 40-43.

Schut J. (1978). Basic meat emulsion technology. Meat Industry Res. Conf. Proc., 1978, 1-15.

Smith L, Fantozzi P, Creveling RK. (1983). Study of triglyceride-protein interaction using a microemulsion filtration method. J. Amer. Oil Chem. Soc. 60: 960-967.

Swasdee RL, Terrell RN, Dutson TR, Lewis RE. (1982). Ultrastructural changes during chopping and cooking of a frankfurter batter. J. Food Sci. 47: 1011-1013.

Swift CE, Lockett C, Fryar AJ. (1961). Comminuted meat emulsions. The capacity of meat for emulsifying fat. Food Technol. 15: 468-473.

Theno DM, Schmidt GR. (1978). Microstructural comparison of three commercial frankfurters. J. Food Sci. 43: 845-848.

Townsend WE, Witnauer LP, Riloff JA, Swift, CE. (1968). Comminuted meat emulsions. Differential thermal analysis of fat transitions. Food Technol. 22: 319-323.

Discussion with Reviewers

A.M. Hermansson: In the preparation of the meat batters for electron microscopy the dehydration procedure is bound to affect the fat phase one way or another. Corroborative studies by freeze etching would be needed for the full evidence of fat exudation, the presence of pores and the distribution of the fat phase. Could the authors specifically comment upon the limitations of the preparation process?

Authors: All conventional electron microscopical (EM) preparation protocols involve a series of chemical and physical processes which can alter the microstructure of the specimen. Fixation with osmium tetroxide (OsO_4) can cause up to 30% specimen swelling, however this is often offset to some extent by the shrinkage which occurs later on in the preparation process (Hayat, 1981). Most of the structural modification of EM specimens occurs during alcoholic dehydration and critical point drying (CPD) for SEM and during embedding for TEM (Chabot, 1979; Dawes, 1988). Dehydration with alcohol can cause translocation of fat, fat leaching from the specimen and invariably, specimen shrinkage. This shrinkage is exacerbated by CPD for SEM and by shrinkage during embedding for TEM. These all produce artefacts which must be controlled by careful observation of sound EM preparation practices during specimen processing. However, their effects cannot be eliminated and together they affect the structure of the processed specimens which are viewed by EM. One must therefore be cognizant of the presence of these artefacts when interpreting electron micrographs.

The freeze-etching technique has not been utilized in our studies but we agree that it would be very useful for the kind of study undertaken in this paper. However, we have used cryo SEM (and surface etching by sublimation) to study meat batter systems. Figures 13 to 15 show some of the microstructural features described in the text as revealed by cryo SEM of chicken meat batters.

J.M. Regenstein: The whole issue of the amount of rancidity in the experimental samples and its implication for the interpretation of the data needs to be considered.

Authors: The extent of rancidity in the samples could affect the protein-lipid interactions. However, all treatments were made from the same source of meat so the variations in fat rancidity between treatments was controlled. In addition, many of these microstructural features have also been observed with other batters prepared from different meat and fat sources (unpublished data).

A.M. Hermansson: The fat observed in this study was part of chicken meat. Both the properties of the fat and the meat raw material may have a bearing on the final structure of a cooked meat system and it may be dangerous to generalize from studies made on one system. Have the authors studied the phenomenon of "fat exudation" or the nature of interfacial films of any other meat system?

F.W. Comer: In your formulations the only fat is coming from MDCM. Due to the recovery procedures for MDCM (mechanical shear and high pressure) it is unlikely that any cellular fat structure is retained, and in fact some protein coating may occur during mechanical deboning. Have you examined meat homogenates containing pork back fat or other adipose tissues? I would be interested to know whether the "speckled egg" pattern in Figure 1 has been observed in this type of meat homogenate.

Authors: In subsequent studies we have used a

chicken breast meat/pork back fat system to study the interactions involved in the stabilization of meat batters (unpublished data). The results of these studies have indicated that fat exudation and the multilayered IPF structure presented here also exists in these systems. We have not yet examined red meat systems but intend to do so.

C.M. Lee: All studies related to meat emulsion stability should include light microscopic data which would serve as supporting evidence to the EM data. Please comment.
Authors: We have used LM to examine the gross morphology sections from the same tissue blocks used for TEM sections. However, it was felt that because of the nature of this study, the resolution offered by light microscopy was not high enough to assist in clarifying the material under investigation.

J.M. Regenstein: Storage time of the meat batter will affect its properties, mainly leading to a stiffening of the material. This suggests that changes in the matrix may be more important than the authors identify and that the thin layer of liquid fat immediately after chopping may not be of fundamental importance. Please comment.
Authors: It was not our intention to suggest that changes in the protein matrix are not important. In fact, there can be no denying the vital role which protein gelation during cooking plays in the development of texture as well as water- and fat-binding. However, available research suggests that interfacial protein film (IPF) formation does take place in meat batters. We therefore believe that its role in batter stabilization should be considered.

J.M. Regenstein: Our work on timed emulsification and cream layer formation does not necessarily favour the emulsion theory. In fact later work with insoluble muscle systems would suggest that solubility and possibly the activity at the interface may not be the critical element. Please comment.
Authors: We are aware of this work (Gaska and Regenstein, 1982a,b; Perchonok and Regenstein, 1986a,b; Huber and Regenstein, 1988). We have also found that insoluble proteins may be important in fat binding in raw $CaCl_2$ batters (Gordon and Barbut, submitted). However, our work to date suggests that regardless of the origin of the proteins forming the protein film, the IPF works in conjunction with matrix protein gelation to stabilize raw and cooked batters. Our studies on $CaCl_2$ meat batters also suggest that the source of the proteins (soluble or insoluble) which form the IPF may be more important in determining fat stability during cooking than it does in the raw state.

F.W. Comer: It was clear from the first part of this study (Gordon and Barbut, 1989) that the major reason for differences in stability between treatments with various salts was the effect upon the protein matrix. The divalent cations produced "highly aggregated matrices" which resulted in large water losses. Differences in fat losses were relatively small. In this paper it is shown that the divalent ions produce thicker protein coating. Does this imply that more protein is extracted by the divalent salts? Intuitively, I would expect thicker protein coats to increase stability.
Authors: A recent study has shown that divalent chloride salts extracted less protein from meat than monovalent chloride salts (Gordon and Barbut, in preparation). Consequently, the thick protein coat in these batters cannot be due to soluble proteins. However, insoluble proteins are capable of participating in IPF formation (Schut, 1978; Gaska and Regenstein, 1982 a,b; Huber and Regenstein, 1988). Subsequent studies done in our laboratory have suggested that insoluble proteins do form an IPF around some fat globules in the divalent salt batters (Gordon and Barbut, unpublished). Because of the nature of these proteins, they appear to be distributed unevenly around the circumference of the globules (pointer, Fig. 4) resulting in weak (thin) areas at points on the circumference of the globules. These points were predisposed to rupture during cooking, thereby causing fat loss from the globule (Fig. 6). It should be noted that Jones and Mandigo (1982) also found that overly thick protein coats around fat globules reduced their stability.

J.M. Regenstein: Do rough globules have a protein envelope?
Authors: It appears that they do. However, this envelope tends to be of uneven thickness (see Figs. 4 and 6) and appears to be bound to the protein matrix and this may be what results in the "rough" appearance after fracturing and viewing by SEM (Figs 2 and 8a). Some globules had both rough and smooth areas (Figs 2 and 3) and this may represent differences on the circumference of the globule between areas with a defined IPF and those where the matrix proteins were directly in contact with the fat (See Fig 5a).

J.M. Regenstein: In the TEM, how do you decide if something is really a protein envelope around an oil droplet, i.e., I presume that means it serves as an interfacial film in part versus the fact that the matrix needs to terminate when it gets to a discontinuity. (Is it possible that the binding of the matrix to the fat is important, but that the traditional film formation is not?).
Authors: You have raised some very important points. In our TEM preparation procedure, secondary fixation with osmium tetroxide (OsO_4) was employed. Osmium tetroxide reacts mainly with the unsaturated fatty acids and, in addition to stabilizing the fat, it imparts greater electron density to areas where these fatty acids are concentrated. These unsaturated fatty acids would be concentrated on the outside of the fat globule where a thin film of liquid fat is believed to be located (Jones, 1984). The OsO_4 also produces acidic binding sites for the heavy metal ions (mainly the lead) which are later used to increase the contrast of the components within the sections (Dawes, 1988). In addition, OsO_4 also reacts with proteins, the extent of which depends (among other things) on protein conformation (Hayat, 1981). All the proteins within the system were exposed to OsO_4 but those at the interface would react differently from those in the matrix because they

assume different conformations (Graham and Phillips, 1979) or are different proteins (Gordon and Barbut, in preparation). Hence, all of these interactions result in an increased electron density on the circumference of fat globules when an IPF is formed which is distinct from cases where the matrix merely terminates next to a fat particle. Other researchers have shown that the use of OsO_4 improves the image of fat globule membranes in emulsions (Liboff et al., 1988).

The binding of the matrix to the fat is important and the great majority of fat particles within a meat batter are bound directly to the matrix (Fig. 13 and 14) in both raw and cooked batters. However, this direct binding appears to require the mediation of a protein coat which at least covers a part of the fat particle thereby allowing some level of immobilization of the fat once it is bound to the matrix. In recent work (Gordon and Barbut, in preparation) we have shown that it appears that the stability of $CaCl_2$ raw batters is due to the formation of an IPF around fat globules by the insoluble proteins which are also a part of the matrix. Earlier, Hermansson (1986) had suggested that the IPF proteins may be a part of the protein matrix. Consequently, even in a case where soluble proteins are not available for IPF formation, the insoluble (but surface-active) proteins such as actomyosin (and some myosin) appear to play a role in fat binding. It should be noted that whether soluble or insoluble proteins form the IPF, its binding to the matrix makes it an integral part of the protein gel network in meat batters.

G.R. Schmidt: Could it be possible that the same conditions necessary for a fine protein matrix are also necessary to form a pore free coating on fat droplets and that this coating actually entraps the lipid and prevents it from coalescing and assuming a non spherical shape? I notice that spheres are only fully coated when the entire protein gel is a fine laced aggregate.
Authors: It is generally true that the proteins involved in matrix formation also function in forming the IPF. It seems that conditions which favour the formation of a fine protein matrix will also result in an increased number of pore-free globules being formed. These conditions may include adequate extraction of myosin and actomyosin (Gordon and Barbut, in preparation). However, even batters with fine structured matrices had several fat globules with pores in their protein coats present (see Figs. 2 and 3) as a result of differences in the thickness and type of coat. Therefore, the actual occurrence of pores in the IPF may not be affected by the above-mentioned conditions since they appear to be present in each batter. However, the number of pore-bearing globules, the number of pores per globule, the size of the pores and whether or not they become rupture holes all appears to be affected by the same conditions which influence matrix structure.

We agree that the coating entraps the fat and helps to prevent it from coalescing and becoming non-spherical. The protein coat also serves as an intermediary to lipid-matrix binding as shown in this study (Figs. 3, 13 and 14) and in a previous study (Gordon and Barbut, 1990). This further helps to prevent coalescence.

C.M. Lee: You stated "it is difficult to see how fat not localized within a membrane could be stabilized by this entrapment mechanism during cooking". How do you justify this statement? Authors should be aware that entrapment follows localization, the formation of IPF is a result of protein-lipid interaction in which protein molecule orient to stabilize its molecular structure upon interaction with fat molecule. This can occur in the small surface area as in the case where fat is finely dispersed in relatively uniform size without disrupting matrix continuity. However, in either case when fat is not uniformly dispersed (e.g. low melting point fat or high chopping temperature) or when a noncohesive matrix is prepared with meat of poor functionality, no continuous and cohesive matrix is available to entrap the dispersed fat. One good example why the matrix continuity should be a prerequisite to the stable fat dispersion, is making a meat emulsion with squid protein which has a high level of salt soluble actomyosin to form IPF sufficient to cover the fat globules dispersed, but failed to form a stable meat batter (Saffle, 1973). It is mainly because squid protein is not capable of forming a continuous, rigid matrix which can entrap the fat particles and keep them from coalescing.
Authors: We have suggested that localization precedes entrapment, as you have pointed out. The cohesiveness and continuity of the matrix is undoubtedly of importance and its importance to fat stabilization was not questioned. We merely draw attention to the fact that mobile, liquid fat would move relatively freely through the openings in the protein matrix during cooking if it was not in some way localized within the system and kept away from other fat particles (see Fig. 6).

J.M. Regenstein: How does one determine that a droplet has lost fat and is still round?
Authors: The pores in the protein film are sites of fat loss from the globules (Fig. 4). It is therefore assumed that globules which show several pores by SEM have undergone at least limited fat exudation (Jones and Mandigo, 1982; Barbut, 1988). These globules still appear to retain their oval or spherical shape (Figs. 1 and 2). In addition, both TEM (Fig. 5) and SEM (Fig. 8) showed that globules in the process of exudation still kept their basic shape except for the section of the protein film surrounding the exuding fat.

F.W. Comer: Figure 1 shows an interesting collection of globules, two of which are identified as having thick rough coats. The number of holes is amazing. What is left inside? Has the fat exuded out and left empty "egg shells"? Other micrographs suggest a "budding" effect from a single pore. If fat were to exudate from a membrane-coated globule, I would expect some type of collapsed structure. Why is this not observed?
Authors: The globules shown in Figure 1 represent extreme cases of pore formation in thickly coated fat globules in an unstable treatment. In these extremely porous globules it is likely that some of the fat has been lost. However, because of the uniformity of distribution of the pores around the globules, extensive fat loss as shown in Fig. 4 probably did not occur and instead several small

amounts of fat probably exuded through each pore (see comparable situation in Fig. 5a), leaving a fair amount of the fat still inside the globules. Collapse of these structures was not seen possibly because the thick protein film denatured during cooking to form a rigid "shell" while the fat was still expanding (and exuding). Because the coat is protein, primary fixation with the aldehydes would further stabilize this rigid structure and prevent collapse during further processing in EM preparation. In addition, the protein coat is also bound to the rigid protein matrix which could help in retaining the shape despite some fat loss. However, if extensive, rapid fat loss occurs, before the protein coat has "set" during cooking then some collapse of the structure would be expected.

J.M. Regenstein: The fact that the procedure led to exudate in all cases would suggest that the conditions may not be realistic for real meat systems.
Authors: A certain degree of fat exudation was observed in all treatments with sufficient frequency to merit discussion as to its possible role in fat stabilization. However, it should be noted that not all fat globules showed exudation and that the phenomenon appeared to be related to the uniformity and thickness of the IPF around fat globules. Globules with very uniform protein coats (thick or thin) quite often did not show fat exudation. Thickly-coated, uniform globules are probably able to stabilize fat by virtue of their mechanical strength of their IPF while thinly coated, uniform globules would rely more on the elasticity of their IPF to retain fat and prevent fat loss.

A.M. Hermansson: An alternative to the proposed exudation mechanism, illustrated in Figure 8, could be flocculation of smaller droplets onto bigger globules and partial coalescence of the semicrystalline fat during cooling or during the preparation process for EM. Partial coalescence will not necessarily result in a lack of the spherical shape.
Authors: The main fat globules in Figure 8 show continuity of their protein coats with that of the smaller globules. This suggests that the protein coat around the "parent" and "daughter" globules is the same. The long connecting "neck" of protein in Figure 8a would not be seen in the case of coalescence. The unity of the protein coat around parent and exuded globules is seen quite clearly by TEM ("E", Fig 5b). In the case of flocculation, each globule would have its own distinct protein coat. With coalescence, protein residues would be seen within the fat (Fig. 4, unstable globule) as has been shown in other studies (Comer and Allan-Wojtas, 1988; Gordon and Barbut, 1989). Hence, while it is perhaps difficult to be definitive about fat exudation from SEM micrographs, TEM makes the distinction between exudation and coalescence clear.

G.R. Schmidt: In the TEM pictures, openings in the membrane are occasionally seen, but the pores seen in the SEM photos appear very deep. Why don't we see these deep pores in the TEM pictures?

Authors: This may be because the depth of the pores (as seen by SEM) is dependent on a) the thickness of the IPF and b) the internal organization of the fat globule. If the fat globule has an internal protein structure which is connected to the protein coat at the point of pore formation, then the pore will appear to extend deeply into the globule because it is merely an extension of the internal protein.

A.M. Hermansson: The multilayered structure shown in Figure 10 is interesting and focuses the attention to the potential of membrane residues of comminuted meat systems as stabilizers. Have the authors any information about variations in the multilayered structures?
Authors: In a follow-up study on the role of the IPF in raw meat batters, it was found that the multilayered structure varied between treatments and sometimes within the same meat batter (unpublished). The structure of the IPF appears to vary from a single layer to up to four different layers. We have found that several different soluble proteins are involved in IPF formation and that insoluble proteins may also form an IPF around fat globules (Gordon and Barbut, 1990 in preparation). We therefore believe that the structure of the protein coat varies depending on the types of proteins of which it is composed.

A.M. Hermansson: The statement of the domain shown in Figure 11 of being a large fat globule is not convincing. This could be a partly broken down fat cell aggregate where the network is residues of the collagen rich cell walls or some other structural component in the complex meat system. Please comment.
Authors: Your analysis of Fig. 11 could be correct. However, the size of each of these compartments (<1μm in diameter) makes it unlikely, in our opinion, that they are remnants of cell wall structures. In addition, such internal structures have been observed in several other large globules in this study (not shown) and in several of our other studies.

F.W. Comer: The presence of protein material inside fat globules has been observed before, but Figure 11 is possibly the best published example. You have attributed this to "protein which coats internal fat". I believe that this may be due to coalescence of protein coated fat globules (or alternatively, residual fat cell membranes which may be less likely for MDCM). It has always surprised me, that if protein coatings are prevalent in comminuted meat products, why are they not observed in coalesced fat pools? Protein should be pressed against protein in a restricted mobility environment, and some (partially) regular pattern observed. What do you believe happens to the protein coats when fat globules coalesce in a gelled meat system?
Authors: Residual protein coats within pools of coalesced fat are occasionally seen (Fig 4) and were highlighted in our previous study (see Fig. 2c, Gordon and Barbut, 1989). In fact, in some of your work (Comer and Allan-Wojtas, 1988) you presented micrographs which we believe show a similar situation. However, this occurrence is not

very common in unstable batters. We believe that this is because instability results either from the rupture of the protein coat (thereby releasing fat) during cooking or its absence around much of the fat prior to cooking as has been shown in another study (Gordon and Barbut, submitted). It would therefore be the free fat itself in most cases which coalesces and not so much the fat particles/globules. The protein coats (if any) originally present around these globules would remain bound to the protein matrix and not be present (in most cases) within the coalesced pool of fat.

C.M. Lee: I would agree with the authors view on the role of the IPF as described in the paper. But, I must point out that the formation of an IPF is a mere consequence of physicochemical interactions bewteen the protein and lipid which determine the fate of the thermal stability of meat emulsions. They include protein functionality, the extent of protein solubilization, matrix integrity, fat dispersion pattern (particle size and density) and other factors that further alter the fat morphology, independent of the formation of an IPF.

Authors: As you have indicated, there are many factors which influence batter stability. We believe that there may be a greater interdependence among these factors than is generally acknowledged and that IPF formation is one of the more important factors which interacts with others to determine meat batter stability.

Additional References

Barbut, S. (1988). Microstructure of reduced salt meat batters as affected by polyphosphates and chopping time. J. Food Sci. 53, 1300-1304.

Chabot JF. 1979. Preparation of food science samples for SEM. Scanning Electron Microsc. 1979; III: 279-286, 298.

Dawes, CJ. (1988). Introduction to biological electron microscopy: theory and techniques, p86-91, 117-125. Ladd Research Industries Inc., Vermont, USA.

Gaska MT, Regenstein JM. (1982a). Timed emulsification studies with chicken breast muscle: soluble and insoluble myofibrillar proteins. J Food Sci. 47, 1438-1443.

Gaska MT, Regenstein JM. (1982b). Timed emulsification studies with chicken breast muscle: Whole muscle, low-salt washed muscle and low-salt soluble proteins. J. Food Sci. 47, 1460-1462.

Graham, DE, Phillips MC. (1979). Proteins at liquid interfaces lll. Molecular structures of adsorbed films. J. Colloid Int. Sci. 70, 427-439.

Hayat, MA. (1981). Fixation for electron microscopy, p157-159, 299-306. Academic Press Inc., New York, NY.

Huber DG, Regenstein, JM. (1988). Emulsion stability studies of myosin and exhaustively washed muscle from adult chicken breast muscle. J. Food Sci. 53, 1282-1286, 1293.

Liboff M, Goff HD, Haque Z, Jordan WK, Kinsella JE. (1988). Changes in the ultrastructure of emulsions as a result of electron microscopy preparation procedures. Food Microstr. 7, 67-74.

Perchonok MH, Regenstein JM. (1986a). Stability at comminution chopping temperatures of model chicken breast muscle emulsions. Meat Sci. 16, 17-29.

Perchonok MH, Regenstein JM. (1986b). Stability at cooking temperatures of model chicken breast muscle emulsions. Meat Sci. 16, 31-42.

Saffle, RL. (1973). The use of squid in meat emulsions. J. Food Sci. 38, 551-552.

FOOD STRUCTURE, Vol. 9 (1990), pp. 91-95
Scanning Microscopy International, Chicago (AMF O'Hare), IL 60666 USA

1046-705X/90$3.00+.00

THE EFFECT OF TUMBLING, SODIUM CHLORIDE AND POLYPHOSPHATES ON THE MICROSTRUCTURE AND APPEARANCE OF WHOLE-MUSCLE PROCESSED MEATS

P. D. Velinov, M. V. Zhikov & R. G. Cassens*

Institute of Meat Industry
65, Cherni Vrah Blvd.
1407 Sofia, Bulgaria

Abstract

The properties of a whole-muscle processed meat were determined. The complex action of sodium chloride, polyphosphates and mechanical agitation caused extraction of myofibrillar protein, swelling of fibers and loss of cross-striations. A new functional ability was found for the extracted proteins to form a fine cover or membrane on the surface of the whole muscle during cooking. These changes produced a product with improved cooking yield and color appearance.

Initial paper received November 21, 1989
Manuscript received May 13, 1990
Direct inquiries to R.G. Cassens
Telephone number: 608 262 1792

Key Words: Muscle, Mechanical Treatment, Processed Meat

*Address for correspondence:
Robert G. Cassens, Muscle Biology Lab.,
1805 Linden Drive, University of Wisconsin,
Madison, WI 53706 U.S.A., Phone (608)262-1792

Introduction

Microscopical studies of processed meats have concentrated on two areas -- the structure of the so-called emulsion in products such as frankfurters and the structure of the protein matrix which binds together the pieces of meat in restructured products. In the former area, initial investigations elucidated the structure as being a dispersion of fat droplets embedded in a protein matrix (Hansen, 1960; Borchert et al., 1967; Schmidt, 1984). Subsequent work has been focused on relating quantitative measurements of the fat droplets to properties of the final product (Cassens and Schmidt, 1979; Hermansson, 1987), and interest continues in using microscopy of the raw emulsion as a predictive or quality control technique during the manufacturing process.

In regard to restructured products, effort has focused on the extraction and functionality of the muscle proteins as affected by mechanical agitation and composition of the added brine (Theno et al., 1978a). Theno et al. (1978b) have described the protein matrix at the interface of bound pieces of meat as being emulsion-like.

In Bulgaria, there are special meat products made from whole, intact muscles. These are made by incorporating a brine and then subsequently heating and smoking. Our objective was to study the internal microstructure and the surface characteristics of these products and to compare traditionally made products with products which had an improved brine composition and also received a period of mechanical agitation during manufacture. The aim was to determine if the complex action of the improved brine and mechanical treatment had an effect and if so if it could be used to improve the technological process.

Materials & Methods

The experiments were conducted on pork muscle from animals with a live weight of 100 to 110 kg. Thirty-five animals were slaughtered in the usual manner and the muscles were checked to insure they fell within the normal range of pH (5.5 to 6.0) and did not exhibit either pale or dark appearance. Longissimus dorsi muscles were

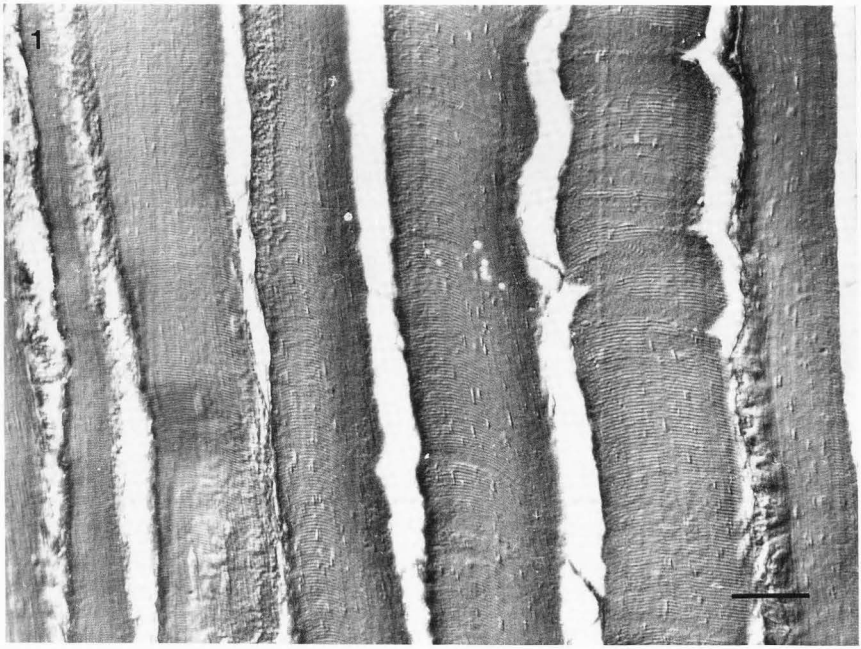

Figure 1: Microstructure of control muscle showing normal shrinkage and good preservation of banding pattern. Scale bar is 25μm.

removed intact from both sides of the carcass following 24 hr. of chilling at 4°C. The muscles from the left side of the carcass served as controls and those from the right side were treated.

The control muscles were immersed in brine for 5 days. The brine was a typical 15° brine prepared with 160 L of water, 30 kg sodium chloride, 0.8 kg sucrose, 0.6 kg sodium nitrite and 0.4 kg sodium nitrate.

The treated muscles were manufactured in a complete, complex line made by "Langen" of Holland. The injection of the muscles took place directly in the tumbling apparatus during a period of 30 minutes with a calculated brine uptake of 12%. In this case, the brine was made from a commercial preparation and contained sodium chloride, polyphosphate, sodium nitrite and sodium nitrate. The tumbling process took place under vacuum and over a 24 hr. period. Active tumbling was done intermittently for a total of 150 min during the 24 hr.

All muscles were processed (at 85-90°C) to an internal temperature of 72° in a smokehouse with natural wood smoke. The muscles were chilled for 12 hr following removal from the smokehouse.

Frozen sections of muscle were prepared and stained with hematoxylin and eosin or with picro ponceau S. Sections were examined with a Zeiss microscope using interference optics. Color characteristics of the cut surface of the products were determined spectrophotometrically, and a visual assessment of the surface of the uncut whole muscle was made.

Results and Discussion

The microstructure of the control and treated samples is illustrated in Figures 1 and 2 respectively. The control muscle appears essentially normal. The interfiber spaces are apparently empty, and the fibers show cross

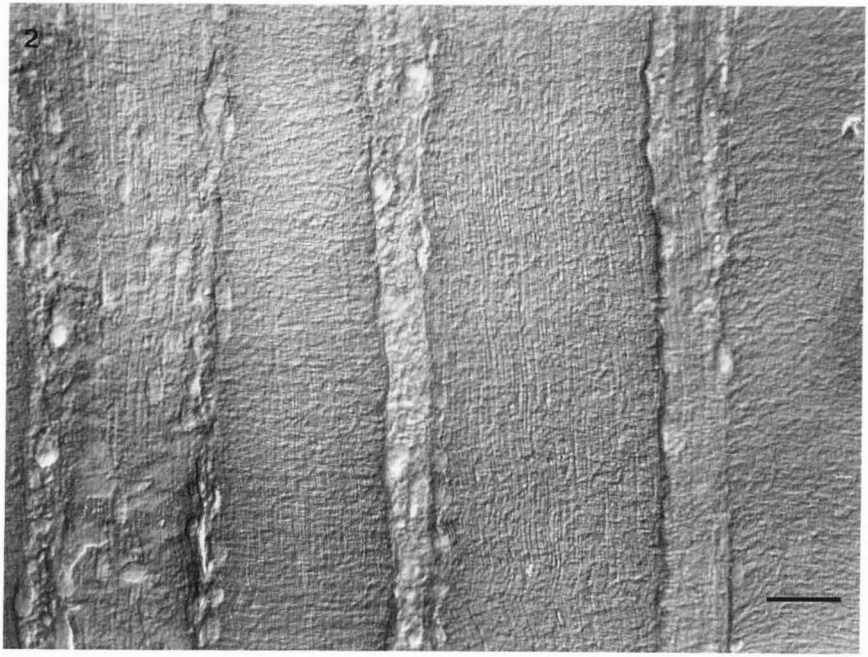

Figure 2: Microstructure of treated muscle showing swollen fibers, loss of striation and filling of intrafiber spaces. Scale bar is 25μm.

striations except in a few focal areas. On the other hand, the microstructure of the treated muscle is quite different. The fibers appear swollen and the cross striations are, for the most part, absent. In addition, the interfiber spaces appear to be filled with a substance which we concluded is extracted and coagulated protein.

It is apparent from the micrographs that the multi-needle injection and mechanical agitation of tumbling resulted in good distribution of brine in the treated samples. Further, the brine components (sodium chloride and polyphosphates) were then able to exert their extractive capabilities with the result that the structure of the muscle was partially disintegrated and the proteins brought into solution were able to move about within the framework of the remaining muscle. As a result of heating, the proteins were coagulated in the interfiber spaces.

In addition, the extracted proteins also found their way to the surface of the whole muscle. The structure of the coagulated protein at the surface resembles that of an emulsion. Objective measurement of the cut surface (Table 1) revealed that the treated samples had a more pronounced red color while the controls were less intense red and were lighter in appearance. Visually, the treated whole muscle had a darker red color. The coagulated protein layer on the surface obviously affects the color appearance.

Table 1. Effect of tumbling on color appearance and cooking loss.

	Treated	Control
Calculated "a" value[1]	19.4	15.4
Cooking yield in %	79.4	72.3

[1] Higher "a" value indicates redder color.

The color difference observed may also be influenced, in part, by the observation that the intracellular spaces in the treated samples are filled with coagulated protein, and, in all likelihood, there is less free water present. The surface layer of coagulated protein may also play a role in shelf life stability of the treated samples.

The complex action of sodium chloride, polyphosphates and mechanical action resulted in the structural changes discussed above and affected cooking yield (Table 1). The higher cooking yield of the treated samples is due to the swollen fibers and the extracted protein which is more or less dispersed throughout the structure of the muscle. This, together with the surface layer of coagulated protein function to hold the water within the muscle during cooking.

Offer and Trinick (1983) concluded that changes in the volume of myofibrils affected meat color and cooking yields. Schmidt (1984) pointed out that swollen meat tissue has an enhanced ability to retain fat and water during heat processing. Lewis et al. (1986) concluded that increased yields are generally associated with increased dispersion of myofibrillar proteins.

In our case, the more efficient injection of the improved brine coupled with mechanical agitation resulted in a product with more attractive color and less cooking loss. The procedure is used now in commercial production.

Acknowledgements

The work reported here formed a portion of the Doctorate of Science thesis of P. D. Velinov entitled "Morphological Studies of Meat Products: The Effects of Proteases and Physical Treatment on Improving Processing Procedures and Quality Control". This process is a portion of innovation number 39326 of The INRA of Bulgaria. Appreciation is expressed to E. Atanasova for technical assistance.

References Cited

Borchert LL, Greaser ML, Bard JC, Cassens RG, Briskey EJ (1967) Electron microscopy of a meat emulsion. J. Food Sci. 32:419-421.

Cassens RG, Schmidt R (1979) Texture and lipid phase morphology of some processed meats. J. Food Sci. 44:1256-1257.

Hansen LJ (1960) Emulsion formation in finely comminuted sausage. J. Food Technol. 14:565-569.

Hermansson AM (1987) Meat raw materials in comminuted meat products. 33rd Intl. Cong. Meat Sci. and Tech. Helsinki, Finland. Vol. 2, 290-293.

Lewis DF, Groves, KHM, Holgate JH (1986) Action of polyphosphates in meat products. Food Microstructure. 5:53-62.

Offer G, Trinick J (1983) On the mechanism of water holding in meat: the swelling and shrinking of myofibrils. Meat Sci. 8:245-281.

Schmidt GR (1984) Processing effects on meat product microstructure. Food Microstructure. 3:33-39.

Theno DM, Siegel DG, Schmidt GR (1978a) Meat massaging: effects of salt and phosphate on the microstructural composition of the muscle exudate. J. Food Sci. 43:483-487.

Theno DM, Siegel DG, Schmidt GR (1978b) Meat massaging: effects of salt and phosphate on the microstructure of binding junctions in sectioned and formed hams. J. Food Sci. 43:493-498.

Discussion with Reviewers

S. H. Cohen: What is meant by a complete, complex line?
Authors: In this system, the injection and tumbling steps are combined. The tumbling apparatus contains injection needles and as the meat pieces are tumbled the needles pierce into the meat and achieve a better distribution of brine.

S. H. Cohen: Could the authors explain what the cross striations are?
Authors: The cross striations we refer to are the alternating dark and light bands, known respectively as A and I bands, in skeletal muscle as viewed in longitudinal section.

S. H. Cohen: How might the surface layer of coagulated protein affect shelf life stability?
Authors: We believe the surface covering or membrane may present a physical barrier to bacterial invasion and spoilage, and it may also retard oxidative changes.

A. M. Hermansson: It appears from the figures that the sample may have cracked during preparation. What were the conditions for freezing and sectioning?
Authors: The samples were frozen in isopentane precooled in liquid nitrogen and then sectioned at -20° C in a cryostat.

A. M. Hermansson: How do the authors know that the intrafiber spaces are filled with extracted and coagulated protein? This material may as well consist of partly melted collagen. How have myofibrillar proteins been differentiated from collagen/gelatin?
Authors: We concluded the intrafiber spaces in the treated muscle were filled with protein because of the staining density in the micrograph compared to the apparent absence of staining in the intrafiber spaces of the control muscle. We do not have any information about the exact composition of the proteins in question.

A. M. Hermansson: It is not apparent from one micrograph showing part of three fibres that there is a good distribution of brine in the heat treated sample.
Authors: Many more micrographs supporting our contention are shown in the thesis of Velinov.

A. M Hermansson: What were the criteria for the resemblence of the surface structure to that of an emulsion? A micrograph is needed to show details of this structure.
Authors: The concept of using proteins, extracted by mechanical working of meat in the presence of a brine, as a binding agent in

restructured products is well known, and the references we cited by Theno et al provide structural details. Again, the thesis by Velinov provides detail found by employing light, polarized light, interference and transmission electron microscopy.

G. W. Offer: The treated muscles differed from the controls, not only in the way the brine was introduced into the meat and in being tumbled, but in the chemical composition of the brines used. The brine used with the injected and tumbled samples contained polyphosphate, that used for the control muscles did not. We have shown (Voyle, C. A., Jolley, P. D., Offer, G. W. 1984. Food Microstructure 3, 113-126) that in the presence of polyphosphate the A-bands of muscles treated with brine are disrupted even in the absence of mechanical agitation. It is well known that polyphosphates enhance the solubilisation of myosin and reduce cooking losses, probably by forming a myosin gel which traps water (see Offer, G. & Knight, P. In : Developments in Meat Science-4 (Lawrie, R. ed.) Elsevier Applied Science pp 63-71). Is it not possible that the difference in appearance between the injected and tumbled samples and the control samples was largely due to differences in their chemical treatment rather than to differences in their mechanical treatment?
Authors: The basis for our work was to compare two different technologies under actual commercial manufacturing conditions. We used structural studies as one means to determine quality of the products produced. In Bulgaria, we need such information for improving old technologies and creating new and better products. So, our work was not conducted in a laboratory or using a model system but rather in a plant where we compared an older procedure with one combining new and advanced technologies. It is quite apparent that the information now available (ie effect of polyphosphates and mechanical agitation) does indeed give vast improvement in the resulting products.

H. J. Swatland: What apparatus was used for reflectance spectrophotometry and how were the "a values" calculated?
Authors: These studies were carried out with a Beckman DK2 with reflectance curves collected within the wave length range 550 to 750 nm. The color determination was conducted with the Y-axis selected method (BDS 10537-72) for 10 wave lengths within the range of the indicated scope. For calculations, we used the color difference formulas CIELAB as recommended by the International Lighting Committee.

FOOD STRUCTURE, Vol. 9 (1990), pp. 97-104
Scanning Microscopy International, Chicago (AMF O'Hare), IL 60666 USA

1046-705X/90$3.00+.00

MICROSCOPIC MEASUREMENT OF APPLE BRUISE

N.-K. Kim and Y.-C. Hung*

Department of Food Science and Technology
University of Georgia Experiment Station
Griffin, GA 30223

Abstract

Microstructural differences between unbruised and bruised apple tissues were evaluated. Cell connections appeared to be looser in bruised tissue than in unbruised tissue. Bruised tissue exhibited more empty regions which are not occupied by cells than unbruised tissue. Empty regions in unbruised and bruised tissues were about 0.7 and 2.4 per mm^2, respectively, comprising 0.7% and 2.7% of the respective total volume. Stereology is a body of mathematical methods relating three-dimensional parameters defining a structure to two-dimensional measurements. Two methods based on a stereological principle were also used to quantify the fraction of total volume occupied by cells. In unbruised tissue, about 99.5% of the volume was occupied by cells compared to only 97.4% in bruised tissue. Both methods successfully quantified microstructural differences between unbruised and bruised apple tissues.

Initial paper received November 6, 1989
Manuscript received June 4, 1990
Direct inquiries to Y.-C. Hung
Telephone number: 404 228 7284

Key Words: Apple cellular structure, bruised apple tissue, scanning electron microscopy, image analysis, empty region, volume ratio, pendulum impactor, bruise volume.

*Address for correspondence:
Y.-C. Hung
Department of Food Science and Technology
University of Georgia Experiment Station
Griffin, GA 30223 Phone No. (404) 228-7284

Introduction

Bruising is the damage to plant tissue by external forces which results in physical changes in texture and/or eventual chemical alteration of color and flavor (Mohsenin, 1978; O'Brien et al., 1984). An external force applied to plant tissue initiates bruising which is manifested by a combination of chemical and physical changes (O'Brien et al., 1984).

Goff and Twede (1979) observed that most physical damage to fruits in the retail chain occurred during distribution, which made it difficult to find an unbruised apple in a supermarket. They observed that the incidence of bruising in the retail chain from tree to consumer for 'McIntosh' apples in 3 lb bags ranged from 80 to 100 bruises per bag.

The high incidence of bruise damage in packaged apples and pears was also reported by Schoorl and Williams (1972, 1973). They showed that 10-15% and 15-24% of apples were bruised in tray packs and in patterned pack cases, respectively, after a journey of 1600 kilometers and six handling operations.

The most common method to measure bruises on apples, pears and peaches is to measure the diameter, depth, weight or volume of browned tissue (Dedolph and Austin, 1962; Schoorl and Holt, 1974; Mohsenin, 1978; Holt and Schoorl, 1977; Holt et al., 1981; Klein, 1987). The browning reaction in bruised tissue (O'Brien et al., 1984) is an indirect index of mechanical damage. However, direct measurement of bruise size is very subjective due to the difficulty of locating the bruise boundary. There is an intermediate zone where the color changes from white to brown are not clear. A more precise method to evaluate bruise damage is needed.

Electron microscopic techniques have been applied extensively to imaging of animal and plant tissues (Davis et al., 1976a, b; Carroll and Jones, 1979; Chabot, 1979; Davis and Gordon, 1977, 1978, 1980, 1982; Buchheim, 1981, 1982). Many studies with fruits were reported using scanning electron microscopy (SEM) (Gough and Shutak, 1972; Jewell, 1979; Bomben and King, 1982; Glenn et al., 1985; Trakoontivakorn et al., 1988).

Apple tissue bruised by impact became brown and corky during storage not only because of

mechanical damage to cells, but also as a result of enzymatic reactions of polyphenolases and substrates released from ruptured cells (O'Brien et al., 1984). Quantitative differentiation of microstructures between unbruised and bruised apple tissues may be used to follow the progress in the development of the bruise and also can be used to determine the boundary between bruised and unbruised tissues.

'Image analysis' is a numerical method for quantitatively describing geometric or densitometric features of an image (Bradbury, 1979). This method may be applied directly on a specimen or photomicrographs (Underwood, 1969; Bradbury, 1979; Dziezak, 1988). Stereology is a body of mathematical methods relating three-dimensional parameters defining a structure to two-dimensional measurements obtainable on sections of the structure (Weibel, 1980). The method is based on the principle that on a selected phase of a random section through a microstructure, equality exists among volume, area, linear and point ratios (Underwood, 1969).

The objective of this study was to establish an objective method to quantify microstructural differences between unbruised and bruised apple tissues through image analysis.

Materials and Methods

Test Materials

'Rome Beauty' apples were manually harvested from the Northeast Branch of Georgia Experiment Station of the University of Georgia at Blairsville, Georgia on September 29, 1987. They were packed using a shrink wrap machine (Model T14-8, Bestronic, Beseler Corp., Florham Park, NJ) in a gas permeable plastic film (Plastic wrap, D955, CRYOVAC, Simpsonville, SC) and stored at 4°C until evaluated.

Bruise Damage

Five apples were used for this study. Before impact testing, apples were taken from the cooler and unwrapped. Unwrapped apples were impacted at room temperature with a pendulum impactor (Prussia et al., 1987). The apparatus consisted of a 90 mm diameter wooden sphere (135 g) attached to a cord so that the center of the sphere was 1.0 m from the pivot point. The wooden sphere was released from a 45° angle which impacted the apple held at the bottom of the pendulum's swing.

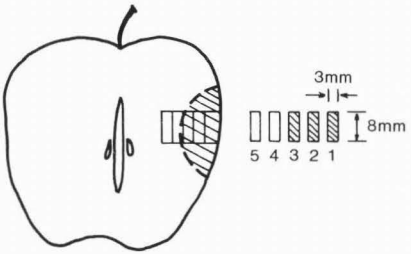

Fig. 1 Excision of specimen from the bruised apple, where shaded area represents a bruise, numbers 1 through 5 represent section 1 to 5.

Calculations of Absorbed Energy and Bruise Volume

The amount of energy absorbed by the apples during impact was calculated as the difference between total impact and rebound energy (Prussia et al., 1987).

$$E_a = m\ g\ (h_1 - h_2) \qquad (1)$$

where E_a = energy absorbed (J); m = mass of the wooden sphere (kg); g = gravitational constant, 9.8 m/s^2; h_1 = drop height (m); h_2 = rebound height (m).

After impact, bruises on apples were allowed to develop at room temperature for 24 h. Bruised apples were cut along the stem-calyx axis from the center of the impact point. The radius of apples and the diameter and depth of the browned tissue on the cut surface were measured. Bruise volume was calculated based on the formula described by Holt and Schoorl (1977).

Five sections from each apple in the shape of rectangular bars (3 x 3 x 8 mm) were taken starting from the skin and proceeding to the core through the center of the bruised area (Fig. 1). The sections were assigned numbers 1 through 5 from the skin toward core. Sections 1, 2 and 3 were excised from the brown bruised tissue whereas sections 4 and 5 were excised from the unbruised area (Fig. 1).

Sample Preparation for SEM

The excised sections were fixed for 2 h in 2 % glutaraldehyde/0.1 M phosphate buffer (pH 7.2) at 0°C. Fixed sections were washed with 0.1 M phosphate buffer (pH 7.2) for at least 30 min at 0°C and post-fixed in 1% phosphate buffered osmium tetroxide solution for 1 h at 0°C. After another washing step with phosphate buffer, tissues were immediately dehydrated with a series of ethanol concentrations and time as follows: 40% (5 min), 50% (5 min), 60% (5 min), 70% (15 min), 80% (10 min), 90% (15 min), and 100% three times for 10 min each.

The fixed and dehydrated sections were frozen and fractured based on the method described in Humphreys et al. (1974). Fractured specimens were dried using a critical-point drier (Samdri-780A, Tousimis Research Corporation, Rockville, MD), and mounted on aluminum stubs with silver paste. Mounted specimens were coated with gold/palladium by a Hummer X Sputter Coater (ANATECH Lim., 5510 Vine St., Alexandria, VA) to a thickness of 40 to 60 nm and stored in a dessicator until examined.

A Scanning Electron Microscope (Model 505, Philips Electronic Instruments, Inc., Mahwah, NJ) with a secondary electron detector operated at an accelerating voltage range between 15 and 20 KeV was employed to examine apple specimens. Specimens were tilted and rotated to obtain uniform scanning and brightness over the viewed specimen surface. Photographs were taken at magnifications to allow viewing a whole specimen under the SEM.

Image Analysis

A 20.3 by 25.4 cm print (8 by 10 inch) was developed from the Polaroid (665 P/N Instant Pack Film, ISO 80/20°, Polaroid Corp., Cambridge, MA) negative. Kodak polycontrast RC 11 F print paper was used to reduce the contrast between the bright cell wall area and the dark intracellular area.

Empty regions were defined as regions not occupied or covered by apple cells. They were marked by scratching the areas on the photomicrographs with a sharp needle. The area of each marked region was measured with a digitizer (Hitachi Tablet Digitizer, Model HDG-1111B, Hitachi Seiko, Ltd, Japan) connected to a microcomputer (Zenith-200) using a program written in BASIC.

The total number of empty regions (TN) on photomicrographs of each specimen and surface area of the specimen viewed under the SEM were evaluated. Since the viewed surface area varied among specimens, TN was divided by the specimen area and expressed as the number of empty regions per unit area (NPA). Total area of empty regions (TA) was also measured from the photomicrographs and expressed as the total area of empty regions per unit area of specimen (APA).

The volume ratio has been defined as the ratio between volume occupied by cells and total volume and is directly equal to either area or length ratio (Underwood, 1969). For the area or length ratio measurements, test circle was super-imposed at random on the photomicrographs (Fig. 2). Three sizes of circles (diameters of 5.1, 6.4 and 7.6 cm) were tested for consistency in volume ratio measurements.

VRL, the volume ratio from linear fraction measurements was calculated as follows:

$$VRL = \frac{\sum \ell_i}{L} \times 100$$

where $\sum \ell_i$ is the total distance across intersected cells and L is the total length on the test line.

VRL was measured from at least ten different locations by randomly super-imposing test circles on the photomicrographs. Consistency of VRL measurements was evaluated by calculating the coefficient of variation (CV) from each size of test circle (SAS, 1985).

The volume ratio is also directly equal to the area ratio (Underwood, 1969). Volume ratio from area fraction (VRA) was calculated from the portion of the area occupied or covered by cells over the total area inside the test line (Fig. 2).

$$VRA = 100 - \frac{\sum a_i}{A} \times 100$$

where, A is the total area inside the test line and $\sum a_i$ is the area inside the test line which was not occupied by the apple cell. Ten VRA measurements were also obtained from each photomicrograph as described in VRL measurements.

Statistical analysis was performed using ANOVA procedures (SAS, 1985). The effects of apple and section on measured parameters were also analyzed.

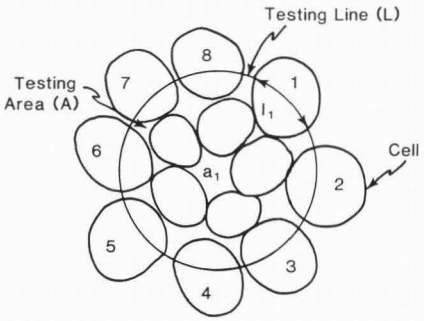

Fig. 2 Sketch drawing of a test circle, super-imposed on the apple cells.

Results and Discussion

Measurement of Bruise

Apple diameters and absorbed energies at impact are presented in Table 1. Apple A had a particularly large diameter compared with the other four apples. Apples A and B had slightly higher absorbed energy than the other three apples which was due to the lower angle of rebound during impact. This phenomenon may be due to different textural properties of apples.

Diameter and depth of bruised areas and the calculated bruise volumes for five apples are presented in Table 1. Apple A had particularly large bruise diameter and volume which may be due to the larger contact surface with the wooden sphere. The larger the apple diameter, the greater the contact surface during impact resulting in a larger bruise diameter. Bruise

Table 1. Apple diameter, absorbed impact energy and Bruise measurements of 'Rome Beauty' apples.

			BRUISE MEASUREMENT		
APPLE	APPLE DIAMETER (mm)	ABSORBED ENERGY (J)	DIAMETER (mm)	DEPTH (mm)	VOLUME (cm^3)
A	84.0	0.37	27	9	3.6
B	72.0	0.38	22	8	2.1
C	68.9	0.36	21	8	1.9
D	69.6	0.36	20	9	2.0
E	67.8	0.36	20	8	1.8

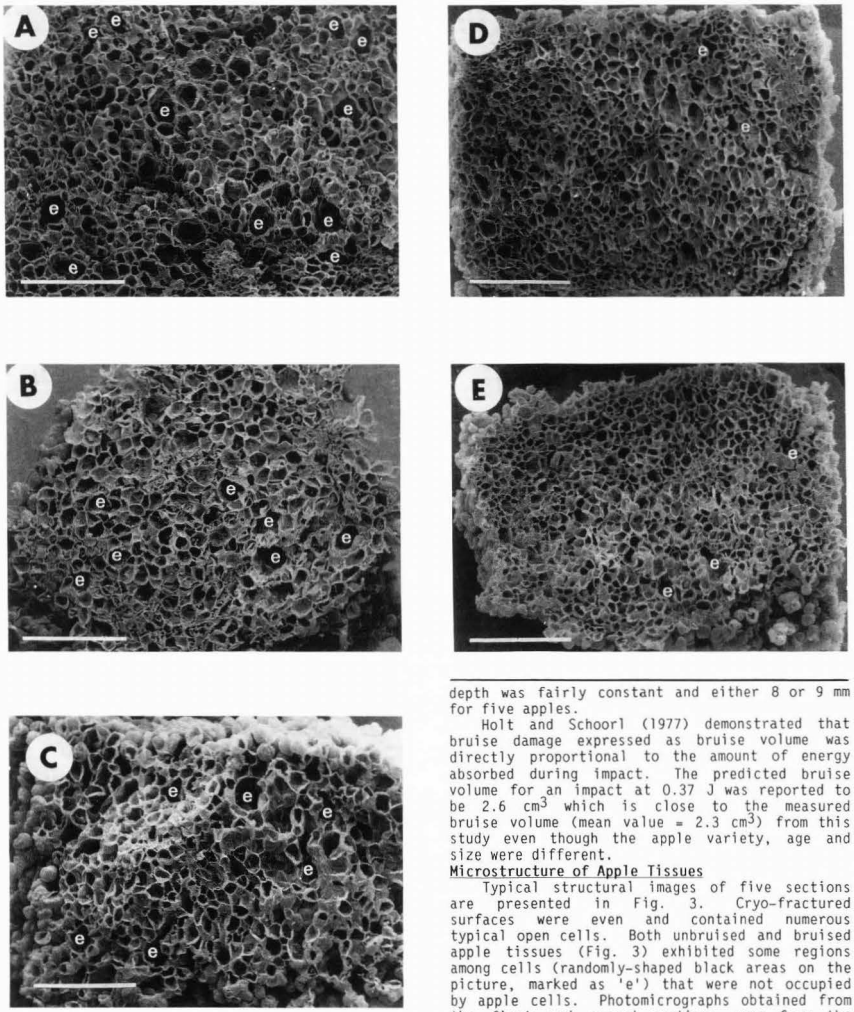

Fig. 3 Microstructure of apple tissue (A) section 1; (B) section 2; (C) section 3; (D) section 4; (E) section 5. Bar = 1mm. "e" illustrates empty region.

depth was fairly constant and either 8 or 9 mm for five apples.

Holt and Schoorl (1977) demonstrated that bruise damage expressed as bruise volume was directly proportional to the amount of energy absorbed during impact. The predicted bruise volume for an impact at 0.37 J was reported to be 2.6 cm^3 which is close to the measured bruise volume (mean value = 2.3 cm^3) from this study even though the apple variety, age and size were different.

Microstructure of Apple Tissues

Typical structural images of five sections are presented in Fig. 3. Cryo-fractured surfaces were even and contained numerous typical open cells. Both unbruised and bruised apple tissues (Fig. 3) exhibited some regions among cells (randomly-shaped black areas on the picture, marked as 'e') that were not occupied by apple cells. Photomicrographs obtained from the first and second sections were from the bruised tissue and contained numerous large empty regions among loosely connected cells which exhibited larger extracellular spaces (Figs. 3A and 3B). The third section (Fig. 3C) was taken from the brown tissue adjacent to the uncolored tissue and had similar numbers of

empty regions as with the first and second sections, but the orderly cell structure remained unaffected. Figs. 3D and 3E were taken from the unbruised tissue and exhibited fewer empty regions and less extracellular spaces than photomicrographs taken from the bruised tissue (Figs. 3A, 3B and 3C). Bruised apple tissue appeared to lose compactness when compared with unbruised apple tissue (Fig. 3).

Number and Area of Empty Regions

The number and area of empty regions measured from the photomicrographs of five sections are presented in Table 2. Sections 1, 2, and 3 had 19.7, 18.0, and 14.9 empty regions, respectively; whereas sections 4 and 5 had only 6.3 and 3.7 empty regions, respectively. This indicated that sections 1, 2 and 3 had more damage than sections 4 and 5.

The total number of empty regions per unit area viewed (NPA) results for each section are presented in Table 2. Sections 1, 2 and 3 obtained from bruised apple tissue had NPA values of 2.41, 2.55 and 2.00 per mm^2, respectively. Sections 4 and 5 obtained from unbruised apple tissue had NPA values of 0.91 and 0.45 per mm^2, respectively. Statistical analysis indicated that section 5 exhibited the least NPA among the sections and section 4 exhibited smaller NPA value than sections 1, 2 and 3 (Table 2).

The total areas of empty regions (TA) are presented in Table 2. Bruised tissue exhibited larger TAs than unbruised tissue. Sections 1, 2 and 3 had TA values of 0.24, 0.21, and 0.18 mm^2, respectively; whereas sections 4 and 5 had TA values of 0.06 and 0.05 mm^2, respectively. This implies that bruised apple tissue had more areas occupied by empty regions than unbruised tissue.

To account for the variation in the specimen area in view, the percentage of empty area per unit specimen area (APA) was calculated. The greater APA value measured correlated with greater damage in the specimen. Sections 1, 2 and 3 from bruised apple tissue had 2.87, 3.00 and 2.36% of the area occupied by the empty regions, respectively. Section 4 had 0.82% and section 5 had 0.56% of the area occupied by the empty regions. The difference in APA results obtained from bruised and unbruised tissues were significant ($P < 0.05$). However, the difference of APA values within bruised or unbruised tissues was not significant.

Either NPA or APA were found to be useful as an index to distinguish the bruised apple tissues from the unbruised tissues. However, NPA measurement consumed less time than the APA measurement.

Size Selection of Test Circle

Three different sizes of circles were employed to calculate the volume ratio from linear fraction (VRL). Coefficient of variation (CV) is a measurement often used in describing the amount of variation in a population (SAS, 1985). The CV of the VRL for three circles are presented in Table 3. VRL results measured by using a circle with 5.1 cm diameter had the greatest CV whereas VRL results measured by using a circle with 7.6 cm diameter had the smallest CV (Table 3). This implies that the variation among repeated VRL measurements using a 7.6 cm diameter circle was the lowest. Because of the low CV, the 7.6 cm diameter circle was selected for further image analysis on photomicrographs.

Table 2. Number and area of empty regions, measured from different sections.*

SECTION	TOTAL NUMBER (#)	TOTAL NUMBER PER UNIT AREA VIEWED (#/mm^2)	TOTAL AREA (mm^2)	TOTAL AREA PER UNIT AREA VIEWED (%)
1ST	19.7^a	2.41^{ab}	0.24^a	2.87^a
2ND	18.0^a	2.55^a	0.21^{ab}	3.00^a
3RD	14.9^b	2.00^b	0.18^b	2.36^a
4TH	6.3^c	0.91^c	0.06^c	0.82^b
5TH	3.7^c	0.45^d	0.05^c	0.56^b

*Mean values of five apples, values in the same column not followed by the same letter are significantly different ($P < 0.05$).

Table 3. Coefficient of variation of volume ratio measured from linear fraction using three sizes of circles.

	COEFFICIENT OF VARIATION (%)		
	CIRCLE DIAMETER		
SECTION	5.1 cm	6.4 cm	7.6 cm
1ST	19.46	5.45	2.60
2ND	17.34	6.45	2.62
3RD	20.21	5.57	2.73
4TH	16.92	4.47	1.09
5TH	18.68	3.56	1.58

For three sizes of circles, VRL results measured from sections 4 and 5 always had lower CV values than those obtained from sections 1, 2 and 3. This implies that the VRL results measured from unbruised apple tissues (fourth and fifth sections) were more consistent than from bruised tissues (first, second and third sections).

Volume Ratio from Linear (VRL) and Area Fraction (VRA)

VRL results from five apples measured by using a 7.6 cm diameter were ranged from 98.07 to 99.08% and exhibited no statistical difference ($P > 0.05$) among apples. The VRA results ranged from 97.67 to 98.36% and also exhibited no statistical difference ($P > 0.05$)

among apples. This demonstrated that VRL and VRA results obtained from different apples were consistent.

VRL results from different sections are presented in Table 4. Sections 1, 2 and 3 had mean VRL values of 97.88, 97.92 and 97.61% whereas sections 4 and 5 had 99.66 and 99.62%, respectively. Bruised tissue exhibited an average of 2.2% of the total space not occupied by the apple cells, whereas sections from unbruised tissue exhibited only 0.35%. Standard deviation of VRL from different sections is also presented in Table 4. Sections obtained from the bruised tissue had larger standard deviation than sections obtained from the unbruised tissue.

Table 4. Volume Ratio by Section from Linear and Area Fraction Measurements.*

	VOLUME RATIO FROM LINEAR FRACTION (%)		VOLUME RATIO FROM AREA FRACTION (%)	
SECTION	MEAN	STANDARD DEVIATION	MEAN	STANDARD DEVIATION
1ST	97.88[a]	0.83	97.22[a]	0.91
2ND	97.92[a]	1.09	96.91[a]	1.19
3RD	97.61[a]	1.07	96.97[a]	0.99
4TH	99.66[b]	0.35	99.25[b]	0.54
5TH	99.62[b]	0.31	99.61[b]	0.18

*Mean values of five apples, values in the same column not followed by the same letter are significantly different ($P < 0.05$).

The mean VRA results and standard deviation obtained from different sections are presented in Table 4. Sections 1, 2 and 3 were obtained from bruised apple tissue and had mean VRA values of 97.22, 96.91 and 96.97%, respectively. Sections 4 and 5 were obtained from unbruised apple tissue and had mean VRA values of 99.25 and 99.61%, respectively. Sections obtained from the bruised tissue exhibited about 3% of the total space not occupied by apple cells (empty regions), whereas sections obtained from the unbruised tissue exhibited only 0.6%. Sections 4 and 5 obtained from unbruised tissue and also had lower standard deviations on VRA results than the bruised tissue (sections 1, 2 and 3).

The measured VRL and VRA differences between bruised and unbruised tissues were statistically significant. This demonstrated that the VRL and VRA measurements can be used to distinguish the microstructural difference between bruised and unbruised apple tissues.

From the visual observation of photomicrographs (Fig. 3), specimens obtained from bruised apple tissue exhibited more empty regions than from unbruised apple tissue. Image analysis data support the visual observation and provide numerical results for statistical analysis. Direct measures of empty regions (APA) (Table 2) ranged from 2.36 to 3.00% for bruised tissue and 0.56 to 0.82% for unbruised tissue. Both VRL and VRA results agreed with the APA measurements and can quantify the microstructural difference between bruised and unbruised apple tissues; however, VRA measurements required more time than the VRL measurements.

Major interferences for image analysis on photomicrographs of biological materials are structural complexity and lack of grey level discrimination (Bradbury, 1979; Bolin and Huxoll, 1987). The semi-automatic method (VRL) developed in this study consists of visual observation and computerized data collecting and processing. Structural complexity and different grey levels on photomicrographs were handled manually, but data collection and processing were handled by microcomputer. This method can effectively quantify the microstructural differences between bruised and unbruised apple tissue.

Summary and Conclusions

Apples damaged by a pendulum impactor developed the bruise volumes ranging from 1.8 to 3.6 cm^3. Structural images obtained from cryo-fractured samples revealed that some regions were not occupied by cells. The bruised tissue exhibited more empty regions than the unbruised tissue based on a visual observation. This criterion was used for image analysis of apple tissues.

There was a clear difference in NPA and APA between bruised and unbruised tissues. NPAs ranged between 2.00 and 2.55 per mm^2 for bruised tissues and between 0.45 and 0.91 per mm^2 for unbruised tissues. APAs ranged between 2.36 and 3.00% for bruised tissues and between 0.56 and 0.82% for unbruised tissues. Statistical analyses of the data showed that both NPA and APA values can be used to quantify microstructural differences between unbruised and bruised apple tissues.

Three different sizes of circles (7.6, 6.4 and 5.1 cm diameter) were used to measure the VRL. The 7.6 cm diameter circle had the smallest coefficient of variation (CV) and is recommended for the volume ratio measurement.

There were no significant differences among apples for both VRL and VRA results. This indicates that the measured VRL and VRA among apples were consistent. Both VRL and VRA measured from the unbruised tissue had significantly lower values than the unbruised tissue. By using either VRL or VRA measurements, the microstructural difference between bruised and unbruised apple tissues can be quantified and distinguished objectively. However, the VRL method required less measurement time and is recommended.

Acknowledgment

The authors would like to thank Mr. Jim Dobson and the supporting staff at the University of Georgia Mountain Branch Station for providing apples for this study, and Drs. Stanley Prussia and Romeo Toledo for their constructive comments and suggestions in the preparation of this manuscript.

References

Bolin HR, Huxsoll CC (1987) Scanning electron microscope/Image analyzer determination of dimensional postharvest changes in fruit cells. J. Food Sci. 52, 1649-1650.

Bomben JL, King CJ (1982) Heat and mass transport in the freezing of apple tissue. J. Food Technol. 17, 615-632.

Bradbury S (1979) Microscopical image analysis : problems and approaches. J. Micros. 115, 137-150.

Buchheim W (1981) A comparison of the microstructure of dried milk products by freeze-fracturing powder suspensions in non-aqueous media. Scanning Electron Microsc. 1981; III, 493-502.

Buchheim W (1982) Aspects of sample preparation for freeze-fracture/freeze-etch studies of proteins and lipids in food systems. A review. Food Microstruc. 1, 189-208.

Carroll RJ, Jones SB (1979) Some examples of scanning electron microscopy in food science. Scanning Electron Microsc. 1979; III, 253-260.

Chabot JF (1979) Preparation of food science samples for SEM. Scanning Electron Microsc. 1979; III, 279-286, 298.

Davis EA, Gordon J (1977) Morphological comparison of two varieties of carrots during growth and storage: SEM. Home Econ. Res. J. 6, 15-23.

Davis EA, Gordon J (1978) Application of low temperature microscopy to food systems. J. Microsc. 112, 205-214.

Davis EA, Gordon J (1980) Structural studies of carrots by SEM. Scanning Electron Microsc. 1980; III, 601-611.

Davis EA, Gordon J (1982) Food microstructure: An integrative approach. Food Microstruc. 1, 1-12.

Davis EA, Gordon J, Hutchinson TE (1976a) Specimen preparation of raw and cooked carrot phloem and xylem for the scanning electron microscope. Home Econ. Res. J. 4, 163-166.

Davis EA, Gordon J, Hutchinson TE (1976b) Scanning electron microscope studies on carrots: Effect of cooking on the xylem and phloem. Home Econ. Res. J. 4, 214-224.

Dedolph RR, Austin ME (1962) The Evaluation of impact bruises on apple fruit. Amer. Soc. for Hort. Sci. 80, 125-129.

Dziezak JD (1988) Microscopy and image analysis for R & D. Food Technol. 42(7), 110-124.

Glenn GM, Poovaiah BW, Rasmussen HP (1985) Pathways of calcium penetration through isolated cuticles of 'Golden Delicious' apple fruit. J. Amer. Soc. Hort. Sci. 110, 166-171.

Goff JW, Twede D (1979) Boxes, bags and cases. Performance of packages for the transportation of agricultural products. Special Report No. 14. Michigan State Univ., School of Packaging. pp. 1-49.

Gough RE. Shutak VG (1972) Fine structure of the apple cuticle and storage scald. Hortsci. 7(6), 561-562

Holt JE, Schoorl D (1977) Bruising and energy dissipation in apples. J. Text. Stud. 7, 421-432.

Holt JE, Schoorl D, Lucas D (1981) Prediction of bruising in impacted multilayered apple packs. Trans. ASAE. 24, 242-247.

Humphreys WJ, Spurlock BO, Johnson JS (1974) Critical point drying of ethanol-infiltrated, cryo-fractured biological specimens for scanning electron microscopy. Scanning Electron Microsc. 1974; I, 275-282.

Jewell GG (1979) Fruits and vegetables. Food Microscopy. Vaughan, J. G. Ed. Academic Press. pp. 1-32.

Klein JD (1987) Relationship of harvest date, storage conditions, and fruit characteristics to bruise susceptibility of apple. J. Amer. Soc. Hort. Sci. 112(1), 113-118.

Mohsenin NN (1978) Physical Properties of Plant and Animal Materials. Gordon and Breach Sci. Publishers. New York. pp. 394-396.

O'Brien M, Singh RP, Garrett RE (1984) The effect of bruising on dried fruit quality. Trans. ASAE 27, 274-277.

Prussia SE, Hung YC, Shewfelt RL, Jordan JL (1987) Latent damage in apples and peaches. American Society of Agricultural Engineers (ASAE) Paper 87-6520, ASAE, Chicago, IL.

SAS (1985) SAS User's Guide: Basics and Statistics, 1985 edition. SAS Institute Inc., Cary, NC.

Schoorl D, Holt JE (1974) Bruising and acceleration measurements in apple packs. Queensland J. Agr. Anim. Sci. 31, 83-92.

Schoorl D, Williams WT (1972) Prediction of drop-testing performance of apple packs. Queensland J. Agr. Anim. Sci. 29, 187-197.

Schoorl D, Williams WT (1973) Robustness of a model predicting drop-testing performance of fruit packs. Queensland J. Agr. Anim. Sci. 30(3), 247-253.

Trakoontirakorm G, Patterson ME, Swanson BG (1988) Scanning electron microscopy of cellular structure of Granny Smith and Red Delicious apples. Food Microstruc. 7, 205-212.

Underwood EE (1969) Stereology, on the quantitative evaluation of microstructures. J. Microsc. 89(2), 161-180.

Weibel ER (1980) Stereological Methods. Volume 2. Theoretical Foundations. Academic Press. London.

Discussion with Reviewers

B.G. Swanson: Do you have any evidence to suggest these data will apply to other apple cultivars?

Authors: No, we do not believe that degree of structural damage will be the same from one apple cultivar to another; however, we believe that the method developed in this study can be

applied to another cultivar in order to quantify microstructural damage.

B.G. Swanson: Why would you want to differentiate bruised apple tissue by SEM or Image Analysis when we can see discoloration and textural differences?
Authors: Color and texture changes are indirect indicators of bruise damage. However, microscopic observation on bruised apple tissue provides information to support the bruising mechanism that mechanical force ruptures cells to give tissue softness and releases polyphenolases responsible for browning reaction. The microscopic observation on bruised apple tissues in this study provides quantitative data for structural damage and supports the bruising mechanism.

E.A. Davis: Would the authors discuss some of the practical applications in using this technique in evaluating apple damage to the apple industry. Do you think it can implemented in some sort of quality control-decision making capacity? Do you see any reason why this same technique could not be applied to other cellular tissues with similar problems?
E. Kovacs: How can you use this method in practice?
Authors: Since SEM sample preparation and semi-automatic image analysis are time-consuming and labor-intensive, the technique developed in this study may not be directly applied to quality control purposes. This study was designed to investigate the bruising mechanism. Similar types of structural damage induced by impact in peaches and pears was reported in the literature. The method developed in this study can be adapted to other cellular tissues with similar problems.

E. Kovacs: In your opinion, which cells are more susceptible to damage? (In Fig 3A. it can be seen, that the damaged cells did not occur systematically)
Authors: Based on our observation on bruised apple tissues, cell damages occurred randomly. It was impossible to notice which cells were more susceptible to mechanical damage.

E. Kovacs: In your opinion, is bruising dependent on the variety?
Authors: Bruise susceptibility of apple depends on both variety and maturity.

R.P. Cavalieri: You report that intact cells occupy 2.4% less volume in the bruised tissue. You attribute this to the impact induced bruise. Do you see any evidence of a cell rupture pattern through the tissue from the point of impact or are the ruptured cells more randomly distributed as shown in the figures? If you do see a pattern in some specimens and not in others, can you attribute this to any identifiable difference in structure?
Authors: Cell ruptures occurred randomly without any pattern in all bruised tissues. Based on our observations, distance from the impact point did not affect the degree of structural damage on damaged tissue; in other words, microstructural damages in sections 1, 2 and 3 appeared the same. This was also demonstrated statistically in Table 4.

H.R. Bolin: The bruise, as depicted in Fig. 1, is not a static event, as shown, but is dynamic. How would you envision taking this into account in your "bruised" "not bruised" formula?
Authors: We suppose that the structural damage happens at the time of impact and ruptured cells release enzymes responsible for browning reaction. Released enzymes and substrates play a role for browning reaction. Browning reaction in apple is completed in 12 hours after impact as demonstrated in the literature (Klein, 1987). If our hypothesis is correct, dynamics of bruise is restricted only to color changes which result from enzymatic browning reaction.

FOOD STRUCTURE, Vol. 9 (1990), pp. 105-108 1046-705X/90$3.00+.00
Scanning Microscopy International, Chicago (AMF O'Hare), IL 60666 USA

A METHOD FOR THE EXAMINATION OF THE MICROSTRUCTURE OF STABILIZED PEANUT BUTTER

Clyde T. Young* and William E. Schadel

Department of Food Science
North Carolina State University
Raleigh, NC 27695-7624

Abstract

A method for light and scanning electron microscopy of damaged resting peanut seed tissue was adapted as a research tool for evaluating the microstructural features of commercially available stabilized peanut butter. This method was used in the present study to evaluate the degree of homogenization of stabilized peanut butter by examining the spatial relationship which exists among the microstructural features. Light and scanning electron microscopy of three commercially available stabilized peanut butters revealed varying degrees of homogenization of broken cell and tissue fragments, protein bodies, and starch grains within a matrix of stabilized oil.

*Paper number 12528 of the Journal Series of the North Carolina Agriculture Research Service, Raleigh, NC. The use of trade names in this publication does not imply endorsement by North Carolina Agriculture Research Service of the products named, nor criticism of similar ones not mentioned.

Initial paper received February 3, 1990
Manuscript received June 4, 1990
Direct inquiries to C.T. Young
Telephone number: 919 737 2964

Key Words: Light microscopy, scanning electron microscopy, microstructure, fixation, peanuts, peanut butter, protein, starch, oil.

Introduction

During the grinding of peanuts into butter, various liquid additives such as stabilizers may be introduced by means of metering units complete with proportioning pumps. Woodroof (1983) claims that achieving a thorough, homogenous mix during the grinding process is extremely difficult. Improper homogenization may result in an undesirable lack of uniformity which may affect the texture and consistency of the peanut butter.

Over the years, our peanut laboratory has performed a substantial number of quality evaluations on different types of commercially available peanut butters as well as other peanut products. Recently Young and Schadel (1989) developed a method for light and scanning electron microscopy of damaged resting peanut seed tissue. The purpose of the present study is to adapt this method as a research tool for evaluating the microstructural features of commercially available stabilized peanut butter. By examining the spatial relationship which exists among the microstructural features, the degree of homogenization in smooth peanut butter can be determined.

Materials and Methods

Sources of Stabilized Peanut Butter

One jar of each of the three leading commercial brands of stabilized peanut butter as purchased at a local grocery store were used. In the present study, these will be referred to as Commercial Brands #1, #2, and #3.

Fixation Method for Light and Scanning Electron Microscopy

Peanut butter samples (1 mm^3) were carefully sectioned from the contents of the three jars with razor blades. These samples were dropped directly into a Karnovsky's (1965) fixative as modified by Young and Schadel (1989). Our modified fixative, as originally devised for damaged resting peanut seed tissue and adapted for peanut butter, was prepared by mixing 25 mL of 8% formaldehyde, 3.6 mL of 70% glutaraldehyde and 28.6 mL of 0.1 M sodium phosphate buffer (hereinafter referred to as buffer). The pH of the mixture was adjusted to 7.0. The peanut butter samples were fixed under vacuum for 30 minutes at room temperature and then at atmospheric pressure for 48 hours at 4°C. Following a 24 hour wash in 6 changes of 0.1 M buffer (4°C, pH 7.0), the material was post-fixed for one hour in 1% osmium tetroxide in 0.1 M buffer (4°C, pH 7.0). After

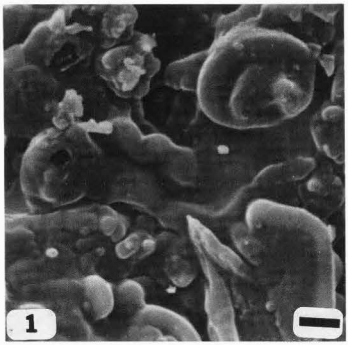

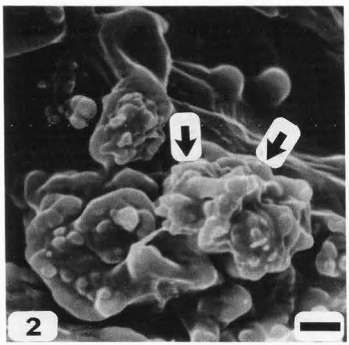

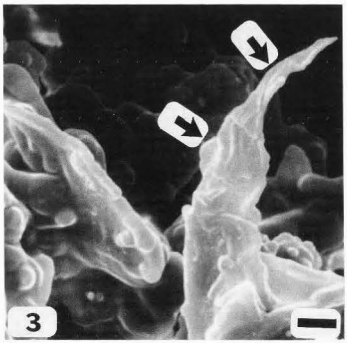

Bars = 10 micrometers on each figure.

Figures 4-6 on the color plate, facing page.

Fig. 4. Light micrographs of Commercial Brand #1: **a)** representative section of a stabilized peanut butter with a high degree of homogenization of microstructural features; and **b)** section in which broken cell wall fragments (W), protein bodies (P), and starch grains (S) are well-dispersed in a matrix of stabilized oil (O).

Fig. 5. Light micrographs of Commercial Brand #2 sample showing: **a)** incomplete homogenization of microstructural features; and **b)** cellular contents (primarily protein bodies) that remained coalesced (arrow) and incompletely dispersed.

Fig. 6. Light micrographs of Commercial Brand #3 sample revealing: **a)** incomplete homogenization of microstructural features; and **b)** comparatively large cell and tissue fragments (arrows).

post-fixation, the material was washed for 30 minutes in 0.1 M buffer (4°C ph 7.0) and dehydrated at 15 minute intervals in a graded series of aqueous ethanol (10, 25, 50, 75, and 95%) and then finally for 30 minutes in absolute ethanol producing the dehydrated samples.

Preparation for Light Microscopy

Dehydrated peanut butter samples were embedded in Spurr's resin using the methodology of Spurr (1969) for long pot-life resin. Sections, 3 micrometers in thickness, were cut using a Reichert ultramicrotome and glass knives. After mounting sections on glass slides, the sections were stained with acid fuchsin and toluidine blue using the methods of Feder and O'Brien (1968). Stained sections were photographed using a Wild light microscope fitted with a 35 mm camera.

Preparation for Scanning Electron Microscopy (SEM)

Dehydrated peanut butter samples were prepared for SEM by critical point drying in a Tousimis PVT-3B unit using liquid CO_2. Dried samples were mounted on aluminum specimen stubs using double-sided tape and silver conducting paint. Prepared stubs were coated with 30 nm gold-palladium alloy at room temperature in a Hummer V sputter coater fitted with a Technics Digital Thickness Monitor. Specimens were viewed with a Philips 505T SEM at a working distance of 15 mm and an accelerating voltage of 15 kV.

Results

Scanning Electron Microscopy (SEM)

Observations with SEM revealed differences in the degree of homogenization among the three commercially available brands of stabilized peanut butter.

Figures 1-3 (at left). Scanning electron micrographs of samples from Commercial Brands #1, #2, and #3 respectively. **Fig. 1** is representative of a stabilized peanut butter with a high degree of homogenization of microstructural features. Note the broken cell wall fragments, protein bodies, and starch grains are well dispersed in a matrix of stabilized oil.

Fig. 2 shows a sample with a variable degree of homogenization in which cellular contents remained coalesced (arrows) and incompletely dispersed.

Fig. 3 shows a sample with a variable degree of homogenization in which comparatively large cell wall fragments (arrows) protrude from the surface.

Commercial Brand #1 is representative of a stabilized peanut butter with a high degree of homogenization of microstructural features. Broken cell wall fragments were well-dispersed in a matrix of stabilized oil (Fig. 1). Commercial Brand #2 possessed a variable degree of homogenization in which cellular contents remained coalesced and incompletely dispersed (Fig. 2). Commercial Brand #3 also possessed a variable degree of homogenization in which comparatively large cell and tissue fragments were observed (Fig. 3).

Light Microscopy (LM)

Observations with LM also revealed differences in the degree of homogenization among the commercially available brands of stabilized peanut butter. Commercial Brand #1 possessed a high degree of homogenization in which broken cell wall fragments, protein bodies, and starch grains were consistently well-dispersed in a matrix of stabilized oil (Figs. 4a and 4b). Commercial Brand #2 possessed a variable degree of homogenization which ranged from high (Fig. 5a) to intermediate (Fig. 5b) in which cellular contents (primarily protein bodies) remained coalesced and incompletely dispersed. Commercial Brand #3 also possessed a variable degree of homogenization which ranged from high (Fig. 6a) to intermediate (Fig. 6b) in which comparatively large cell and tissue fragments were observed.

Discussion

The use of SEM has limited capability for evaluating the differences among stablized peanut butters. Although SEM was capable of detecting incompletely homogenized cellular contents and tissue fragments protruding from the specimens, the additional use of LM provided an excellent complement to SEM for a more thorough understanding of the spatial relationship of the microstructural features. This spatial relationship is best preserved by plastic embedding which enables thin-sectioning for LM examination without disruption of the spatial relationship. By preserving the spatial relationship, the degree of homogenization of the microstructural features of stablized peanut butter can be determined. For example, Commercial Brand #2 exhibited a coalescence of protein bodies (Figs. 2 and 5b) which indicated incomplete homogenization.

Vix et al. (1972) reported pressure as the cause of coalescence of protein bodies in partially defatted, hydraulically pressed peanuts. We believe that the observance of coalesced protein bodies in stabilized peanut butter may also be related to incomplete homogenization.

Lastly, the use of plastic embedding for LM also enables the observance of large tissue fragments that would otherwise be crushed by smearing the peanut butter on a slide for examination under the light microscope.

References

Feder N, O'Brien TP. (1968). Plant Microtechnique: some principles and new methods. Am. J. Bot. 55:123-124.

Karnovsky MJ. (1965). A formaldehyde glutaraldehyde fixative of high osmolarity for use in electron microscopy. J. Cell Biology 27:137A.

Spurr AR. (1969). A low-viscosity epoxy resin embedding medium for electron microscopy. J. Ultrastructure Res. 26:31-43.

Vix HLE, Gardner HK, Lambou MG, Rollins ML. (1972). Ultrastructure related to cottonseed and peanut processing. In "Seed Proteins" (GE Inglett, ed.), Van Nostrand Reinhold Co., NY, pp. 212-230

Woodroof JG. (1983). Peanut butter. In "Peanuts: Production Processing, Products" (JG Woodroof, ed.), Van Nostrand Reinhold Co., NY, pp. 181-227.

Young CT, Schadel WE. (1989). A method for light and scanning electron microscopy of drought induced damage of resting peanut seed tissue. Food Microstructure 8:253-256.

Discussion with Reviewers

N. Krog: Is there any correlation between your structural observations and the rheological properties, surface shine, etc. of the different peanut butter samples?

I. Heertje: Is the difference in homogenization between the three samples in some way reflected in the organoleptic properties?

Authors: Yes, our structural observations reveal differences between the three samples in which homogenization of microstructural features varies from complete to incomplete and is correlated with the smoothness character note of peanut butter during eating, and is also related to changes in rheological properties and surface shine.

I. Heertje: Is a fixation time of 1 hour in osmium tetroxide adequate for fixing the continuous oil phase? I would fear that, under those conditions, part of the oil would be lost during the washings with ethanol. Consequently the distribution of the dispersed particles may have been affected.

Authors: A fixation time of one hour in 1% osmium tetroxide is adequate for samples that are approximately 1 mm^3 in size. Since the osmium tetroxide completely blackens the oil in the samples, any potential oil loss should appear as a stream of blackened oil from the sample during the ethanol washings. Neither the removal of blackened oil nor sample size changes (i.e. shrinking) were observed during the ethanol washings.

F.O. Flint: Would 5 mm diameter cryostat sections give more reliable results than plastic embedded sections that are only 1 mm in diameter?

Authors: The sample size of 1 mm^3 is determined by the fixation requirements of the plastic embedding of peanut butter. Our experience with larger cryostat sections is that the peanut butter is smeared during cryostat sectioning and, therefore, is unsatisfactory since the method of preparation alters the sample.

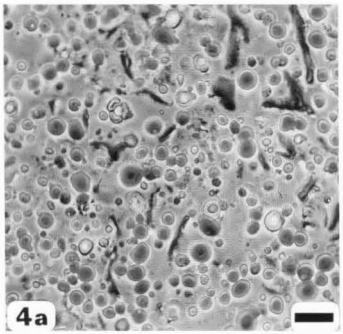

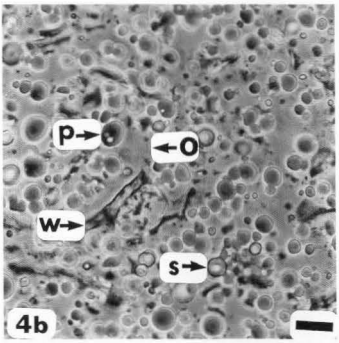

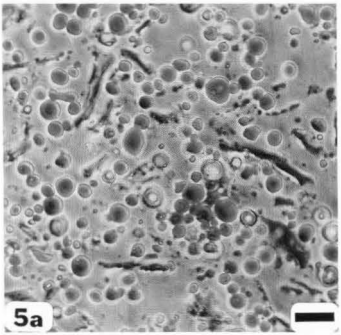

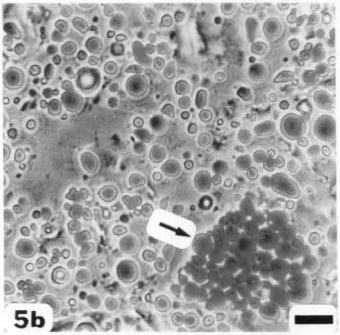

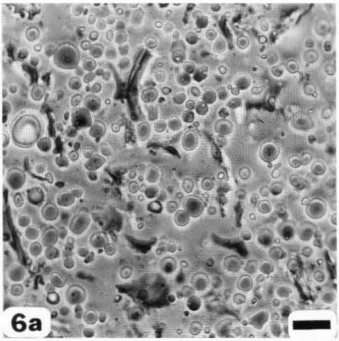

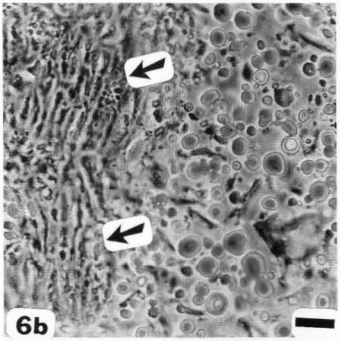

Bars = 10 micrometers on each figure.

FOOD STRUCTURE, Vol. 9 (1990), pp. 109-112 1046-705X/90$3.00+.00
Scanning Microscopy International, Chicago (AMF O'Hare), IL 60666 USA

TRANSMISSION AND SCANNING ELECTRON MICROSCOPY OF PEANUT (Arachis hypogaea L. CV. FLORIGIANT) COTYLEDON AFTER ROASTING

Clyde T. Young* and William E. Schadel

Department of Food Science
North Carolina State University
Raleigh, NC 27695-7624

Abstract

Changes in the microstructure of peanut (Arachis hypogaea L. cv. Florigiant) cotyledon after roasting at a temperature of 160°C for 16 minutes were investigated with transmission and scanning electron microscopy. Thermal modifications were documented with photomicrographs of the cytoplasmic network, protein bodies, starch grains and cell-to-cell junctions after oven roasting. These thermal modifications include disruption of the cytoplasmic network, distension of protein bodies, decreased stain affinity of starch grains, and disintegration of middle lamellae in some cell-to-cell junctions.

*Paper number 12559 of the Journal Series of the North Carolina Agriculture Research Service, Raleigh, NC. The use of trade names in this publication does not imply endorsement by North Carolina Agriculture Research Service of the products named, nor criticism of similar ones not mentioned.

Initial paper received February 18, 1990
Manuscript received June 4, 1990
Direct inquiries to C.T. Young
Telephone number: 919 737 2964

Key Words: Fixation, thermal modification, peanuts, scanning electron microscopy, transmission electron microscopy, starch, protein, staining.

Introduction

Observation of the changes in the microstructure of peanut cotyledons after oven roasting enables investigators to understand thermal modifications that occur during roasting. Young and Schadel (1990) first noted thermal modifications of oven roasted peanut cotyledons microstructure using light and scanning electron microscopy (SEM). The purpose of the present study was to use transmission electron microscopy (TEM) in conjunction with SEM to achieve a greater resolution of the thermal modifications of peanut cotyledon microstructure after oven roasting.

Materials and Methods

Fixation Methodology

Cotyledons of peanuts (Arachis hypogaea L. cv. Florigiant) were obtained from the Tidewater Research Station, Suffolk, VA. Raw peanut cotyledons with intact skins were roasted in a hot air oven at 160°C for 16 minutes. Both raw and roasted peanut cotyledons were then prepared for TEM and SEM. Tissue blocks (1 mm^3) of outer surface epidermis, mid-region parenchyma, and inner surface epidermis were cut from both the raw and roasted peanut cotyledons and fixed in a Karnovsky's (1965) fixative as modified by Young and Schadel (1989). Our modified fixative was prepared by mixing 25 mL of 8% formaldehyde, 3.6 mL of 70% glutaraldehyde and 28.6 mL of 0.1 M sodium phosphate buffer (hereinafter referred to as buffer). The pH of the mixture was adjusted to 7.0. The tissue blocks were fixed under vacuum for 30 minutes at 23°C and then fixed at atmospheric pressure for 48 hours at 4°C. Following a 24 hour wash in 6 changes of 0.1 M buffer (4°C, pH 7.0), the material was post-fixed for one hour in 1% osmium tetroxide in cold 0.1 M buffer. After post-fixation, the material was washed for 30 minutes in 0.1 M buffer (4°C pH 7.0) and dehydrated at room temperature in a graded series of aqueous ethanol (10, 25, 50, 75, and 95%) and then finally in absolute ethanol.

Preparation for TEM

Dehydrated tissue was embedded in Spurr's resin using the methodology of Spurr (1969) for long pot-life resin. Ultrathin sections cut using a Reichert ultramicrotome were stained with 4.0 % uranyl acetate for 1 hour, followed by 0.4% lead citrate for 4 minutes. Sections were examined with a JEOL 100S TEM.

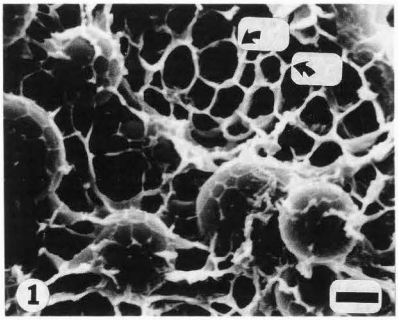

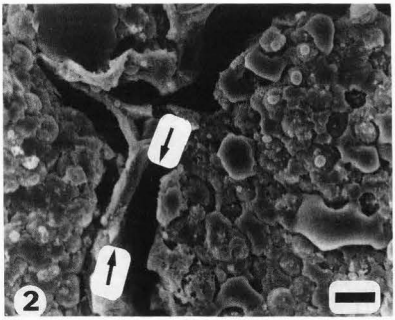

Figures 1 and 2. Scanning electron micrographs of cross-sections of parenchyma cells in the mid region of raw (Fig. 1) and oven roasted (Fig. 2) peanut cotyledons. **Fig. 1** shows the cytoplasmic network (arrows) surrounding the storage reserve bodies of protein and starch, and the spaces once occupied by lipid bodies before removal of the lipid bodies by alcohol during specimen dehydration. **Fig. 2** shows the loss of cellular organization and the absence of cytoplasm along the periphery of the cells (arrows).
Bars = 2 micrometers (Fig. 1) and 10 micrometers (Fig. 2).

Preparation for Scanning Electron Microscopy (SEM)

Dehydrated tissue was critical point dried in a Tousimis PVT-3B unit using liquid CO_2. Subsequently, the dried sections were mounted on aluminum specimen stubs with double-sided tape and silver conducting paint. Prepared stubs were coated with 30 nm gold-palladium alloy at room temperature in a Hummer V sputter coater fitted with a Technics Digital Thickness Monitor. Specimens were viewed with a Philips 505T SEM at a working distance of 15 mm and an accelerating voltage of 15 kV.

Results and Discussion

The majority of peanut cotyledonary tissue is made up of parenchymal cells. The major subcellular organelles of these parenchymal cells are lipid bodies, protien bodies and starch grains surrounded by a cytoplasmic network. With SEM, the cytoplasmic network can be observed to surround the almost spherical protein bodies, starch grains and spaces once occupied by lipid bodies before removal of the lipid bodies by alcohol dehydration during specimen preparation (Fig. 1). However, protein bodies and starch grains cannot be distinguished from one another with SEM since both of these organelles appear as indistinguishable smooth spheres. The use of SEM in observing the microstructure of parenchymal cells from oven roasted cotyledons (Fig. 2) is even more limited because oven roasting has disrupted the cytoplasmic network and distended protein bodies and starch grains. Therefore the use of TEM, in addition to SEM, is necessary to achieve a more thorough understanding of the thermal modifications of peanut cotyledonary microstructure after roasting.

When viewed with TEM, the cell-to-cell junctions are characterized by a distinct middle lamella (Fig. 3) existing between parenchymal cells of raw peanuts. After oven roasting some of these middle lamella (Fig. 4) separate as a result of thermal modifications which occur primarily within the first mm of tissue beneath the rounded outer cotyledon surface. In the raw cotyledon, the protein bodies are almost circular in outline and are surrounded by numerous lipid body membranes (Fig. 5). The electron dense protein bodies have a grainy appearance which is distinct from the smooth appearance of electron dense starch grains. After oven roasting the protein bodies are distended (Fig. 6). In the raw cotyledon, the starch grains appear compact and electron dense, and the cytoplasmic network is intact (Fig. 7). After oven roasting, the starch grains have some electron transparent regions and cytoplasmic network has been disrupted (Fig. 8). In the raw peanut cotyledon, the cytoplasmic network

Figures 3-8. Transmission electron micrographs of:
Fig. 3. A cross-section of a cell-to-cell junction of parenchymal cells in a raw peanut cotyledon. Note the distinct middle lamella (arrow).
Fig. 4. A cross-section of a cell-to-cell junction of parenchymal cells in an oven roasted peanut cotyledon. Observe that thermal modification has caused the cell walls to separate along the middle lamella (arrow).
Fig. 5. A protein body (P) surrounded by the cytoplasmic network within a raw peanut cotyledon. Note that the electron dense protein body is almost circular in outline and has a grainy appearance.
Fig. 6. A protein body (P) within an oven roasted peanut cotyledon. Note that the thermal modification has caused the protein body to become distended.
Fig. 7. A cross-section of a starch grain (ST) within a raw peanut cotyledon. Note the electron dense nature (arrow) of the starch grain and the continuous cytoplasmic network (points).
Fig. 8. A cross-section of a starch grain (ST) adjacent to disrupted cytoplasm (large arrows) within an oven roasted peanut cotyledon. Observe the electron transparent nature of some regions of the starch grains (small arrows).

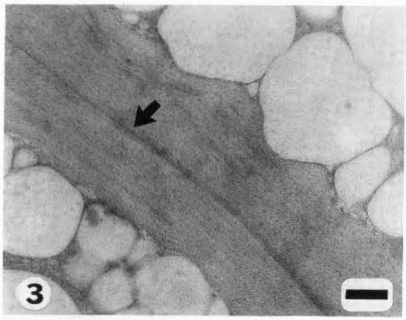

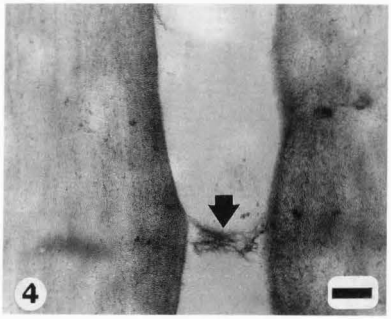

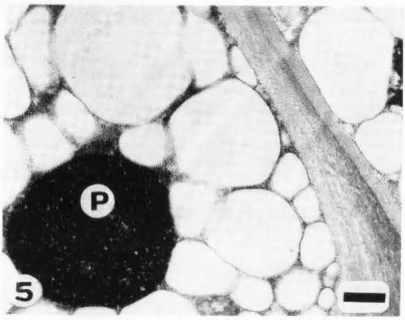

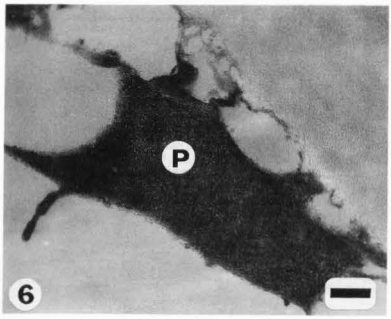

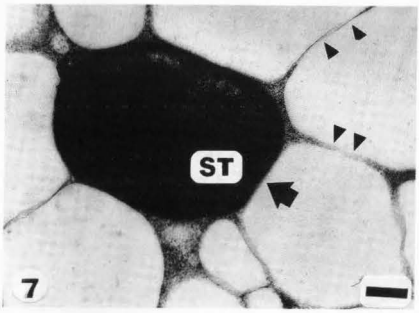

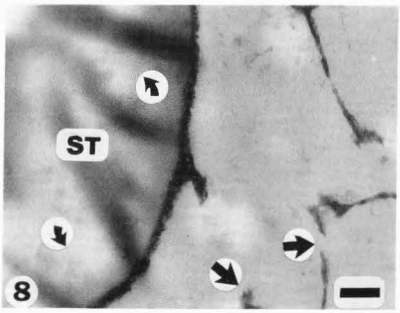

Bars = 0.5 (Figs. 3, 7 and 8), 0.25 (Figs. 4 and 6) and 0.75 (Fig. 5) micrometers.

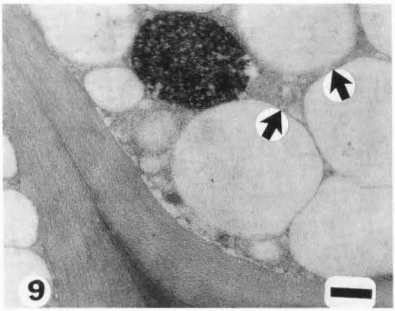

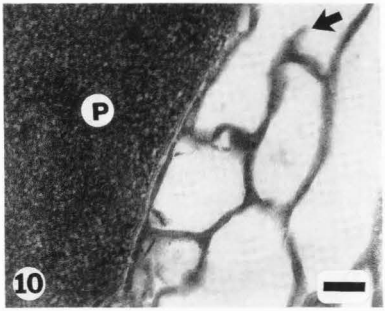

Figures 9 and 10. Transmission electron micrographs of:

Fig. 9. A cross-section of a parenchyma cell in a raw peanut cotyledon. Note that the cytoplasmic network is continuous (arrows). Bar = 0.75 micrometers.

Fig. 10. A cross-section of the disrupted cytoplasmic network (arrow) adjacent to a protein body (P) in an oven roasted peanut cotyledon. Bar = 0.75 micrometers.

surrounding the lipid body membranes (Fig. 9) is continuous. After oven roasting, the heat has disrupted the cytoplasmic network (Fig. 10).

In summary, observations with TEM, in conjunction with SEM, reveal that oven roasted peanut cotyledonary parenchymal cells possess the following characteristics as a result of thermal modification:

(1) some cell wall separations primarily within the first mm of tissue beneath the rounded outer cotyledon surface,

(2) distended protein bodies,

(3) starch grains with decreased stain affinity, and

(4) disruption of the cytoplasmic network.

References

Karnovsky MJ. (1965). A formaldehyde glutaraldehyde fixative of high osmolarity for use in electron microscopy. J. Cell Biology 27:137A-138A.

Spurr AR. (1969). A low-viscosity epoxy resin embedding medium for electron microscopy. J. Ultrastructure Res. 26:31-43.

Young CT, Schadel WE. (1989). A method for light and scanning electron microscopy of drought induced damage of resting peanut seed tissue. Food Microstructure 8:253-256.

Young CT, Schadel WE. (1990). Light and scanning electron microscopy of peanut (Arachis hypogaea L. cv. Florunner) cotyledon after roasting. Food Struct. 9:69-73.

FOOD STRUCTURE, Vol. 9 (1990), pp. 113-122
Scanning Microscopy International, Chicago (AMF O'Hare), IL 60666 USA

1046-705X/90$3.00+.00

SCANNING ELECTRON MICROSCOPY: TISSUE CHARACTERISTICS AND STARCH GRANULE VARIATIONS OF POTATOES AFTER MICROWAVE AND CONDUCTIVE HEATING

J. Huang[1], W.M. Hess[1], D.J. Weber[1], A.E. Purcell[2], and C.S. Huber[2]

[1]Department of Botany, [2]Department of Food Science and Nutrition,
Brigham Young University, Provo, UT 84602 USA

Abstract

In order to determine cytological effects of microwave heating compared to conductive heating, whole potatoes were heated in a microwave oven in plastic bags for 0.5, 1 and 2 minutes and in boiling water for 5, 10 and 20 minutes. Both heating treatments caused swelling and partial disruption of starch granules. However, as observed with scanning electron microscopy, swelling patterns of starch granules were different in potatoes using the two heating processes. In conductive heating potatoes were heated from the outside to the inside. Microwave heated potatoes were heated fairly uniformly in different regions of tubers. The weight loss of potatoes was insignificant with both heat treatments. The softening of potatoes heated in boiling water corresponded with conductive heating patterns. With both conventional heating and microwave heating potatoes were softer outside than inside, although this pattern did not correspond with heating patterns with microwave heating.

Initial paper received November 20, 1989
Manuscript received June 1, 1990
Direct inquiries to W.M. Hess
Telephone number: 801 378 2451

KEY WORDS: Scanning electron microscopy, starch granules, microwave heating, conductive heating

Address for correspondence:
W.M. Hess, Electron Optics Laboratory
129 WIDB, Brigham Young University
Provo, UT 84602 USA
Phone No. (801)378-2451

Introduction

The use of microwave energy for processing and cooking foods has increased greatly in recent years. Microwave heating offers rapid and economic methods for processing food products of high organoleptic and nutritional value. Heating that occurs as a result of microwave energy is caused by molecular vibration in foods. Therefore, microwave energy has a much greater penetration depth than the heat produced by conventional methods (Knutson et al., 1987). In food applications microwave energy penetrates to the center of the food in a relatively short time and heats the food quickly. In terms of energy cost differentials, industrial microwave food processing has become more economically attractive in recent years, as costs of gas and oil have risen and use of coal and nuclear energy sources for generating electrical power has increased (Mermelstein, 1989).

Although many acceptable food products are produced by microwave energy, less satisfactory results are obtained with some starch-based foods. The reason for this may be related to fast heating rates, difference in heat and mass transfer mechanisms, or specific interaction of the components of the food with microwave radiation (Goebel et al., 1984).

Today, potatoes provide 25% of the world's food from plants and play a major role in the diet of many people. Few studies have been conducted on the effects of microwave heating on starches of potato. Collison and Chilton (1974) found that microwave-heated samples of potato starch were damaged more rapidly than forced air convection-heated samples. They also suggested that the starch:water ratio was more important than heating rate in determining the extent of damage. Goebel et al. (1984) studied starch granule swelling over a range of water levels commonly found in starch-based food systems and developed a classification of the stages of granule swelling. They indicated that at each starch:water ratio the range of stages of swelling and matrix development was smaller in convection-heated samples than in microwave-heated samples, but the convection-heated samples

were at more advanced stages of gelatinization than the comparable microwave-heated samples.

Chen et al. (1971) studied textural changes of the potato tissue caused by heat. When the temperature of a potato is raised above 50C, starch granules start to swell and begin to gelatinize at 64-71C. This process results in cells becoming less angular and in cell separation. Sogginess of the tissue may also occur (Roberts and Proctor, 1955). Reeve (1954) reported that upon prolonged heating, the hemicellulose and cellulose components undergo some breakdown. Collins and McCarty (1969) observed that microwave energy produced comparable softening in about one-third the time required by boiling water. They also reported that a sensory panel was unable to distinguish significant differences in texture between potatoes cooked in water and by microwaves. Preliminary observations indicated that the microwave-cooked potatoes might possess a more mealy texture.

Different heating patterns with microwave heating have been reported by several researchers. Chen et al. (1971) conducted heating studies on whole white potatoes with microwave energy (1 kW at 2450 MHz) and boiling water, using white potatoes with a mean radius of 1.95 cm and a mean weight of 29 g. When temperature measurements were made after various treatment durations, a temperature gradient from core to periphery was observed with microwave heating which was opposite to the gradient for heating in boiling water. Later Ohlsson and Risman (1978) carefully studied temperature distribution in spheres and cylinders of potatoes heated with microwave energy. They found more pronounced core heating at 2450 MHz in spheres with diameters in the 2- to 6- cm range. However, earlier work by Collins and McCarty (1969), in which microwave energy was compared with boiling water, indicated a temperature gradient from the surface to the core instead of the core to the surface shown by Chen et al. (1971) and Ohlsson and Risman (1978). It is difficult to generalize across a number of studies in which heating conditions are different.

Physical properties of foods are very often correlated with their microscopic structure. The purpose of this study was to determine swelling patterns of starch granules and heating patterns of potatoes during microwave and conductive heating. Scanning electron microscopy (SEM) was used to characterize changes in potato starch granules during microwave heating and conductive heating.

Materials and Methods

Raw Potatoes

Russet potatoes were selected from a commercial supplier. Whole potatoes with uniform size, mean radius (5.8-6.1 cm) and mean weight (117-162 g), were used.

Conductive Heating Process

Whole potatoes were heated in boiling water according to the stages listed in Table 1. Temperatures at the center, side, and end regions of potatoes were measured with a DM 302 series thermocouple. Iron constantin thermocouples were inserted so that one was at the mass center of the potato, one at 2-3 mm deep at one end and another at 2-3 mm on the side. Heating experiments were replicated four times

Temperatures were recorded every minute during the heating process. After heating, samples were cooled immediately with running tap water. Tissues from the center, side, and end regions of each conductive-heated potato were chosen as representative regions of potatoes for SEM studies.

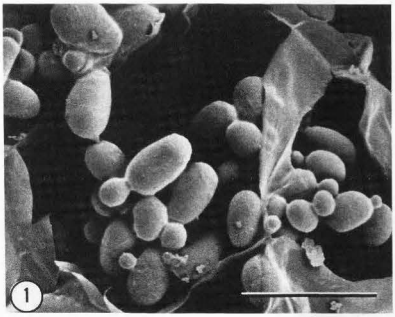

Fig. 1. Starch granules in raw potatoes. Bar = 100 μm.

Table 1. Temperature and Heating Time of Each Stage During Treatments

Stage[1]	Boiling Water		Microwave	
	Center temp. °C	Heating time minutes	Center temp. °C	Heating time minutes
1	46	5	38	0.5
2	65	10	66	1
3	90	20	80	2

[1]Stages:
1. Center of potatoes heated to temperatures which are below their starch gelatinization.
2. Center of potatoes heated to temperatures where starch gelatinizes.
3. Center of potatoes heated to temperatures which are above starch gelatinization.

Fig. 2. Center region of boiled potato sample heated to 46C. Fig. 3. Side region of boiled potato sample heated to 46C. Fig. 4. End region of boiled potato sample heated to 46C. Fig. 5. Center region of boiled potato sample heated to 65C. Fig. 6. Side region of boiled potato sample heated to 65C. Fig. 7. End region of boiled potato sample heated to 65C. Bar = 100 μm.

Potato starch granules

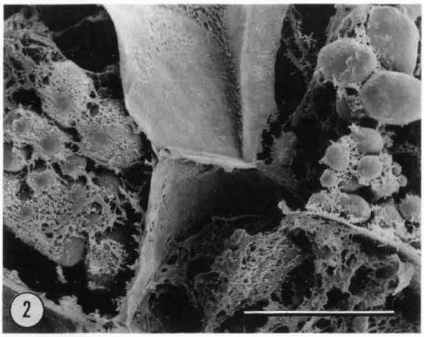

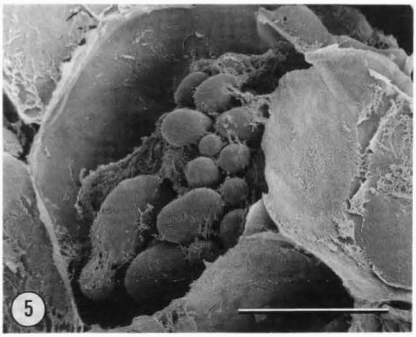

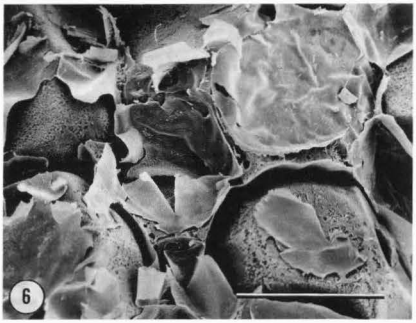

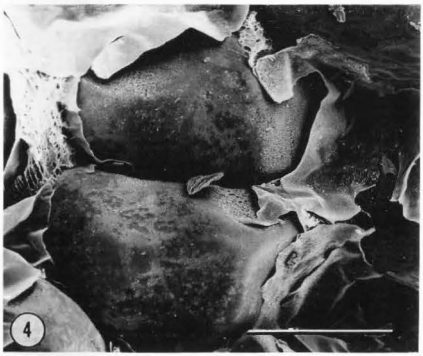

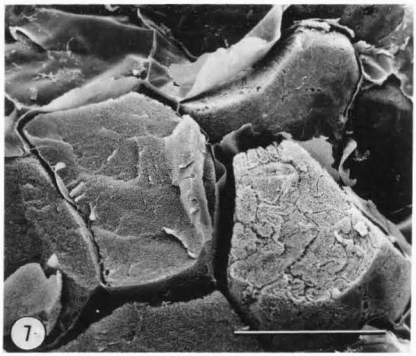

Table 2. Characteristics of Progressive Gelatinization of Boiling Potatoes

Stage	Center Region	Side Region	End Region
1	mostly individual small grains	clumped small granules	large clustered granules filled whole cell
2	small to medium clumped granules	large swollen granules	large swollen granules
3	swollen granules with reticulated structure	swollen granules with reticulated structure	swollen granules with reticulated structure

Table 3. Characteristics of Granulation of Microwave and Treated Potatoes

Stage	Center Region	Side Region	End Region
1	small individual granules	small clumped granules	small clumped granules
2	clustered large granules filled whole cell	large swollen starch granules, individual granule no longer visible	large swollen starch granules
3	large swollen starch granules	large swollen starch granules	large swollen starch granules

Sampling and Microwave Heating Process

Whole potatoes were placed in plastic bags and heated in the center of a microwave oven according to the stages listed in Table 1. The microwave oven was operated at 2450 MHz frequency. Immediately after heating, thermocouples were inserted as in conventional heated potatoes. Temperatures at the center, side, and end regions of each sample were measured at 30 second intervals until the temperatures at the center began to decrease. Samples were then quickly cooled with running tap water. Tissues from the center, side, and end regions of microwave heated potatoes were chosen as representative regions of potatoes for SEM studies. Heating experiments were replicated four times.

Preparation For SEM

After processing, samples from representative regions of potatoes, including the unheated control, were frozen in liquid freon followed by liquid nitrogen before being fractured with razor blades. Fractured samples were then freeze-dried 12-24 hours. The temperature of the condensing plate was -65C. The dry samples were mounted on aluminum stubs and a modified Polaron E5300 freeze-drier was used to gold sputter samples. The fractured surfaces of samples were examined with an JEOL 840A SEM.

Water Loss and Hardness Measurement

Potato samples were weighed before and after heat treatments so that water loss could be measured. Firmness of the heated potatoes was measured by use of a Voland-Stevens-LFRA Texture Analyzer using a 1.6 mm diameter stainless steel plunger. The plunger was positioned to penetrate to the center of potatoes at a right angle to the surface. Force (kg/cm^2) required to penetrate into the center of each potato was recorded as hardness. Travel speed of the plunger was 0.5 mm/sec.

Results

Unheated Control Samples

Starch granules in unheated potatoes were smooth and small and were not fused (Fig 1). Individual granules were distinct.

Swelling Pattern of Conventional Heated Samples

Representative regions from each stage are shown in Figures 2-10 and the characteristics of each region at every stage are summarized in Table 2. In Stage 1 (Figures 2-4) starch granules progressively clumped and were swollen at the edges of potatoes. Figures 5-7 show that at Stage 2 coalescence occurred only in outer regions of boiled samples while a considerable number of unswollen starch granules was still present in the inner region. Figures 8-10 show that for Stage 3 all the starch granules were swelled. In the center region the starch was coarsely reticulated (Fig. 8). In the side region, where temperatures were higher, the reticulation was finer (Fig. 9). In the end region, where temperatures were near boiling temperatures, the cell contents were homogenous (Fig. 10). In summary, gelatinization first occurred in end regions of stage 1, and advanced until it reached stage 3 where most of the starch appeared to be gelatinized. Separation of adjacent cell walls did not occur even after boiling the potatoes for twenty minutes in stage 3.

Fig. 8. Center region of boiled potato sample heated to 90C. Fig. 9. Side region of boiled potato sample heated to 90C. Fig. 10. End region of boiled potato sample heated to 90C. Fig. 11. Center region of microwaved potato sample heated to 38C. Fig. 12. Side region of microwaved potato sample heated to 38C. Fig. 13. End region of microwaved potato sample heated to 38C. Bar = 100 μm.

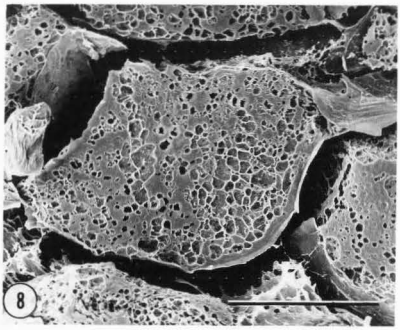
8

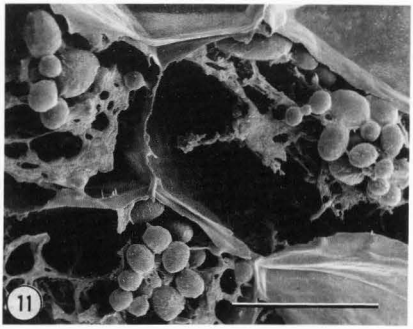
11

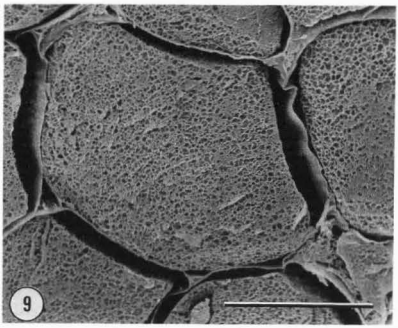
9


12

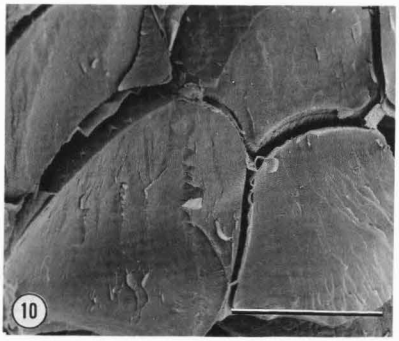
10

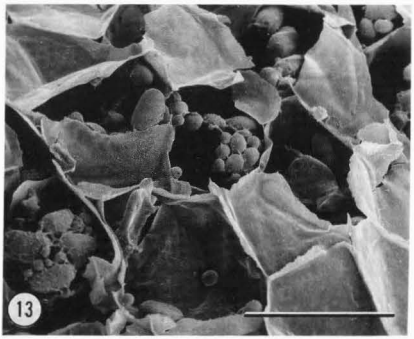
13

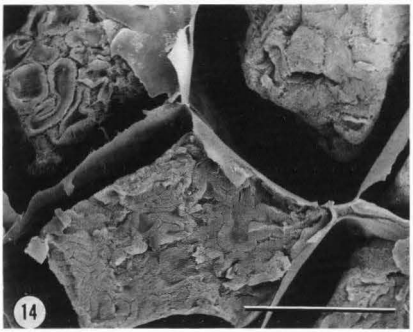
14

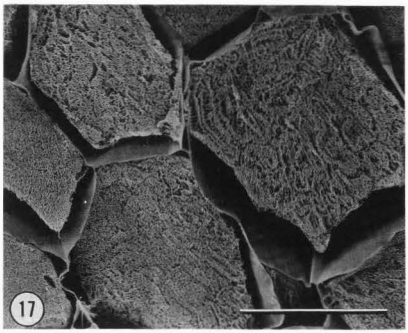
17

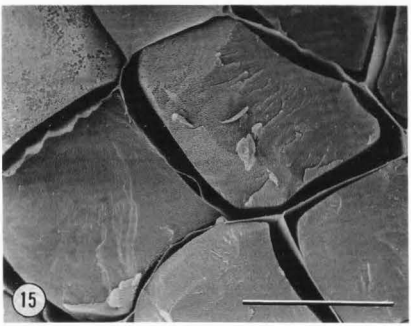
15

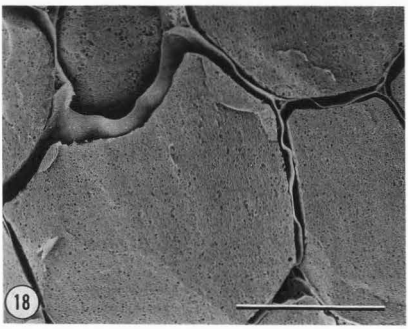
18

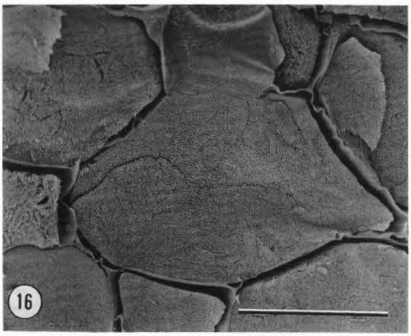
16

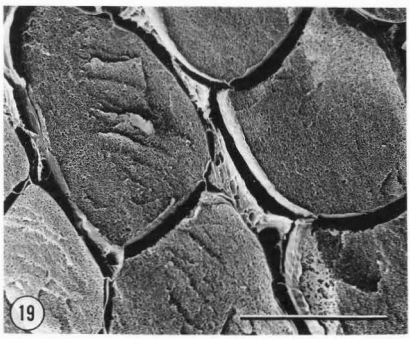
19

Table 4: Weight Losses of Treated Potatoes

Temperature (°C)	Weight (g) Before Treatment	Weight (g) After Treatment
Conventional Treated		
40	179	179
62	185	185
90	178	177
Microwave Treated		
41	192	191
62	199	192
82	200	191

Swelling Patterns of Microwave Heated Samples

Representative regions of microwave treated samples from each stage are shown in figures 11-19. The characteristics of each region at each stage are summarized in Table 3. No granulation occurred in stage 1 (Figs. 11-13). However, the small unswelled granules appeared to be different from the original unheated sample. The granules in this stage started to clump.

In stages 2 and 3 (Figures 14-19) coalescence of starch grains occurred in both inner and outer regions of the microwave samples. The whole potato appeared to be evenly gelatinized at these stages and irregular shaped granules filled the whole cells in both the outer and inner regions of potatoes. In addition there were large intercellular spaces in the samples.

Heating Patterns

The time-temperature profiles for the boiling water and microwave treated samples are shown in Figs. 20-23. With microwave heating, shorter times (approximately ten times shorter) were required for the potato starch to reach gelatinization temperatures in the center of potatoes.

There was a significant difference in time-temperature profiles between microwave and conductive heating. During conductive heating the temperature of boiled samples was higher in peripheral potato tissues. The temperature of peripheral regions of potatoes reached about 90 C within one to two minutes when put into boiling water and remained at this temperature throughout the heating, while the temperature in the center regions of potatoes increased slowly to 90C. (Figs. 20-22). On the other hand, microwave heating temperatures were fairly uniform in different regions of tubers (Fig. 23).

Fig. 14. Center region of microwaved potato sample heated to 66C. Fig. 15. Side region of microwaved potato sample heated to 66C. Fig. 16. End region of microwaved potato sample heated to 66C. Fig. 17. Center region of microwaved potato sample heated to 80C. Fig. 18. Side region of microwaved potato sample heated to 80C. Fig. 19. End region of microwaved potato sample heated to 80C. Bar = 100 μm.

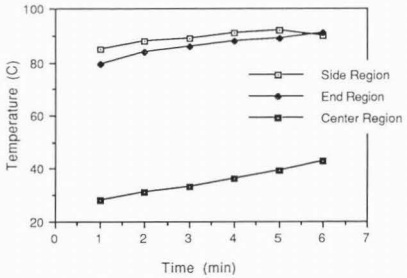

Fig. 20. Penetration of heat into potato treated by boiling water during stage 1.

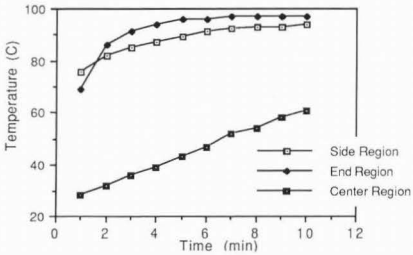

Fig. 21. Penetration of heat into potato treated by boiling water during stage 2.

Weight Loss and Texture of Treated Potatoes (Microwave versus Boiling Water)

The weight loss (Table 4) of potatoes, for the most part, was insignificant with both treatments. However, the weight loss of microwave treated potatoes was more evident than with the boiling water treated potatoes (Figs. 24-25).

The hardness of raw potatoes and treated potatoes is shown in Figs. 26-28. The hardness of boiling water heated potatoes increased from the outside layer to the inside layer. The hardness of the center part did not decrease until the center part was heated to gelatinization temperatures (Fig. 27). With raw potatoes (Fig. 26), boiling water heated potatoes (Fig. 27), and microwave heated potatoes (Fig. 28) the skin offered resistance to penetration. Once the skin was penetrated, stress depended upon the hardness of the tissue. The softest point of the tissue was evident by the minimum values on the stress/depth curves (Fgis. 26-28).

The hardness of microwave heated potatoes stayed at about the same level at stage 1 while the hardness at stages 2 and 3 increased from the outside to the inside as was observed with the boiling water treated samples (Fig. 28). The

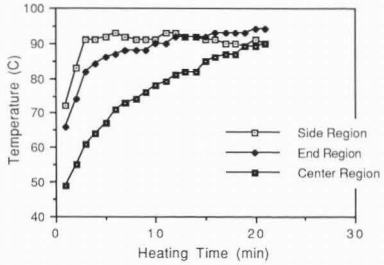

Fig. 22. Penetration of heat into potato treated by boiling water during stage 3.

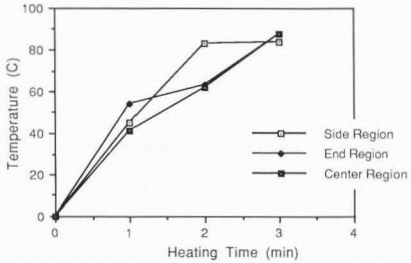

Fig. 23. Penetration of heat into potato treated by microwave during stage 1, 2, and 3.

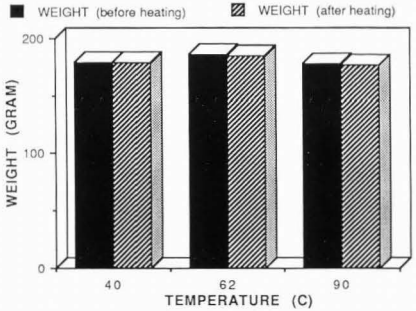

Fig. 24. Weight loss of potatoes during boiling water heating.

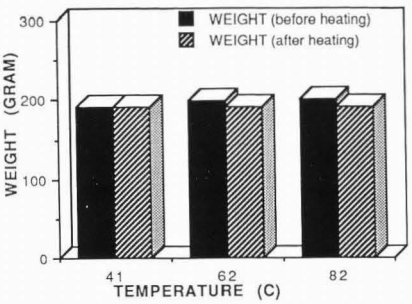

Fig. 25. Weight loss of potatoes during microwave heating.

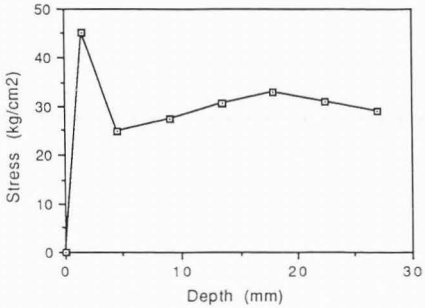

Fig. 26. Hardness of raw potatoes.

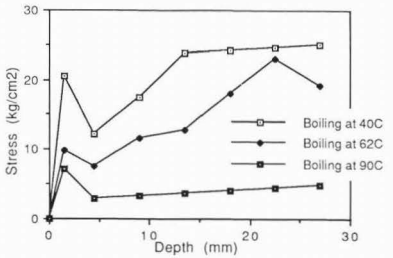

Fig. 27. Hardness of potato treated by boiling water at stage 1, 2 and 3.

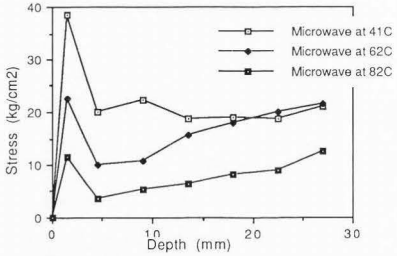

Fig. 28. Hardness of potato treated by microwave at stage 1, 2 and 3.

hardness of the center regions generally did not change much until the center regions were heated to gelatinization temperatures.

Discussion

Goebel et al. (1984) studied the distribution of gelled, chalky and paste areas of wheat starch-water dispersions heated in beakers with microwave ovens and conventional ovens. They indicated that the gelled regions where granulation first occurred were the inner regions of the microwave samples and the outer regions of the convection samples. Contrary to this report, we found that the coalescence of starch grains occurred in both inner and outer regions of the microwave samples. Nevertheless, the gelatinization did first occur in the outer region of the conventional samples. During normal cooking in boiling water the heated potatoes at stage 1 primarily consisted of unswelled starch granules. Only some outer regions contained swelled starch granules (Figs. 2-4). However, in microwave heated samples, the starch granules in both outer and inner regions had a similar appearance when they were heated to 40C (stage 1) (See Figs 11-13). At temperatures which caused gelatinization (stage 2), gelatinization occurred in both inner and outer regions with microwave heated potatoes (Figs. 14-16). No apparent structural differences were found between outer regions and center regions at stages 2 and 3 with microwave heating (Figs. 14-19).

There appears to be no consistent temperature gradient between the core and the surface of potatoes with microwave heating (Fig. 23). This suggests that the difference in starch granule swelling patterns could be closely related to different heating patterns between conductive heating and microwave heating. There are a number of reports on microwave heating patterns of potatoes. However, the conclusions were different. For example, Chen et al. (1971) demonstrated a temperature gradient from potato cores to peripheral regions with microwave heating and the opposite gradient for heating in boiling water. Conversely, Collins and McCarty (1969) reported a temperature gradient from the surfaces of potatoes to the cores instead of the core to the surface gradient shown by Chen et al. (1971). Therefore, further research needs to be conducted to clarify the issues of microwave heating patterns.

Turpin (1989) suggested that although conventional and microwave heating methods have the same objective, conduction heating has very different thermodynamic effects. With conduction heating, energy is added to the food molecules in the form of heat. With microwave heating, energy is added in the form of electromagnetic radiation, at a frequency of 2450 MHz and converts to heat at the target. Microwave heating of these samples took about one-tenth as much time as conduction heating to reach pre-determined temperatures (Table 1). It also explains the different starch swelling patterns and heating patterns between microwave and conductive heating.

Large intercellular spaces were evident with samples heated by both methods (Figs. 8-10, 14-19). However, the cell walls remained intact. The possible reasons for the prominent intercellular spaces are: 1) Granule shrinkage may have been due to increased packing density caused by gelatinization and retrogradation of the starch. 2) The intercellular spaces may have been created by partial solubilization of pectin in middle lamellas of cells which lead to easy separation of cells. Sefa-dedeh and Stanley (1979) reported that the greatest structural change of legumes during cooking was the breakdown of the middle lamella leading to the easy separation of intact cells. Nevertheless, they also stated that there was less evidence for the breakdown of the middle lamella in soybeans.

On the other hand, there was a marked difference in the appearance of starch granules between conventionally heated samples and microwave heated samples at stage 3. The starch granules from conventionally heated samples appeared to be more reticulated (Figs. 8-9) while the starch granules from microwave treated products tended to be more compact and dense (Figs. 17-19). This implies that conduction heating may hydrate more starch causing partial disruption of starch granules. Langton and Hermansson (1989) suggested that heat treatment of wheat starch dispersions gave rise to two stages of swelling and solubilization. Solubilization was observed in the center of granules during the first stage of swelling. Further swelling caused granule deformation and caused amylose release. Using an electron microscope, Buttrose (1963) concluded that acid caused corrosion of starch granules. Apparently, the heating treatment used in this study also caused the starch granule disruption (Figs. 8-9, 17-19). Nevertheless different heating methods resulted in different degrees of disruption. The microwave heated samples (Figs. 17-19) appeared to be less hydrated than the conventionally heated samples (Figs. 8-10). The microwave heated samples were less reticulated (Figs. 17-19).

Buttrose (1963) pointed out that starch

granules were made of concentric shells and were spherocrystals. This study showed that starch granules had a layered structure when they were heated to gelatinization temperatures (Figs. 7, 14-16). However, the layered structures were invisible when the temperature was above the gelatinization temperature (Figs. 8-9, 17-19).

The softening trends of conduction heated potatoes corresponded with heating patterns. In other words, softness increased following the increase of temperature (Figs. 20-22, 27). On the other hand, the softening trends of microwave treated potatoes at stages 2 and 3 could not be explained by their heating patterns while softening trends of microwave treated potatoes at stage 1 corresponded with the heating pattern (Figs. 23 and 28). This implies that softness does not solely rely upon temperature with microwave heating. Further investigations are necessary to elucidate the understanding of the relationship between softness, temperature of potatoes, and time exposed to microwave energy. Compared to conventionally heated potatoes, microwave treating did result in a little more moisture loss (Figs. 24-25). However, the relationship between hardness of heated potatoes and their moisture losses seems to be indistinct.

The findings in this study suggest that microwave heating may be more desirable for commercial products than conventional heating because of density. Moledina et al (1978) suggested that round and dense granules were desirable when economy packaging and shipping is used. In addition, he pointed out that round and dense granules also lend themselves well to automatic mashed potato machines which are becoming popular in restaurants and institutions.

Acknowledgements

This research was supported in part by the American Potato Division of Basic American Foods. We also thank Connie Swensen and James V. Allen for technical assistance.

References

Buttrose MS. (1963). Electron-microscopy of acid-degraded starch granules. Die Stärke. 15, 85-92.

Chen SC, Collins JL, McCarty IE, Johnston MR. (1971). Blanching of white potatoes by microwave energy followed by boiling water. J. Food Sci. 36, 742-743.

Collins JL, McCarty IE. (1969). Comparison of microwave energy with boiling water for blanching whole potatoes. Food Technol. 23, 3, 63-66.

Collison R, Chilton WG. (1974). Starch gelation as a function of water content. J. Food Technol. 9, 309-315.

Goebel NK, Grider J, Davis EA, Gordon J. (1984). The effects of microwave energy and convection heating on wheat starch granule transformations. Food Microstructure, 3, 73-82.

Knutson KM, Marth EH, Wagner MK. (1987). Microwave heating of food. Lebensmittel-Wisshenshaft und Technology, 20, 101-110.

Langton M, Hermansson AM. (1989). Microstructural changes in wheat starch dispersions during heating and cooling. Food Microstructure 8, 29-39.

Mermelstein NH. (1989). Microwave food processing. Food Technol. 43, 1, 117-126.

Moledina KH, Fedec P, Hadziyev D, Ooraikul B. (1978). Ultrastructural changes in potatoes during potato granule process as viewed by SEM. Starch Stärke 30, 191-199.

Ohlsson T, Risman PO. (1978). Temperature distribution of microwave heating-spheres and cylinders. J. Microwave Power 13, 303-309.

Reeve RM. (1954). Histological survey of conditions influencing texture in potatoes. I. Effects of heat treatments on structure. Food Res. 19, 323-332.

Roberts EA, Proctor BE. (1955). The comparative effect of ionizing radiations and heat upon the starch containing cells of the potato tuber. Food Res. 20, 254-263.

Sefa-dedeh S, Stanley DW. (1979). Textural implications of the microstructure of legumes. Food Technol. 33, 10, 77-83.

Turpin CH. (1989). Variable microwave power. Microwave World. 10, 8-11.

Discussion with Reviewers

Reviewer I: Were the boiled samples placed in plastic bags to prevent the introduction of additional water into the cells?

Authors: No. We purposely heated the samples with boiling water so that water in the samples would not evaporate. In this way we were able to study the impact of moisture loss on potato structure and softness between conventionally and microwave heated samples. Moisture loss was not evident with conventionally heated samples, but was evident with microwave heated samples.

Reviewer I: Why does Figure 14 look so different from the other micrographs?

Authors: Figure 14 shows the center region of a microwaved sample heated to 66C. In general, potato starch gelatinizes at about 62-65C. The characteristics of starch granules in Figure 14 indicate that starch gelatinized but did not completely coalesce. This phenomenon does not last long. These physical changes in starch take place rapidly thus they are not normally seen.

Reviewer I: J. Grider

FOOD STRUCTURE, Vol. 9 (1990), pp. 123-131
Scanning Microscopy International, Chicago (AMF O'Hare), IL 60666 USA

1046-705X/90$3.00+.00

THERMOTROPIC BEHAVIOR OF COCONUT OIL DURING WHEAT DOUGH MIXING : EVIDENCE FOR A SOLID-LIQUID PHASE SEPARATION ACCORDING TO MIXING TEMPERATURE

Christine LE ROUX, D. MARION, H. BIZOT, and D.J. GALLANT

Institut National de la Recherche Agronomique
Centre de Recherches Agroalimentaires
B.P. 527 44026 NANTES CEDEX 03 (France)

Abstract

Freeze fracture electron microscopy and differential scanning calorimetry were used to study the behavior of coconut oil during cake batter processing. The greatest modifications of fat crystallization are due to the mixing temperature of batter more than the physical state of the fat before its incorporation and the wheat flour hydration. Mixing at a temperature below the melting point of coconut oil involves a liquid/solid fat segregation in the cake batter. The endogenous wheat flour lipids and proteins appear to stabilize this fat partition. These results are likely related to previous observations which correlate loaf volume and mixing temperature of wheat flour dough containing coconut oil.

Initial paper received April 25, 1990
Manuscript received June 14, 1990
Direct inquiries to D.J. Gallant
Telephone number: 33 40 675014

Key Words : Coconut oil, fat crystallization, wheat dough, freeze fracture, differential scanning calorimetry.

Introduction

Fats play an important role in the processing of bakery products. In cake-making a 35 to 50% fat content based on flour weight influences : entrapment of air during mixing process, lubrication of protein and starch particles, emulsification and retention of considerable amounts of liquid to increase softness of the cake. In smaller amounts (1-3%) fats can be used in bread-making to increase loaf volume and to improve slicing properties, crumb grain uniformity and tenderness (Chamberlain et al. 1965). These effects depend on the crystalline form (α, β or β') adopted by the fat; for instance, in cake-making the beta prime form has been found the most appropriate to improve volume and texture of cakes (Hoerr et al. 1966). Furthermore, the liquid/solid ratio of the fat at mixing temperature greatly influences bread or cake volume (Tamstorf et al. 1980).

It has been suggested among many hypotheses that the solid components of the fat facilitate the production of oriented structures in cake batters, which may remain even when the temperature exceeds the melting point of the fat; and these structures favour gas retention in the earliest stages of baking (Bell et al. 1977). In addition, microscopic studies of cake batters have shown that during mixing, air cells are incorporated into the fatty phase and during baking the fat quickly melts and releases the suspended air into the flour water phase (Carlin 1944).

However, the reported hypotheses do not provide a very satisfactory explanation for the role of fats in bread-making or cake-making. In fact very few studies concern the behavior of fat during cake batter processing while a number of factors are known to influence fat crystallization especially nonfat components such as amphiphilic lipid molecules (Timms 1984).

In order to clarify the mechanism of fat crystallization in the cake batter, the coconut oil, usually used in cake factories, has been chosen to take advantage of its low melting point (24-27°C) well apart from starch gelatinization. Moreover simple thermal behavior due to predominating beta-prime polymorph (Riiner 1970), was expected to simplify interpretation.

In the present investigation a dual approach of cake batter structure has been used combining freeze fracture microscopic observations for lipid phase identification and differential scanning calorimetry for the characterization of phase transitions.

Experimental

Cake batter formulations and processing conditions are given in Table 1, with 40% or 60% water content on flour weight basis. The doughs were mixed for 15 min in a Farinograph under controlled temperature and with a mixing speed of 61 rpm.

ADDITION ORDER →

Wheat Flour	Water	Coconut oil	Mixing (°C) Temperature
100g	40g	L 30g L 10g SL 10g	15 - 20 or 30
100g	60g	L 30g L 10g SL 10g	15 - 20 or 30

Wheat Flour	Coconut oil	Water	Mixing (°C) Temperature
100g	L 10g L 30g	40g	15 - 20 or 30
100g	L 10g L 30g	60g	15 - 20 or 30

Table 1. Standard cake batter formulation with sequential procedure, 3 min of mixing after the first adding of water or fat to the flour. Physical state of fat before mixing : L liquid, SL solid/liquid.

Polarized light microscopy was performed with an Olympus Vanox microscope to detect starch birefringence in the cake batters.

Cake batter samples incubated between two copper sheets at mixing temperature were rapidly plunged in an liquid N_2 slush. Other freeze-fracture conditions were as previously described (Marion et al. 1987). Replicas were viewed on a Jeol 100S electron microscope operating at 80 kV. For each mixing condition at least ten replicas were observed.

Thermal measurements were carried out on a temperature programmable, differential heat flux microcalorimeter (DSC111, SETARAM). The samples were placed in 150 µl stainless steel pans. The samples were cooled from their mixing temperature to 1°C, at a rate of 5°C/min, and then heated to 150°C at a rate of 1°C/min. Indium was used to check temperature calibration. Data were collected on a HP 86 microcomputer.

The same coconut oil, stored at 4°C, was used during these experiments and care was taken to reproduce identical "thermal history" for all coconut oil aliquots.

Results

Differential Scanning Calorimetry

Figure 1 shows the DSC thermogram of coconut oil. A large endothermic peak is observed with a T_m (temperature of endothermic peak maxima) at 25°C. The onset temperature of endotherm is obviously below 0°C and represents the melting of the solid β' form, according to results of Hannewijk et al. (1958).

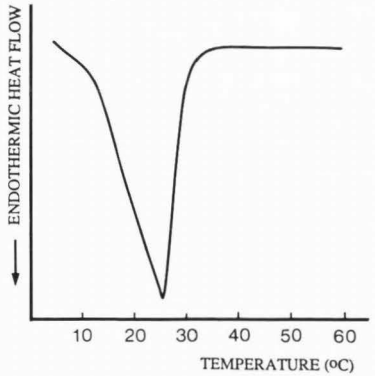

Fig.1 : Representative DSC thermogram of coconut oil. (Heating rate 1°C/min).

The endothermic melting of coconut oil, incorporated in a liquid state into the dough and mixed at 30°C, is not modified (Fig. 2). Furthermore, at a mixing temperature of 30°C, the melting endotherm of coconut oil is not influenced by water or the amount of fat added to wheat flour. In the same way, the melting endotherm does not depend on the order of water or oil addition to the flour.

The two endothermic peaks caused by gelatinization of starch are affected by water content as shown in previous work (Donovan 1979), but not by fat level (Fig. 2).

With cake batter mixing at 30°C the melting coconut endotherm seems to be almost independent of the physical state of the fat added to cake batter (solid-liquid mixture or liquid fat). (Table 2 or Figs. 3 and 4).

After heating to 150°C in the DSC pans, reheating after cooling (5°C/min) restores the initial melting profile of coconut oil. The starch endotherms have disappeared, suggesting complete starch gelatinization.

Studies with polarized light of these cake batters after first heating show the starch granules lose polarization crosses (results not shown). These observations agree with DSC studies, and clearly demonstrate the complete starch gelatinization after a first heating, even at 40% water level.

On the contrary, the endothermic peak shape of coconut oil is greatly modified when cake batter is mixed at 15 or 20°C (Figs. 3 and 4) whatever should be the other processing conditions, such as addition of other ingredients, water content (40% or 60%) and the physical state of fat added to the cake batter (Table 2).

Thus, in regard to the endotherm of coconut oil melting, new peaks appear below and above T_m of coconut oil. This suggests that part of the fat has a higher melting point since a thermal recycling of these cake batters restores the usual pattern of mixture obtained by fat addition at 30°C (Fig. 5).

Mixing Temperature	Water Content			Water Content		
	60% (60g water/100g wheat flour)			40% (40g water/100g wheat flour)		
	Physical state of fat before mixing	1st scan °C	2nd scan °C	Physical state of fat before mixing	1st scan °C	2nd scan °C
15°C	Liquid	13 20 27	22.4	Liquid	N.D. 18.3 26.4	22
	Liq/sol	12 27	22	Liq/sol	N.D.	
20°C	Liquid	18 22.5 29	22.5	Liquid	N.D. 20.7 27	22
	Liq/sol	18.5 23.8 29.6	22.9	Liq/sol	N.D.	
30°C	Liquid	23.2	23	Liquid	23.1	23
	Liq/sol	22.7	23.5	Liq/sol	N.D.	

Table 2. Temperatures of fat melting peak maxima, in the various processing conditions, achieved with DSC.

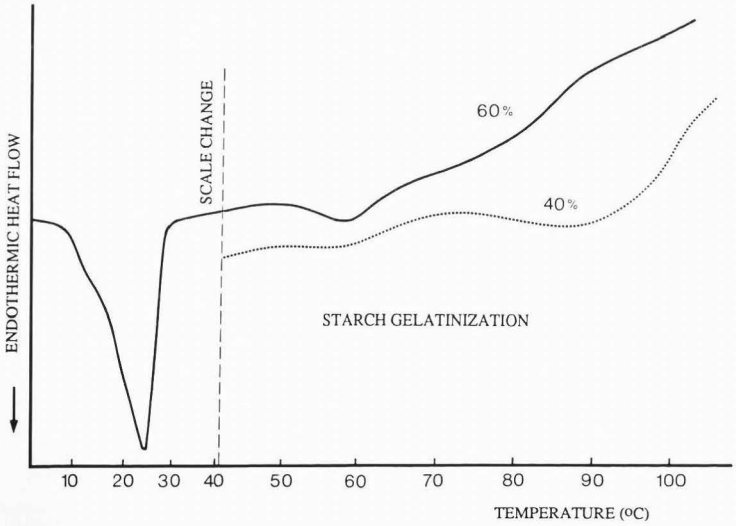

Fig.2 : Representative DSC thermogram of a cake batter (40% and 60% hydration on a wheat flour basis) containing coconut oil, mixed at 30°C.

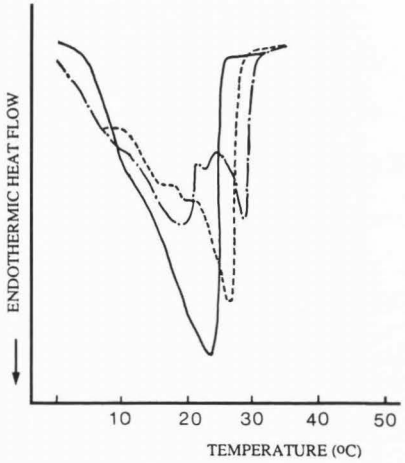

Fig.3 : Representative DSC thermograms of cake batters (60% hydration) containing coconut oil. The fat is incorporated as liquid in the cake batter. Comparison of (—) 30°C, (—·) 20°C, and (---) 15°C mixing temperature.

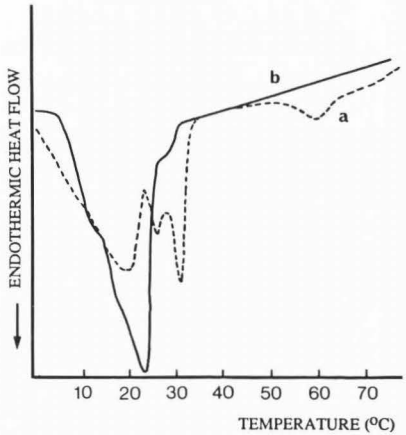

Fig.5 : Representative DSC thermograms of cake batters (60% hydration) containing coconut oil. The fat is incorporated as liquid in the cake batter, with mixing temperature of 20°C. Comparison of (a) the first heating, (b) reheating of this cake batter after a cooling at a rate of 10°C/min.

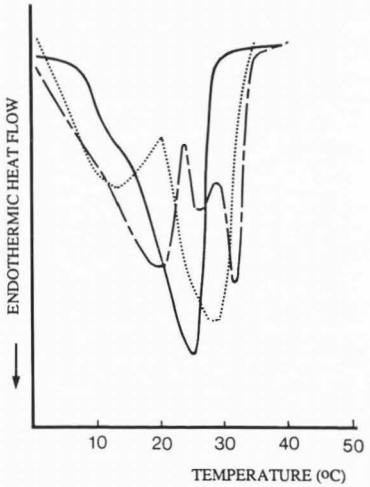

Fig.4 : Representative DSC thermograms of cake batters (60% hydration) containing coconut oil. The fat is incorporated as solid-liquid in the cake batter. Comparison of (—) 30°C, (—·) 20°C, and (···) 15°C mixing temperature.

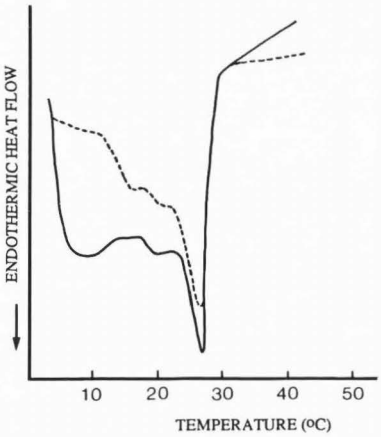

Fig.6 : Representative DSC thermograms of cake batters containing coconut oil. The fat is incorporated as liquid in the cake batter, with mixing temperature of 20°C. Comparison of (—) 40% hydration, and (---) 60% hydration.

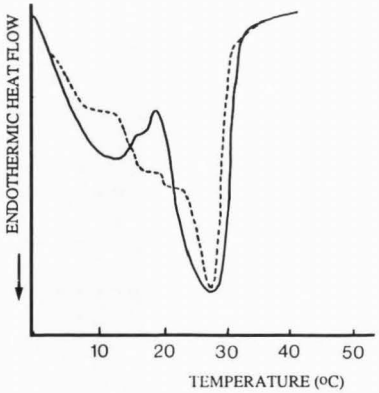

Fig.7 : Representative DSC thermograms of cake batters containing coconut oil, with mixing temperature of 15°C and hydration of 60%. (- - -) Fat incorporated as liquid. (——) Fat incorporated as liquid-solid.

For the mixing temperature of 15 or 20°C, we can even observe the same phenomenon independent of the other processing conditions. This peak is more or less important, depending particularly on water content (Fig. 6), and to some extent on the state of fat (liquid or solid-liquid) incorporated into cake batters (Fig. 7).

Freeze-fracture electron microscopy

Freeze-fracture of the cake batter clearly shows the protein matrix, starch granules and lipids of wheat flour (Fig. 8).

The cake batter with the mixing temperature of 30°C exhibits globular fat droplets with a diameter varying between 0.15 to 2 µm more or less surrounded by the gluten protein network. There are a few small spherical particles (50 to 200 nm in diameter) associated with fat globules (Fig. 9 a-b), which according to previous freeze-fracture studies on wheat flour and gluten (Al Saleh et al. 1986; Marion et al. 1987), could be attributed to endogenous wheat lipids. However DSC studies indicate that these associations do not modify the melting point of coconut oil.

Cake batters mixed at 15 or 20°C exhibit not only comparable fat globules but also irregular crystalline platelet areas (Fig. 9 c-d). These two types of fat structures appear to be more or less separated from each other (Fig. 10 a). It should be mentioned that these crystalline regions are not surrounded by the wheat flour lipidic vesicles, but only by proteic particles. It is noteworthy that less endogenous lipid vesicles are still present in the protein network, suggesting that most of them have been combined with fat droplets (Fig. 10 b).

No distinct changes in the location and structure of fat has been detectable for cake batter mixing temperatures of 15 and 20°C, with fat incorporated either as a solid-liquid mixture or as a liquid. These results are also valid for 40 and 60% water content (Fig. 10 c).

After heating of cake batters mixed below the melting temperature of fat, only globular droplets are observed, suggesting that fusion of fat crystalline structures and oil droplets occured during heating.

Fig.8 : Freeze fracture of a non fat cake batter preparation. S : Starch; L : Lipids of wheat flour; p : Protein network.

Discussion

The results of this study emphasize the importance of mixing temperature at which the cake batter is mixed on fat melting. It is obvious that cake batter mixing at temperatures below 30°C modifies the melting endotherm of coconut oil. This might be explained by changes in fat crystallization implying growth of new crystal structures such as β or α polymorph, or by a separation of solid and liquid fat fraction may then take place inside the dough matrice. In the former hypothesis, it is well known that for a pure triglyceride melting temperature increases from α to β' and to β (Perron et al. 1969); in the latter, few degrees below its melting point, coconut oil is composed of a heterogeneous slurry of crystals in liquid oil. During cake batter mixing, the segregation and stabilization of these two phases, led to the formation of a lower melting solid solution and a higher melting one.

At any rate, freeze-fracture electron microscopy observations indicate that the individual endothermic peaks of thermograms for dough mixing at 15°C and 20°C, are related to a differentiation of at least two distinct fat structures. In addition to fat droplets, there is a peculiar agglomeration of crystalline platelets at 15°C and 20°C. We expect that the highly organized crystalline platelets give the higher melting DSC curves and corresponds to the solid fat while the droplets gives the lower melting curves.

It must be mentioned that both fat fractions are covered by proteins particles, but only fat droplets appear, surrounded by lipid vesicles. Thus, endogenous lipids and proteins appears to stabilize this partition. The fusion of endogenous lipids with exogenous liquid fat implies a loss of lipid vesicles in the protein network. This phenomenon together with the modification of fat crystallization might be

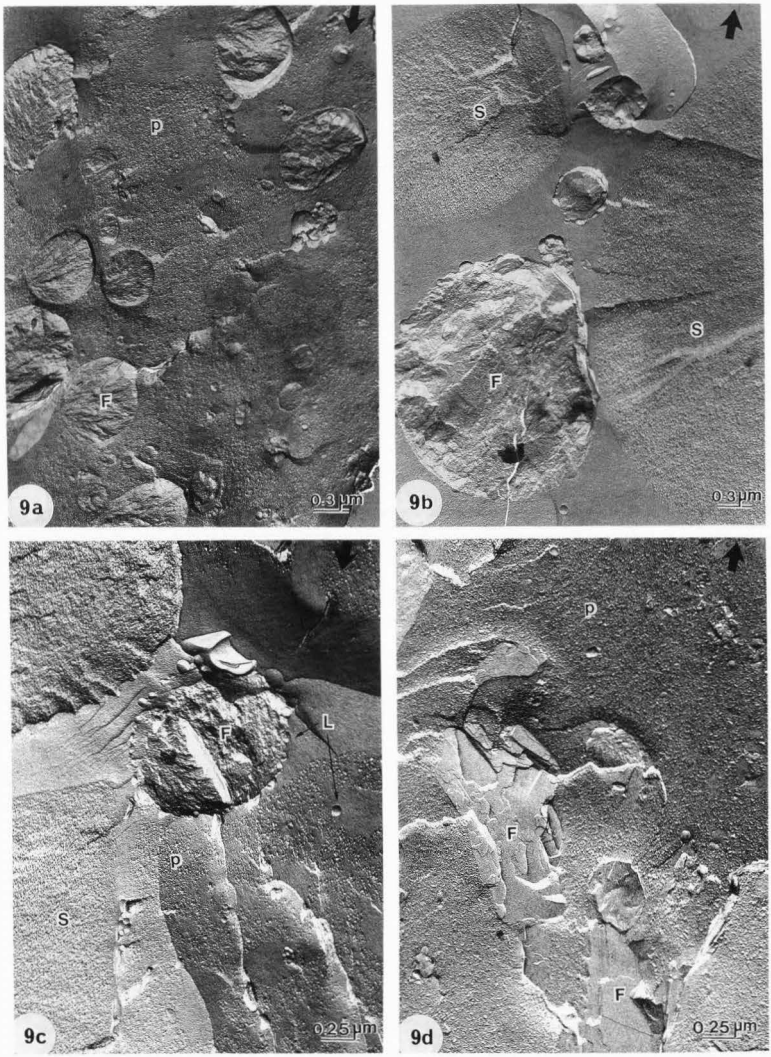

Fig.9 : Freeze fracture of a cake batter preparation (60% water content), containing coconut oil. F : Fat; p : Protein network; L : Lipid vesicle ; S : Starch. a-b : cake batter mixed at 30°C; c-d : Cake batter mixed at 15 or 20°C.

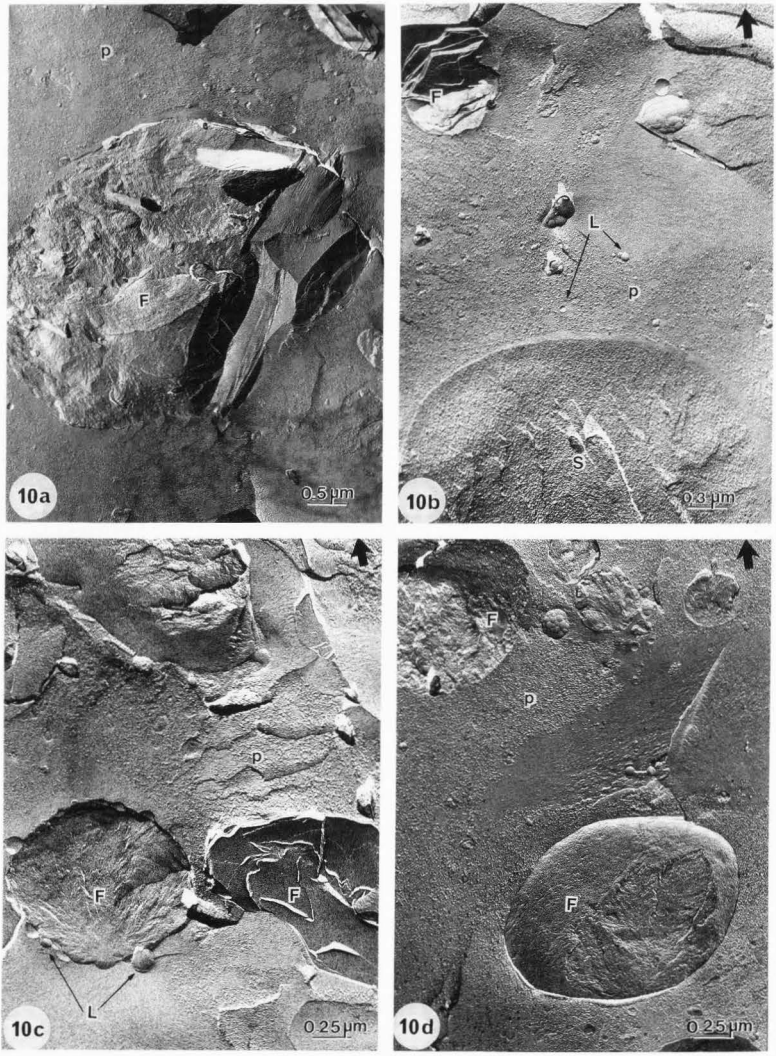

Fig.10 : Freeze fracture of a cake batter preparation containing coconut oil. F : Fat; p : Protein network; L : lipid vesicle; S : Starch. a-b : Cake batter of 60% water content and mixed at 15 or 20°C; c : Cake batter of water content 40% and mixed at 15 or 20°C; d : Cake batter of 60% water content, mixed at 15°C and heated for 30 min at 65°C.

of great importance in relation to the rheological properties of wheat flour cake batters.

In addition, it can be mentioned that the reheating of the cake batters mixed at 15 or 20°C, involves the fusion of the two fat type fractions. This is clearly demonstrated by DSC in which the initial melting endotherm is restored and by freeze-fracture electron microscopy which shows the disappearance of crystalline platelets.

Some slight differences are seen by DSC in peaks between cake batters mixed at 15 and 20°C and according the other processing conditions at these two temperature of mixing (water content, physical state of addition etc...). However, these slight differences are not evidently related to changes in the location and ultrastructure of fat and cake batter.

Concerning starch it is evident that starch gelatinization is not prevented with added fat within the processing conditions studied. These results are in agreement with previous ones (Abboud and Hoseney 1984).

This partition of solid and liquid fat provides an explanation to the results obtained by Baker and Mize (1942) which have shown that dough mixing below the melting point of coconut oil improves bread volume and crumb texture; and this is in agreement with the general idea that fat solid/liquid ratio more than fat source is the determinant on breadmaking technology (Bell et al. 1977).

Furthermore the retention of liquid fat in protein network during gluten washing (Baker and Mize 1942) might be explained by the stabilization of liquid fat droplets at once by endogenous polar lipids and proteins.

Therefore, the results of this work emphasizes the necessity to take into account that fat crystallization may be greatly modified in a dough and thus, that knowledge of fat crystallization before adding to a dough is necessary but not sufficient. Simple DSC tests are sensitive enough to detect changes and can serve as a systematic test to monitored fat segregation as long as sampling problems are overcome.

References

Abboud AM, Hoseney RC. (1984). Differential scanning calorimetry of sugar cookies and cookie doughs. Cereal Chem. **61** (1), 34-37.

Al Saleh A, Marion D, Gallant DJ. (1986). Microstructure of mealy and vitreous wheat endosperms (Triticum durum L.) with special emphasis on location and polymorphic behaviour of lipids. Food Microstruc. **5**, 131-140.

Baker JC, Mize MD. (1942). The relation of fats to texture, crumb, and volume of bread. Cereal Chem. **19**, 84-94.

Bell BM, Daniels DGH, Fisher N. (1977). Physical aspects of the improvment of dough by fat. Food Chem. **2**, 57-70.

Carlin GT. (1944). A microscopic study of the behavior of fats. Cereal Chem. **21**, 189-199.

Chamberlain N, Collins TH, Elton GAH. (1965). The chorleywood bread process : improving effects of fat. Cereal Sci. Today **10**, 415-419, 490.

Donovan JW. (1979). Phase transition of starch-water systems. Biopolymers **18**, 263-275.

Gallant DJ, Guilbot A. (1971). Artefacts au cours de la préparation de coupes de grains d'amidon. Etudes par microscopie photonique et électronique. (Artefacts during the preparation of starch granules sections. Studies under light and electron microscope). Stärke, **23** (7), 244-250.

Hannewijk J, Haighton AJ. (1958). Differential thermal analysis. III. Melting curves of oils and fats. J. Am. Oil Chem. Soc. **35**, 457-461.

Hoerr CW, Moncrieff J, Paulicka FR. (1966). Crystallography of shortenings. Baker's Digest **40** (2), 38-40.

Marion D, Le Roux C, Akoka S, Tellier C, Gallant DJ. (1987). Lipid-protein interactions in wheat gluten : a phosphorus nuclear magnetic resonance spectroscopy and freeze-fracture electron microscopy study. J. Cereal Sci. **5**, 101-115.

Perron R, Petit J, Mathieu A. (1969). Study of palmitic-stearic triglycerides and their binary mixtures by differential thermal analysis (DTA). I. Pure triglycerides. A. Chem. Phys. Lipids **3**, 11-28.

Riiner U. (1970). Investigation of the polymorphism of fats and oils by temperature programmed X-ray diffraction. Lebensm. Wiss. Technol. **3**, 101-106.

Tamstorf S, Jonsson T, Krog N. (1980). The role of fats and emulsifiers in baked products. In : Chemistry and Physics of Baking. J.M.V. Blanshard, P.J. Frazier and T. Galliard (Eds). The Royal Society of Chemistry, London, 75-88.

Timms RE. (1984). Phase behaviour of fats and their mixtures. Prog. Lipid Res. **23**, 1-38.

Discussion with Reviewers

Reviewer II : It is postulated that the native flour lipids are being "dissolved" by the liquid oil fractions and that this may alter the rheological properties. To what extent will this change the finished cake volume and texture? and how?
Authors : Most of the wheat flour lipids have fused with coconut oil so that the polar lipids are no longer available for stabilization of air/water interfaces during cooking and this may affect the cake volume. Furthermore, below the melting point of coconut oil, this phenomenon seems to be associated with a modification of fat crystallisation in cake batter affecting the rheological behavior of fat and therefore cake texture.

Reviewer II : Can the disappearance of the flour lipids be measured quantitatively by electron microscopy and is there enough evidence for this phenomenon?
Authors : In previous work (Marion et al, 1987) we have shown that most of the wheat flour lipids are organized in small vesicles. From analysis of about ten samples for each mixing temperature it is obvious that the quantity of vesicles embedded in the protein network decreases when fat is present.

For applying image analysis on electron micrographs of flour lipids, images need to have sufficient contrast; this contrast enhancement can be achieved by fixation with osmium before embedding and sectioning, so that lipids appear black and are easily distinguished from other structures. The lack of contrast makes quantification in images from freeze-fractured and freeze-etched samples very difficult. The fixation procedure also causes fat extraction which would influence the results of image analysis.

Another kind of measurement could be obtained directly under TEM employing a step by step measurement of different image areas using a special fluorescent screen connected to a sensitive electrometer as already shown by Gallant and Guilbot (1971).

H.C. Hoseney : Coconut oil is a mixture of chemical entities. Would the study be cleaner if pure, sharp melting fats were used?
Authors : Study of binary phase diagrams of some simple triglycerides would give better results but it will be necessary to build a small scale apparatus similar to the Farinograph to

control mixing energy and temperature in order to use small amounts of dough and therefore small amounts of pure triglycerides, which are very expensive.

A.E. Blaurock : Walstra's work offers an alternative interpretation of the modification of coconut oil behavior in cake batter. Walstra has demonstrated that, in a finely divided emulsion, some droplets form crystals and others will not, simply as a result of nucleation in some droplets and not others. In addition, the three different curves shown in figure 3 may result simply from the kinetics of crystallization into different mixtures of the polymorphic forms of coconut oil, as a result of the different thermal histories of the three specimens. In this case, no physical separation need have occured in the dough during mixing.

Authors : Nucleation may explain the slight differences observed in individual peaks depending on (1) mainly, whether the fat is added as solid-liquid or liquid (Figs. 3 and 4, respectively), or (2) the water content of the cake batter (Figs. 6 and 7). However the general behavior characterized by individual peaks of low and high temperature endotherms is sensitive to the mixing temperature (Figs. 4 and 5). It is kept even after an overnight resting at 1°C (result not shown) and cannot be explained by nucleation only. Furthermore, it was impossible to obtain such DSC curves whatever the cooling rate (up to 1°C/sec) above the fat melting temperature. This suggests that liquid-solid mixture is necessary to induce modification of the thermal behavior of the coconut oil in cake batter.

FOOD STRUCTURE, Vol. 9 (1990), pp. 133-138
Scanning Microscopy International, Chicago (AMF O'Hare), IL 60666 USA

1046-705X/90$3.00+.00

CHANGES IN THE RHEOLOGY AND MICROSTRUCTURE OF ROPY YOGURT DURING SHEARING

J.A. Teggatz and H.A. Morris

Department of Food Science and Nutrition
University of Minnesota
Saint Paul, Minnesota 55108

Abstract

Rheological and microstructural changes that occurred in ropy yogurt during shearing were observed. Yogurt made with an exopolymer-producing (ropy) strain of Lactobacillus delbrueckii subsp. bulgaricus and non-ropy strain of Streptococcus thermophilus was subjected to an increasing shear rate from 0-833 s^{-1} using a Haake Rotovisco RV2. Shear stress noticeably increased to a peak value and then decreased to a plateau value as the shear rate continued to increase. Samples taken at eight different shear rates were examined by scanning electron microscopy (SEM). At low shear rates, the exopolysaccharide (EPS) existed as a filamentous network attached to the lactobacilli and casein matrix. At the shear rate where the highest shear stress was recorded, the EPS/bacteria bonds were broken.

SEM micrographs and shear stress curves were used to determine a "bond-strength" of the EPS/lactobacilli interaction. After the interaction was disrupted, the EPS was still incorporated with the casein, where it continued to influence viscosity.

Initial paper received February 8, 1990
Manuscript received May 11, 1990
Direct inquiries to J.A. Teggatz
Telephone number: 612 644 5653

Keywords: Yogurt; exopolysaccharide; ropy lactic acid, bacteria; scanning electron microscopy; rheology

Introduction

Exopolymer (EPS)-producing cultures have been recognized for many years as the cause of slimy or ropy milk (Buchanan and Hammer, 1915; Macy, 1923). Previous researchers investigated the rheological characteristics of fermented milks made with these cultures and found an increase in viscosity and a reduction in susceptibility to syneresis (Schellhaass and Morris, 1985; Giraffa and Berg re, 1987; Cerning et al., 1986).

Many processing problems, such as low viscosity or high syneresis, which occur during yogurt manufacture are often solved by increasing the total solids or adding stabilizers, such as modified starch, carrageenan, guar gum, pectin, gelatin, and sodium caseinate (Winterton and Meiklejohn, 1978; Radema and van Dijk, 1973; Modler et al., 1983; Kessler and Kammerlehner, 1982). However, some feel that these additives adversely affect the true yogurt taste, aroma and mouthfeel (Kroger, 1973; Steinberg, 1979). This suggests that the use of ropy cultures could appeal to those consumers who are looking for a "natural" yogurt (Steinberg, 1979). Ropy cultures are also a potential benefit for yogurt manufacturers in The Netherlands and France, where the addition of stabilizers is prohibited in unfruited yogurt (Humphreys and Plunkett, 1969).

A product's response to an applied stress is determined through rheological measurements. Since yogurt is a non-Newtonian time-dependent fluid (Holdsworth, 1971), rotational viscometers with a concentric cylinder design have been used in recent research at both steady and variable shear rates (Schellhaass and Morris, 1985; Winterton and Meiklejohn, 1978; Macura and Townsley, 1984; Labropoulos et al., 1981; Parnell-Clunies, 1986).

Electron microscopy has often been utilized to study yogurt cultures and yogurt microstructure (Schellhaass and Morris, 1985; Bottazzi and Bianchi, 1986). Variations in heat treatment of the medium, total solids, and thickening agents have all been shown to alter yogurt microstructure (Kalab et al., 1975; Kalab et al, 1976; Davies et al, 1978), but few have integrated this into explanations for rheological behavior. Most studies were also conducted on samples existing in an undisturbed or "static" state and not subjected to any applied stresses.

The objectives of this study were to examine the changes that occur in ropy yogurt when it was subjected to a shear force and to observe what happened to the yogurt microstructure as a result of

shear by using scanning electron microscopy.

Materials and Methods

Yogurt

Yogurt was made from steamed (90°C for 1/2 hour) 11% reconstituted nonfat dry milk (NDM) in 200 ml aliquots contained in 400 ml beakers. The milk was tempered to 32°C and inoculated with 1% each of lactobacilli and streptococci cultures. The cultures for ropy yogurt were Lactobacillus delbrueckii subsp. bulgaricus RR (ropy) and Streptococcus thermophilus C3 (nonropy), while for nonropy yogurt they were Lactobacillus delbrueckii subsp. bulgaricus 880 (nonropy) and Streptococcus thermophilus C3 (nonropy). All of the beakers of yogurt were incubated at 32°C for eleven hours until approximately pH 4.4 was reached and then immediately cooled to 4°C.

The strains of yogurt cultures were obtained from the collection of H.A. Morris (University of Minnesota, St. Paul, MN). They were routinely propagated in steamed (90°C for 1 hour) 11% reconstituted NDM. A 1% inoculum was transferred to the cooled medium and incubated overnight at 37°C.

Rheology of Yogurt

The apparent viscosity of yogurt was measured using a Haake Rotovisco RV2 coaxial cylinder viscometer with a MVII sensor system and 500 measuring head (Haake, Inc., Saddle Brook, NJ). The sample was maintained at 10°C by a circulating waterbath connected to the jacket surrounding the sensor system during testing. The viscometer was programmed so the rotor speed increased from 0 rpm to 925 rpm in three minutes. Scale readings were recorded and calculations for shear stress and shear rate were completed according to Haake Manual 105.

Six samples each of the ropy and nonropy yogurts were sheared in the viscometer and data were plotted as shear stress versus shear rate. In order to observe microstructural changes in the ropy yogurt that were occurring during the various stages of shearing, eight new samples were used and the viscometer was stopped at predetermined times during the programmed cycle so that samples sheared at 0, 139, 167, 194, 222, 250, 278, 416, and 833 sec^{-1} could be removed. These correspond to 0, 0.5, 0.6, 0.7, 0.8, 0.9, 1.0, 1.5, and 3.0 minutes into the shearing cycle. A different sample of yogurt had to be used each time after the cycle was interrupted, but all samples were from the same lot of reconstituted NDM.

Scanning Electron Microscopy of Yogurt

Samples of the sheared yogurt were pipetted into holes (2 mm diameter x 2 mm deep) drilled into aluminum scanning electron microscopy (SEM) stubs. The stubs were gently dipped into a 3% agar sol (45°C) and allowed to solidify. Primary fixation of the stubs was done with 5.6% glutaraldehyde in 0.033M sodium cacodylate buffer (pH 7.0) and 500 ppm ruthenium red for 48 hours at 4°C. The high concentration of glutaraldehyde was used because it had to penetrate the agar coating on the stubs. Three 10 minute rinses in 0.033M cacodylate buffer were followed by post fixation with 2% osmium tetroxide in 0.033M sodium cacodylate buffer and 500 ppm ruthenium red for 1 hour at 4°C. The stubs were then rinsed three times with distilled water (10 minutes each). Primary dehydration was carried out at room temperature in a graded ethanol series (10 minutes each in 25%, 50%, 75%, 99% and 3 times in 100%). Final dehydration was done in a Ladd critical point dryer (Ladd Research Industries, Inc., Burlington, VT) using CO_2 as the transition medium. The agar layer on top of each stub was gently lifted off and mounted upside down on a clean SEM stub using double-coated tape. Any small samples remaining in the stub holes were mounted on another clean stub with the tape. The samples were surrounded by a coat of carbon paint and coated with a layer of gold-palladium using a Kinney vacuum evaporator (model KSE-2AM). Specimens were viewed in a Philips 500X scanning electron microscope at 6 kV.

Results and Discussion

Rheology

The use of exopolymer-producing cultures in yogurt increases the apparent viscosity (Schellhaass and Morris, 1985; Galesloot and Hassing, 1973). The magnitude of increase varies due to differences in culture strains, yogurt total solids, incubation conditions, and methods for viscosity measurement. Yogurt exhibits pseudoplastic or shear-thinning behavior; therefore, it is more appropriate to measure the shear stress at an increasing shear rate (Schellhaass and Morris, 1985) rather than record single point measurements (Cerning, et al., 1986). In the present study, a shear rate range greater than previously explored was evaluated (Schellhaass and Morris, 1985; Labropoulos, et al., 1981) in order to observe the full rheological history from unsheared yogurt to extremely sheared yogurt. Figure 1 shows the magnitude of difference between ropy and nonropy yogurts and points out the three characteristic parts of the curve for ropy yogurt. The ropy yogurt had a noticeable increase in shear stress as the shear rate was increased from 0 to approximately 220 s^{-1}, as indicated by arrow B. Beyond that shear rate, the shear stress decreased to a plateau level where it remained even though the shear rate continued to increase. This unusual "hump" in the shear stress curve was less noticeable in the nonropy yogurt, but its small presence suggests that protein-protein interactions in the yogurt gel structure are broken during the initial period of shearing. This could also happen in the ropy yogurt, but there is obviously another factor involved.

The physical nature of pseudoplastic fluids makes it difficult to apply an empirical equation, such as the power law (1) over a wide shear rate range (Van Wazer, et al., 1963). Figure 2 is a log-log plot of Figure 1 and it exhibits a similar shape with the hump in the center of the curve. Consequently, this research was directed towards using SEM to try to explain why such curves were obtained when using the ropy yogurt.

Scanning Electron Microscopy

Scanning electron micrographs have visually demonstrated that ropy cultures have web-like filaments attached to the cell surface, while nonropy cultures are void of such attachments (Schellhaass and Morris, 1985; Kalab et al., 1983). Figure 3A confirms these findings in yogurt made with ropy L. delbrueckii subsp. bulgaricus and nonropy S. thermophilus. The sample has not been sheared, so the EPS is still attached to the rods. There is no obvious change in the yogurt microstructure as it is subjected to a shear rate of 139 s^{-1} (Figure 3B). Micrographs of yogurt subjected to shear rates up to 167 s^{-1} and 194 s^{-1} are not shown because there is

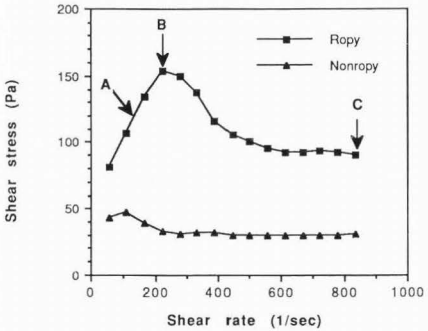

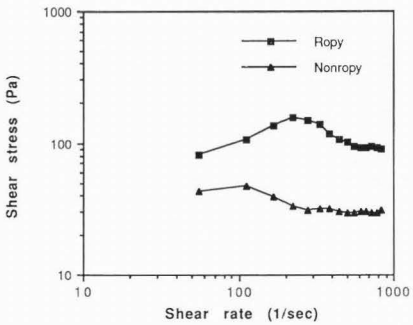

Figure 1 (at left). Shear stress versus shear rate curves of ropy and nonropy yogurt made from reconstituted nonfat milk (11% solids). Yogurt was made by incubating ropy and nonropy strains of Lactobacillus delbrueckii subsp. bulgaricus with nonropy strains of Streptococcus thermophilus at 32°C for 11 hours to pH 4.4. Each line represents the average of six samples. Arrows indicate yogurt sheared at: **A)** 139 s^{-1}; **B)** 222 s^{-1}; and **C)** 833 s^{-1}.

Figure 2 (at right). Log shear stress versus shear rate curves of ropy and nonropy yogurt made from reconstituted nonfat milk (11% solids). Yogurt was made by incubating ropy and nonropy strains of Lactobacillus delbrueckii subsp. bulgaricus with nonropy strains of Streptococcus thermophilus at 32°C for 11 hours to pH 4.4.

little visible difference in the progression.

Several investigators have suggested that the EPS is not only attached to the cell surface, but also to the protein matrix (Schellhaass and Morris, 1985; Tamime et al., 1984). In Figure 3A, the casein is visible as distinct micelles clumped together. It appears that the EPS could be attached to the casein, but this remains to be verified.

There are marked differences in the yogurt microstructure once a shear rate of 222 s^{-1} has been reached (Figure 3C). At this point, less EPS is visibly present and the casein can be described as a more undefined, fluffy mass. Figures 3D, 3E, and 3F show the progression of changes in the microstructure when exposed to shear rates of 250 s^{-1}, 416 s^{-1}, and 833 s^{-1}, respectively. The micrograph of yogurt at a shear rate of 278 s^{-1} is not shown because there is little significant change. The EPS is no longer attached to the rods; therefore, it appears to become aggregated with the casein, though not necessarily attached to the protein. The rough surface of the rods could be casein fragments which were dislodged during shearing and adhered to the bacteria. The casein matrix also continues to appear fluffy at the higher shear rates and less defined in appearance.

Rationalization of Rheological Patterns by Electron Microscopy

The scanning electron micrographs of yogurt under stress might provide a feasible explanation for the unusual rheological behavior exhibited. The initial rapid increase in shear stress or resistance to stretching could be attributed to the bonds between EPS and the rods. At the peak of the stress, the bonds have reached their maximum limit and consequently, they break. This results in a decreased shear stress even though the shear rate continues to increase. One could quantify the breaking point by comparing the SEM micrographs and shear stress curves to determine the "bond-strength" between the EPS and rods. From Figure 1, this appears to be approximately 150 Pa, but could range between 140-160 Pa depending on the sample observed.

Based on our observations, the EPS is actually attached to the casein in addition to the bacteria. The EPS/casein interaction could be weaker in strength than the EPS/bacteria interaction and not have a visible influence on the measured shear stress of the yogurt or the EPS/casein interaction might be very strong and require a much stronger force before it is broken.

Once the EPS is separated from the bacterial cell surface as a result of the shearing, it remains incorporated with the casein in some manner, where it continues to influence the viscosity. This is most likely due to a continued interaction of EPS with casein, which is evidenced in Figure 1, where the ropy yogurt exhibits a greater shear stress than nonropy yogurt even at high shear rates.

Conclusion

The application of SEM to explain rheological behavior when studying EPS-producing cultures was used to help understand the mechanism by which the EPS interacts with its surroundings and influences viscosity. In ropy cultures, the EPS is attached to the bacterial cell surface and also interacts with the casein. The EPS/bacteria interaction is disrupted when the yogurt is sheared at an increasing shear rate to 220 s^{-1}, which is at the peak of the hump in the shear stress versus shear rate curve. The peak shear stress could be defined as the "bond-strength" between the EPS and bacteria and is approximately

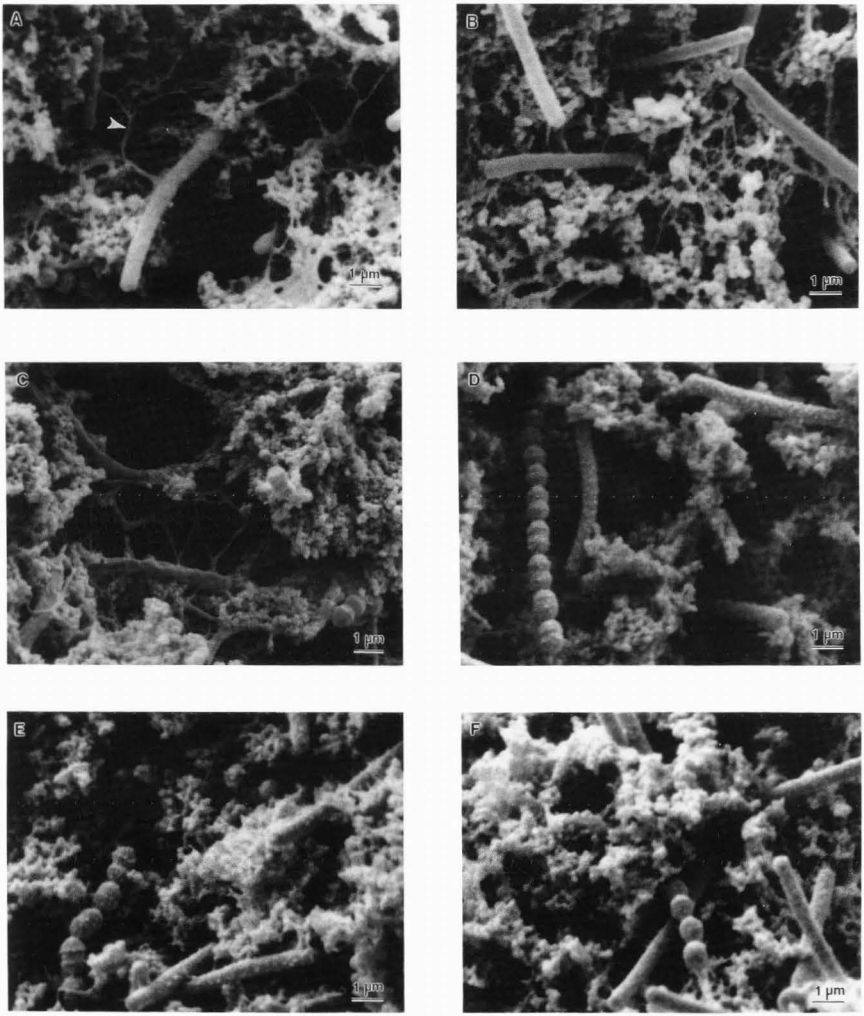

Figure 3. Microstructure (SEM) of ropy yogurt made from reconstituted nonfat milk (11% solids), ropy L. delbrueckii subsp. bulgaricus and nonropy S. thermophilus. Arrow in Fig. 3A indicates filaments of EPS. Casein is present as micelles associated with the bacteria and EPS. Yogurt was sheared to the following shear rates: **A)** 0 sec^{-1}; **B)** 139 sec^{-1}; **C)** 222 sec^{-1}; **D)** 250 sec^{-1}; **E)** 416 sec^{-1}; and **F)** 833 sec^{-1}.

150 Pa. After the EPS is separated from the cell surface, it continues to interact with the casein and influence the viscosity of the yogurt.

Acknowledgement

Published as contribution No. 17,925 of the series of Minnesota Agricultural Experiment Station on research conducted under Project No. 18-75, supported by Hatch Funds and a major grant from Unilever Research Laboratorium, Vlaardingen, Netherlands. We are indebted to Gilbert Ahlstrand for assistance and advice concerning the SEM work and Linda Lofquist for help with viscosity measurements.

References

Bottazzi V, Bianchi F. (1986). Types of microcolonies of lactic acid bacteria, formation of void spaces and polysaccharides in yoghurt. Scienza E Tecnica Lattiero-Casearia. 37, 297-315.

Buchanan RE, Hammer BW. (1915). Slimy and ropy milk. Res. Bul. Ia. Agr. Exp. Sta. 22, 205-295.

Cerning J, Bouillanne C, Desmazeaud MJ, Landon M. (1986). Isolation and characterization of exocellular polysaccharide produced by Lactobacillus bulgaricus. Biotech. Letters. 8, 625-628.

Davies FL, Shankar PA, Brooker BE, Hobbs DG. (1978). A heat-induced change in the ultrastructure of milk and its effect on gel formation in yogurt. J. Dairy Res. 45, 53-58.

Galesloot TE, Hassing F. (1973). Lumps in stirred yoghurt. Dairy Sci. Abstr. 36, 449.

Giraffa G, Bergere JL. (1987). Nature du caractere epaississant de certaines souches de Streptococcus thermophilus: etude preliminarie. Le Lait. 67, 285-298.

Holdsworth SD. (1971). Applicability of rheological models to the interpretation of flow and processing behavior of fluid food products. J. Text. Stud. 2, 393-418.

Humphreys CL, Plunkett M. (1969). Yoghurt: a review of its manufacture. Dairy Sci. Abstr. 31, 607-622.

Kalab M, Emmons DB, Sargant AG. (1975). Milk gel structure. IV. Microstructure of yoghurts in relation to the presence of thickening agents. J. Dairy Res. 42, 453-458.

Kalab M, Emmons DB, Sargant AG. (1976). Milk gel structure. V. Microstructure of yogurt as related to the heating of milk. Milchwissenschaft. 31, 402-408.

Kalab M, Allan-Wojtas P, Phipps-Todd BE. (1983). Development of microstructure in set-type nonfat yogurt - a review. Food Microstruc. 2, 51-66.

Kessler HG, Kammerlehner J. (1982). Factors affecting the stability of natural set yogurt. XXI Int. Dairy Cong. Vol. I, Bk. 1, 283.

Kroger M. (1973). Controlling the quality of yogurt. Dairy and Ice Cream Field. 156, 38-39,61,66-67.

Labropoulos AE, Lopez A, Palmer JK. (1981). Apparent viscosity of milk and cultured yogurt thermally treated by UHT and vat systems. J. Food Prot. 44, 874-876.

Macura D, Townsley PM. (1984). Scandinavian ropy milk - Identification and characterization of endogenous ropy lactic streptococci and their extracellular excretion. J. Dairy Sci. 67, 735-744.

Macy H. (1923). A ropy milk organism isolated from the Finnish "Piima" or "Fiili." J. Dairy Sci. 6, 127-130.

Modler HW, Larmond ME, Lin CS, Froehlich D, Emmons DB. (1983). Physical and sensory properties of yogurt stabilized with milk proteins. J. Dairy Sci. 66, 422-429.

Parnell-Clunies EM. (1986). Influence of heat-induced protein changes in milk on the physical and ultrastructural properties of yogurt. Ph.D. thesis. Univ. of Guelph, Guelph, Ontario, Canada.

Radema L, van Dijk R. (1973). Thickening agents for yogurt. Dairy Sci. Abstr. 36, 449.

Schellhaass SM, Morris HA. (1985). Rheological and scanning electron microscope examination of skim milk gels obtained by fermenting with ropy and non-ropy strains of lactic acid bacteria. Food Microstruc. 4, 279-287.

Steinberg AF. (1979). Yogurt, the Cinderella product. Amer. Dairy Rev. 41, 50F.

Tamime AY, Kalab M, Davies G. (1984). Microstructure of set-style yoghurt manufactured from cow's milk fortified by various methods. Food Microstruc. 3, 83-92.

Van Wazer JR, Lyons JW, Kim KY, Colwell RE. (1963). Viscosity and Flow Measurement. John Wiley and Sons, Inc. NY. 12-17.

Winterton D, Meiklejohn PG. (1978). A modified starch stabilizer for low-cost production of fruit yogurt. Aust. J. Dairy Tech. 33, 55-56.

Discussion with Reviewers

S.M. Schellhaass: Many investigators have observed that incubating at lower than optimum growth temperatures results in increased EPS production. Have you investigated the impact of slower growth conditions (i.e., lower incubation temperatures) on the resistance of the EPS to detachment from the cell surface?

Authors: Rheological measurements and scanning electron microscopy have been conducted on yogurt incubated at higher temperatures (45°C) for comparison to lower temperature incubation (32°C). The higher incubation temperature gave shear stress values that were lower over the entire shear rate range. The micrographs did not clearly indicate that less EPS was present; therefore, this would suggest that lowered resistance to detachment did exist. However, we have not determined the amount recovered when EPS is isolated from yogurt incubated at 45°C versus 32°C.

B.E. Brooker: This study is critically dependent on the ability to image EPS using scanning electron microscopy. Although the so called filaments of EPS are found only in EPS producing strains, what evidence do the authors have that this appearance accurately depicts the polysaccharide in life? If there is no evidence that the polysaccharide is preserved in a natural or near natural state, does this not make the observations in the present paper very difficult to interpret and of doubtful value?

Authors: It is true that we do not know the full effects of electron microscopy preparation techniques, especially the critical point drying, on the exopolysaccharide. However, this conventional SEM method has been used previously on ropy yogurt to obtain similar results (Schellhaass and Morris, 1985).

It has been argued that critical point drying promotes artifacts because the organic solvents may extract gelatinized starch or polysaccharides that are present (Schmidt, 1982; Kalab, 1981). In this research, there are obviously differences occurring in the micrographs during the progression of shear rates. Even if the filaments are not depicted exactly as in their natural state, they will be modified similiarly and there is a significant enough change to warrant the stated observations and conclusions. An alternative method for sample preparation could utilize cryofixation and freeze-fracturing, which would avoid the use of any chemicals (Schmidt, 1982).

R.W. Martin: It remains very difficult to correlate rheology of dairy systems to microstructural characteristics. Are any biochemical or microstructural studies planned to further investigate this correlation?

Authors: No further biochemical or microstructural studies are planned at this time. However, the viscoelastic properties of ropy and nonropy yogurts are being investigated.

Additional References

Kalab M. (1981). Electron microscopy of milk products: A review of techniques. Scanning Electron Microsc. III, 453-472.

Schmidt DG. (1982). Electron microscopy of milk and milk products: Problems and possibilities. Food Microstruc. 1, 151-165.

FOOD STRUCTURE, Vol. 9 (1990), pp. 139-149
Scanning Microscopy International, Chicago (AMF O'Hare), IL 60666 USA

1046-705X/90$3.00+.00

THE ROLE OF CELL WALL STRUCTURE IN THE HARD-TO-COOK PHENOMENON IN BEANS (*PHASEOLUS VULGARIS* L.)

Ilan Shomer*, Nachman Paster, Pinhas Lindner and Rosa Vasiliver

Institute for Technology and Storage of Agricultural Products, Agricultural Research Organization, The Volcani Center, P.O.Box 6, Bet Dagan 50250, Israel.

Abstract

Differences in structure, water uptake and efflux of solubles were found between normal and hard-to-cook beans (*Phaseolus vulgaris* L.). The staining characteristics of hard beans were different from those of the normal in both non-cooked and cooked tissue, especially in the cell walls. The three zones of the cell wall - the middle lamella, the primary and the secondary walls - were found in both normal and hard-to-cook beans. The primary cell wall of both normal and hard beans was partially degraded upon cooking, as seen by bright fields within the fibrillar pattern. The ultrastructure of the non-cooked secondary cell wall was significantly different between normal and hard beans. The middle lamella in normal beans disintegrated upon cooking, while that of hard beans was retained. Hard beans took up less water during soaking but released more solubles to the medium than normal beans.

It is concluded that the resistance of the middle lamella to solubilization upon cooking prevents cell separation, and this results in the hard texture of the hard-to-cook beans.

Initial paper received May 1, 1990
Manuscript received June 20, 1990
Direct inquiries to I. Shomer
Telephone number: 972 3 9683256

KEY WORDS: Bean, Cell wall, Hard-to-cook, Middle lamella, Pectin, *Phaseolus vulgaris*, Ultrastructure.

*Address for correspondence: Ilan Shomer, Institute for Technology and Storage of Agricultural Products, A.R.O., The Volcani Center, P.O.Box 6, Bet Dagan 50250, Israel. Phone No. 972-3-968-3256.

Introduction

The hard-to-cook (HTC) phenomenon in beans manifests itself in prolongation of cooking time, thus reducing the beans' nutritional and textural qualities. This phenomenon, which will be referred to as hardening, was found to be induced by storage at elevated temperatures and high relative humidities (Plhak *et al.*, 1987).

Several suggestions have been given to explain this phenomenon. Varriano-Marston and Jackson (1981) suggested that cytoplasmic changes during storage lead to enhanced cell adhesion, and hence hardening of the beans. Hincks and Stanley (1986, 1987) suggested that polymerization of phenols within the cell wall might lead to bean hardening. Based on the work of Wardrop (1971) and Esau (1977) suggesting that lignin monomers may be secreted into the region of the middle lamella, Varriano-Marston and Jackson (1981) assumed that hardening in beans stored under unfavorable conditions is caused by lignification of the middle lamella. However, no differences were found between normal and hard beans in the degree of lignification, content of tannins and specific activity of peroxidase (Plhak *et al.*, 1987). Histological studies (Varriano-Marston and Jackson, 1981; Jones and Boulter, 1983; Narasimha *et al.*, 1989) revealed differences in the packing density of the cotyledon cells between normal and HTC beans. No evidence relating these changes to specific cell components was presented.

The present study describes the structural changes occurring in the cotyledon tissue of beans as a result of hardening. The involvement of the cell wall, especially the middle lamella, in the hardening phenomenon is described and discussed.

Materials and Methods

Preparation of hard-to-cook beans:

Dry beans (*Phaseolus vulgaris* L. cv. 'Ivory') from local production, stored for about 3 months at ambient temperature and humidity (20-24°C, 50-60% RH) were used for the experiments. The moisture content of the

dry beans, as measured by oven-dry method (Anon., 1966), was 11.5%. Hardness was induced by incubating bean seeds at 42°C and 80% RH (in a desiccator, over a solution of saturated KCl), for 21 days. The incubated beans and a sample of non-treated beans kept at ambient room temperature and humidity were dried to a constant weight at 25°C under reduced pressure (250 mm Hg). The water content of the beans was determined by drying to a constant weight at 70°C at reduced pressure (250 mm Hg). The water content of both samples after drying was 12%.

Soaking and cooking of beans:

Ten g of beans was placed in 100 ml of distilled water in a 250 ml Erlenmeyer flask and shaken at a rate of 50 strokes/min for 18 h at room temperature. The weight of the beans and the volume of the liquid were then determined. The beans were cooked in boiling water at ambient pressure for 30 min; after cooking, distilled water was added to compensate for evaporation. The weight of the beans and the volume of the liquid were then measured. Water uptake was calculated as increase in weight after soaking or cooking, with a correction for the amount of solubles which leaked into the medium from the beans. Leakage of solubles was determined by weighing the residue after lyophilization of 10 ml of soaking or cooking liquid. Hardening was examined by pressing the cooked bean with the fingers; normal beans disintegrated, while the hard-to-cook retained their integrity.

Chemical analyses:

Nitrogen was assayed by the Kjeldahl procedure. Phosphate was analyzed in Kjeldahl digests by a Technicon Automatic Analyzer System (Technicon Corporation, Tarritown, NY). Trichloroacetic acid (TCA) coagulable nitrogen was measured in the precipitates formed by addition of TCA to a final concentration of 15%. Alcohol-insoluble solids (AIS) were precipitated by addition of two volumes of ethanol. The precipitate was washed twice with 70% ethanol, dissolved with 0.05 N NaOH and assayed according to the method of Blumenkrantz and Asboe-Hansen (1973). Total soluble sugars in the soak and cooking water were determined by the phenol-sulfuric acid method (Dubois *et al.*, 1956).

Light and electron microscopy:

Small slices (~1-2 mm^3) from the center of bean cotyledon tissue were fixed in 5% glutaraldehyde in 0.1 M cacodylate buffer (pH 7) for 2 h at 4°C. The slices were then rinsed several times with the same buffer, followed by washing with 0.1 M phosphate buffer (pH 7), postfixed with 2% OsO_4 in the phosphate buffer at 4°C for 2 h, and then washed several times with the phosphate buffer, followed by washing with distilled water. The fixed specimen was dehydrated gradually with ethanol and embedded in Agar 100 Resin (Agar Aid, Cambridge). For light microscopy, sections of ~3µm thickness were prepared by LKB Pyramitome, mounted on a glass slide, and stained with a 10 X diluted solution of toluidine blue and basic fuchsin (0.365 g and 0.135 g, respectively, in 60 mL of 30% ethyl alcohol). For transmission electron microscope (TEM), ultrathin sections were stained with uranyl acetate and lead citrate and examined with a JEOL-100CX TEM at 80 kV.

Results and Discussion

Characteristics of normal and hard-to-cook beans:

Hard-to-cook beans were found to be hard but springy after cooking, while normal control beans stored at room temperature were disintegrated easily when subjected to light finger pressure. The water uptake and efflux of solutes in beans upon soaking and cooking are shown in Tables 1 and 2, respectively. After 18 h of soaking in water, HTC beans took up 20% less water as compared with normal beans. From Table 1 it is seen that HTC beans release approximately tenfold more sugars and nitrogen, and about 45-fold more phosphorus to the soaking water than normal beans. Increased efflux of solubles and lower water imbibition upon soaking of HTC beans were reported by Jones and Boulter (1983). A

Table 1: Uptake of water by, and efflux of solubles from bean seeds soaked in distilled water for 18 h (mg/g dry matter).

Storage conditions	Water uptake	Efflux			
		Sugars[a]	Pectin[b]	Nx6.25[c]	P[d]
	±50	±1	±0.02	±0.5	±0.1
Control	1250	4.0	-	3.0	0.2
42°C at 80% RH[e]	1010	44.0	0.08	24.0	9.0

[a]Total sugars, as glucose, determined by the phenol - sulfuric acid method.
[b]As galacturonic acid
[c]No measurable amount of TCA-coagulable protein
[d]Phosphate
[e]Relative humidity

Figures 1-4. Light micrographs of cross sections of bean cotyledons, stained with toluidine blue and basic fuchsin (S - starch). Fig. 1 - normal bean. Primary cell wall is indicated by sharp arrows and the secondary one by blunt arrows; bar=10 µm. Fig. 2 - cooked normal bean. Primary cell wall is indicated by sharp arrows, and the secondary one by blunt arrows; bar=10 µm. Fig. 3 - non-cooked hard bean. Arrows indicate the cell wall; bar=10 µm. Fig 4 - cooked hard bean. Arrows indicate the cell wall; bar=10 µm.

disparity of views prevails concerning the extent of water uptake of HTC vs normal beans. Thus, Jackson and Varriano-Marston (1981) reported a similar extent of water uptake upon soaking by normal HTC beans. Small amounts of pectin were released from HTC beans upon soaking, while no AIS could be isolated from the soaking water of normal beans. From Table 2, it could be seen that after cooking for 30 min, there was twofold greater water uptake in normal beans than in HTC beans.

Table 2: Uptake of water by, and efflux of solubles from soaked bean seeds during cooking for 30 min (mg/g dry matter).

Storage condition	HTC	Water uptake	Efflux				
			Sug[a]	Pec[b]	Nx6.25 Total	Prot[c]	P[d]
		±50	±1	±0.2	±0.5	±0.1	±0.5
Control	-	520	75	1.8	23.0	3.9	5.8
42°C at 80%RH[e]	+	260	7	t[f]	5.0	0.82	t[f]

[a]Total sugars, as glucose, determined by the phenol-sulfuric acid method

[b]As galacturonic acid.

[c]TCA coagulable protein.

[d]Phosphate

[e]Relative humidity.

[f]Traces

Efflux of carbohydrates, nitrogen and phosphorus was now higher in normal beans. Normal beans released pectin and TCA-coagulable nitrogen (protein) upon cooking. The increased efflux of solubles from HTC beans upon soaking indicates damage caused to the plasmalemma during the storage under adverse conditions. The reduced water uptake by HTC beans upon soaking may be ascribed to partial loss of semipermeability of the plasmalemma as well as to changes in high molecular weight components like pectic material or in intracellular storage proteins. Chemical changes leading to increased crosslinkage, or reduced hydrophilic character of these components will reduce their capacity to take up water during imbibition as well as during the cooking processes.

Light microscopy:

Light microscope observations showed that in cooked normal beans the cells of the cotyledon tissue tend to separate from each other (compare Figs. 1 and 2). However, in cooked HTC beans, cell adhesion and tissue integrity were retained (Figs. 3, 4). These findings are in agreement with those of other studies (Varriano-Marston and Jackson, 1981; Narasimha *et al.*, 1989 Plhak *et al.*, 1989), but the present results revealed distinct differences in the staining characteristics between tissue sections of normal and HTC beans. The most marked differences appeared in the cell walls. In HTC beans all of the cell wall regions were stained intensively (Figs. 3,4).

In the cooked beans, differences also were observed in the staining intensity of starch granules between normal (Figs. 1,2) and HTC (Figs. 3,4) beans. The integrity of starch grains and the residual birefringence observed under polarization microscopy of both normal and HTC beans suggest that starch was not entirely gelatinized upon cooking.

The differences in staining properties of the cell wall indicate a difference in the cell wall characteristics and composition between normal and HTC beans. A detailed study of the ultrastructure of the cell wall was therefore undertaken.

Electron Microscopy:

a. **Non-Cooked Beans:** The ultrastructure of cell walls in swollen normal beans before cooking is shown in Figures 5-9 Usually, the cell wall consists of three distinct regions: the outer region of the middle lamella, the middle region of the primary cell wall, and the innermost region of the secondary cell wall (Fig. 5). Facing the intercellular spaces the middle lamella is thicker, while it is thinner in the adhesion zone between the cells. A higher magnification of the middle lamella in the adhesion zone is shown in Figure 9. In many cases the middle lamella is so thin that it cannot be identified by ultrastructural observation.

The secondary cell wall is thick, adjacent to the intercellular space (Fig. 5), pits (Fig. 6) and disconnection zone (Figs. 7). The detailed structure of the secondary wall with three zones is shown in Figure 8. In cells of non-cooked normal beans the thick region of the secondary wall has a reticulated pattern, with an internal layer of dense structure (Figs. 5-8).

Higher magnification revealed that the structural elements of the reticulum are tubular. This reticulum seems to be embedded in a sparse microfibrillar matrix

Figures 5-9. Ultrathin sections of cotyledons of normal bean. The region of the cell wall includes the middle lamella (ML), primary cell wall (W) and secondary wall (S) with its outer, middle and inner layers (I, II, III, respectively). Figs. 5-7 - The secondary wall found usually adjacent to the intercellular space (ICS), pit (Pit) and disconnecting area (DC). Protein bodies (PB) seen in the cytoplasm (Cy); bar=1 µm. Fig. 8 - High magnification of the secondary cell wall shows reticulum (R), with its cross view seen as a tubular structure (arrows). The reticulum seems to be embedded in a fine fibrillar matrix (FM); bar=10 µm. Fig. 9 - High magnification of the middle lamella (ML) and the primary cell walls (W); bar=0.2 µm.

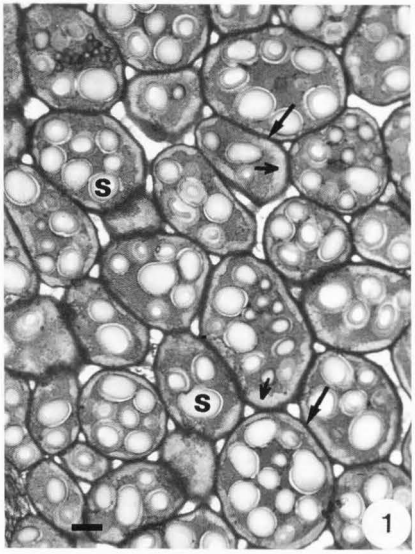
S
S
1

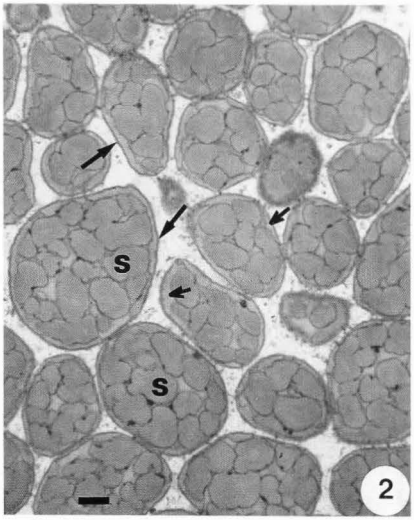
S
S
2

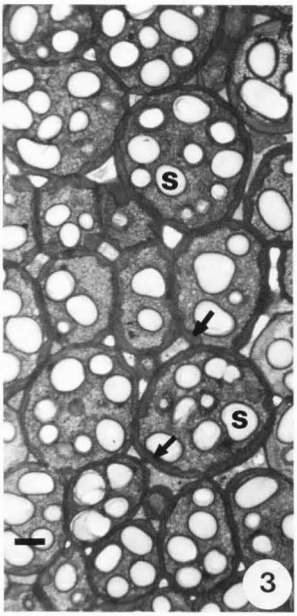
S
S
3

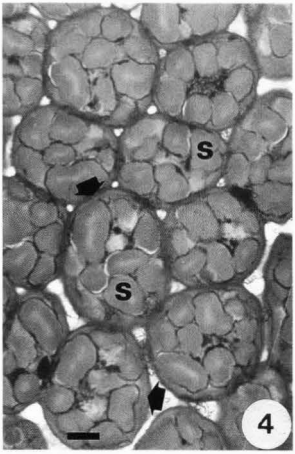
S
S
4

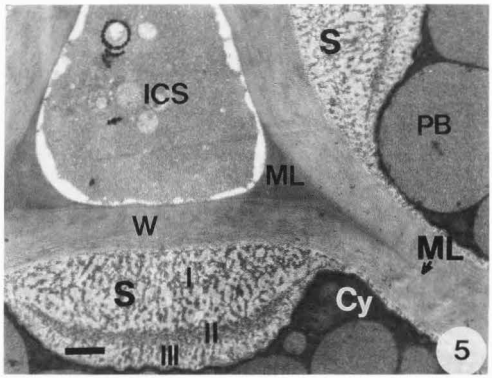
ICS
S
PB
ML
W
ML
S
I
II
III
Cy
5

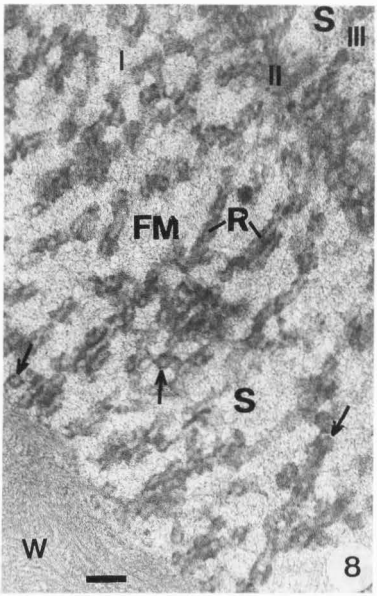
S
III
I
II
FM
R
S
W
8

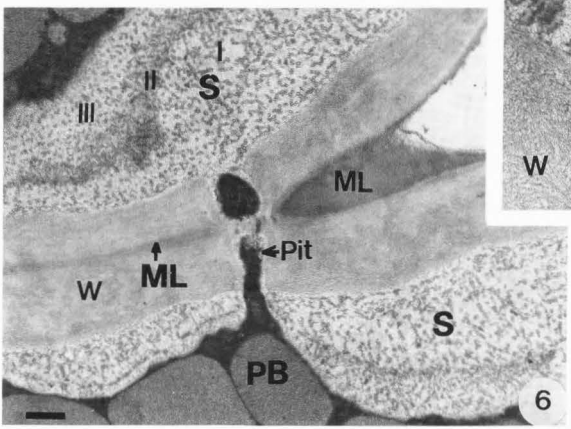
I
II
S
III
ML
Pit
ML
W
S
PB
6

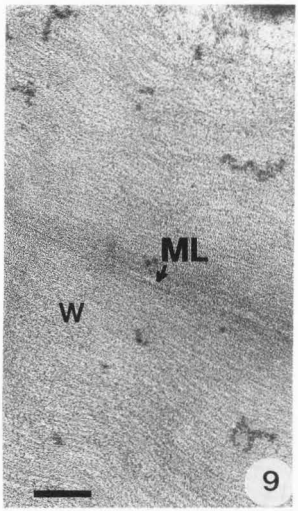
ML
W
9

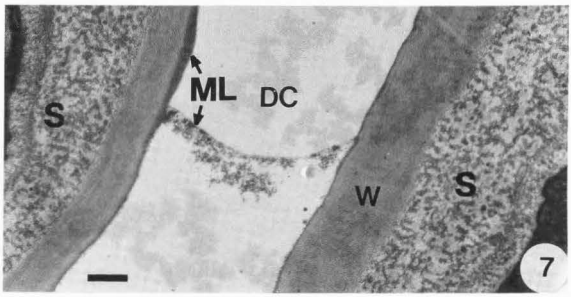
ML
DC
S
W
S
7

(Fig. 8). The zone of the secondary wall shows densely packed tubules.

The cell walls of the non-cooked HTC beans differed from those of the normal beans in their ultrastructure, especially in the secondary cell wall (Fig. 10). The secondary wall is seen also adjacent to pits (Figs. 10,11). The typical reticular pattern of the secondary cell wall is not seen; instead, there appears a pattern of scattered tubuli with fibrillar connections (Figs. 11-13). A similar but less organized pattern is observed in the innermost region of the secondary cell wall (Figs. 13,14).

b. Cooked beans: The cooking process caused significant changes in the cell wall structure of normal beans. The primary cell wall is the most resistant part of the cell wall with respect to structural changes occurring upon cooking (Figs. 15-17), although many weakly stained locations are seen within its fibrillar pattern. It appears that in these locations the cell wall material was degraded upon cooking. The ultrastructure of the normal secondary cell wall (Figs. 5-8) changed dramatically as a result of cooking (Figs. 17,18). The middle lamella became loosened (Figs. 15,19,20). Detailed observations showed two typical zones from which the middle lamella was changed by the cooking process: (i) zones in which adjacent cells are attached to each other (Fig. 16), where the boundary between the cells is not seen clearly, because of the removal of the middle lamella; and (ii) zones in which cell separation is seen clearly and where the residues of the middle lamella are still observed (Figs. 19,20).

The most prominent change in the cell wall as a result of cooking appeared in the secondary wall. The typical reticular structure in non-cooked beans (Figs. 5-8) was lost, and replaced by an amorphous structure embedded within a fibrillar network (Figs. 15-18). The central zone of the secondary wall, where densely packed tubules were visible before cooking, are seen now as masses of dense amorphous matter (compare Figs. 15,18 with Figs. 5,8).

The secondary cell wall of cooked HTC beans (Figs. 21-23) is similar to that of cooked normal beans (Fig. 18). However, in cooked HTC beans the middle lamella retained its integrity (Figs. 21,24-26). In these specimens the primary cell wall contains weakly stained locations (Figs. 21,26), as was observed in the cooked normal beans (Figs. 15-17).

It appears that although part of the primary cell wall is removed as a result of cooking, the middle lamella is retained and still functions as a cementing agent which prevents cell separation upon cooking. This evidence supports the suggestion of Varriano-Marston and Jackson (1981) that the middle lamella is involved in reducing the cooking quality of beans. A possible mechanism by which the middle lamella becomes insoluble was suggested by Jones and Boulter (1983), who showed that during storage under conditions leading to HTC, phytate is partially hydrolyzed and pectin is de-esterified. This results in formation of calcium magnesium pectate, which may insolubilize the middle lamella.

The present study demonstrates in structural details the significance of the middle lamella in the HTC phenomenon. The results of Jones and Boulter (1983) suggests that HTC is due to changes in properties of the pectic components rather than deposition of lignin. Although Hincks and Stanley (1987) provided tentative evidence for lignification of cell wall in hard-to-cook beans, in a later study of Srisuma *et al.* (1988), no significant differences in lignin content were detected between normal and hard-to-cook beans.

Conclusions

The primary and the secondary cell walls respond to cooking similarly in both normal and HTC beans. In contrast, the middle lamella of normal beans is degraded. In HTC beans the middle lamella remains intact in spite of cooking, and hence it prevents cell separation and is thus responsible for the HTC phenomenon. However, the mechanism by which the middle lamellar components become insoluble during storage under unfavorable conditions is still unknown.

The involvement of other cellular components such as lignin, phenols, starch granules and proteins in the HTC phenomenon has not yet been elucidated.

Acknowledgements

Contribution from the Agricultural Research Organization, Bet Dagan, Israel. No. 2817-E, 1989 series. The authors thank Mr. Dan Shavit for the high quality photographs, Dr. Andre Frank for the use of EM, and Mrs. Rina Granit for her technical assistance.

References

Anon (1966) International rules for seed testing. *Proc. Int. Seed Testing Assoc.* Wageningen Netherlands.

Figures 10-14. Ultrathin section of the cotyledon of a hard-to-cook bean. Fig. 10 - The area of intercellular space (ICS) with primary (W) and secondary (S) cell walls and pit (Pit), where the middle lamella (ML) seen clearly near the intercellular space. The cytoplasm (Cy) is seen as dark matrix with starch grains (St); bar=2 μm. Fig. 11 - High magnification of the primary wall (W) and the secondary wall (S) adjacent to the pit (Pit); bar=0.2 μm. Figs. 12-14 - High magnification of the primary cell wall (W) and the outer (OS), middle (S) and inner (IS) secondary cell walls, with tubuli (arrows) and the fibrillar connecting system (F). (Fig. 12 bar=0.2 μm; Figs. 13, 14 bar=0.1 μm.

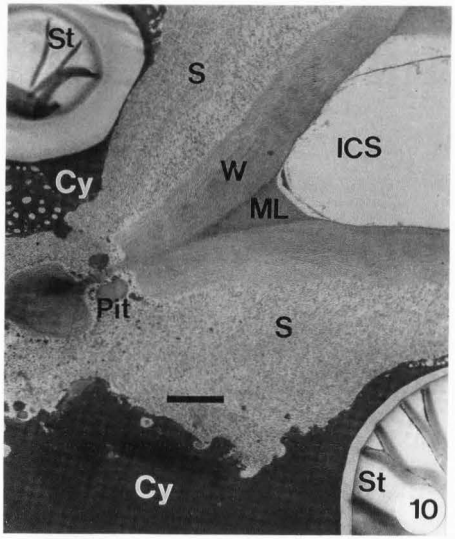
St
S
ICS
W
Cy
ML
Pit
S
Cy
St
10

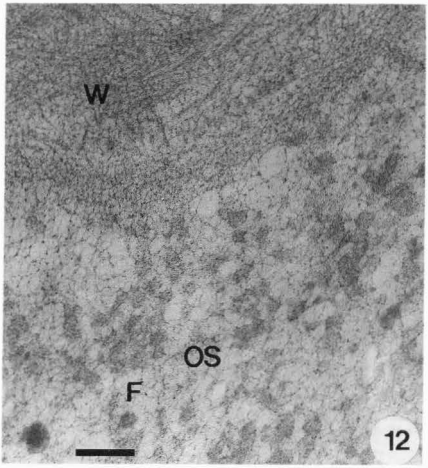
W
OS
F
12

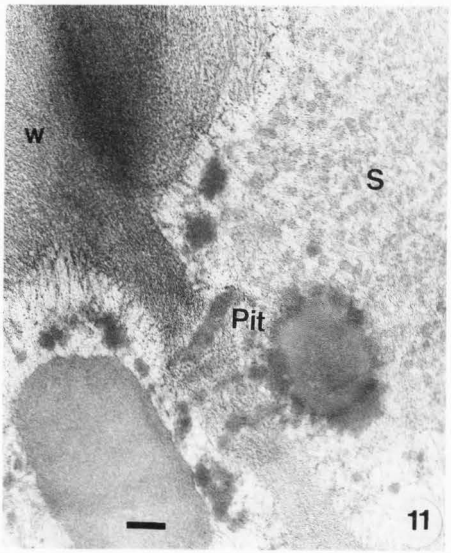
W
S
Pit
11

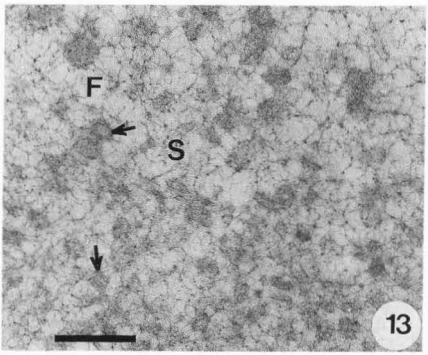
F
S
13

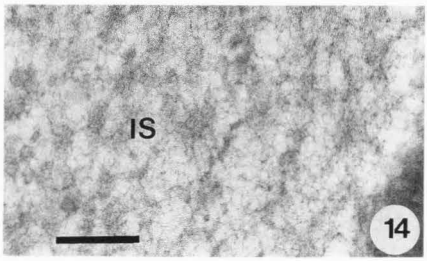
IS
14

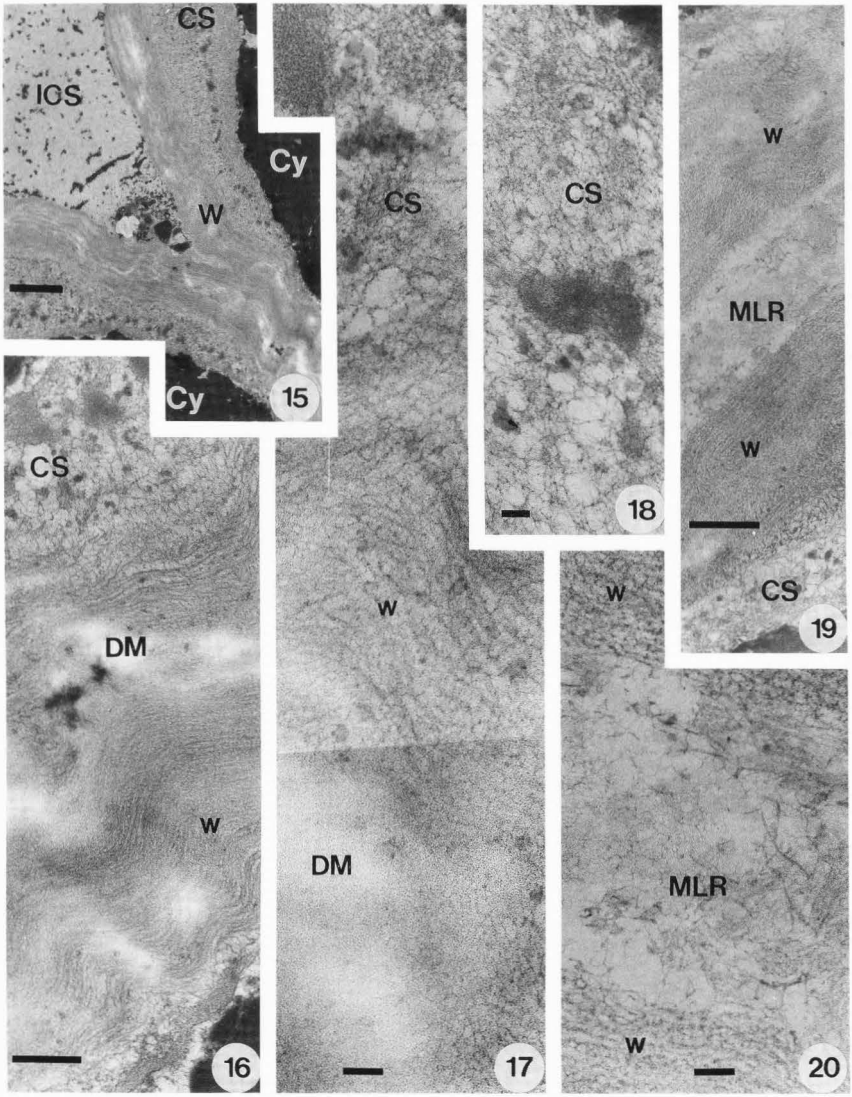
CS
IOS
Cy
W
Cy
15
CS
DM
W
16
CS
W
DM
17
CS
18
W
MLR
W
CS
19
W
MLR
W
20

Blumenkrantz N, Asboe-Hansen G (1973) New method for quantitative determination of uronic acids. *Anal. Biochem.* **54**, 484-489.

Dubois M, Gilles KA, Hamilton JK, Rebers PA, Smith F (1956) Colorimetric method for determination of sugars and related substances. *Anal. Chem.* **28**, 350-356.

Esau K (1977) *Anatomy of Seed Plants*, 2nd edn. John Wiley and Sons, New York.

Hincks MJ, Stanley DW (1986) Multiple mechanisms of bean hardening. *J. Food Technol.* **21**, 731-750.

Hincks MJ, Stanley DW (1987) Lignification: evidence for a role in hard-to-cook beans. *J. Food Biochem.* **11**, 41-58.

Jackson GM, Varriano-Marston E (1981) Hard-to-cook phenomenon in beans: effect of accelerated storage on water absorption and cooking time. *J. Food Sci.* **46**, 779-803.

Jones PMB, Boulter D (1983) The cause of reduced cooking rate in *Phaseolus vulgaris* following adverse storage conditions. *J. Food Sci.* **48**, 623-626, 649.

Narasimha HV, Srinivas T, Desikachar HSR (1989) A histological basis for "hard-to-cook" phenomenon in red gram (*Cajanus cajan*) cultivars. *J. Food Sci.* **54**, 125-131.

Plhak LC, Stanley DW, Hohlberg AI, Aguilera JM (1987) Hard-to-cook defect in black beans - effect of pretreatment and storage condition on extractable phenols and peroxidase activity. *Can. Inst. Food Sci. Technol. J.* **20**, 378-382.

Plhak LC, Caldwell KB, Stanley DW (1989) Comparison of methods used to characterize water imbibition in hard-to-cook beans. *J. Food Sci.* **54**, 326-329.

Srisuma, N, Hammerschmidt R, Uebersax MA, Ruengsakulrach S, Bennink MR, Hosfield GL (1989) Storage induced changes of phenolic acids and the development of hard-to-cook in dry beans (*Phaseolus vulgaris*, var. Seafarer). *J. Food Sci.* **54**, 311-314, 318.

Varriano-Marston E, Jackson GM (1981) Hard-to-cook phenomenon in beans: structural changes during storage and imbibition. *J. Food Sci.* **46**, 1379-1385.

Wardrop AB (1971) Occurrence and formation in plants. In: *Lignins*, KV Sarkanen, CH Ludwig (eds), pp. 19-41. John Wiley and Sons, New York.

Figures 15-20. Ultrathin section of cotyledon of a cooked normal bean. Fig. 15 - The primary cell wall (W) seen with weakly stained locations. The cooked secondary cell wall (CS) seen beside dark cytoplasm (Cy); bar=2 μm. Figs. 16-18. High magnification of the primary (W) and secondary (CS) cell walls. The weakly stained locations (DM) indicate partially dissolved primary cell wall (Fig. 16 bar=0.5 μm; Fig. 17 bar=0.1 μm; Fig. 18 bar=0.1 μm). Figs. 19, 20 - Primary (W) and secondary (CS) cell wall where residues (MLR) of the middle lamella are seen between adjacent cells (Fig. 19 bar=1 μm; Fig. 20 bar=0.1 μm).

Discussion with reviewers

M.C. Bourne: Do you believe that the skin (pericarp) of the bean seeds affects the hard-to-cook behavior?
Authors: Cotyledons cooked without the pericarp exhibit the HTC phenomenon as does the whole bean.

M.C. Bourne: What effects would you expect if the beans were stored at 42°C, 80% RH for periods much longer than 21 days?
Authors: We do not expect significant effects on the aspects studied by us. The beans would continue to be hard and the ultrastructural differences between normal and HTC beans would probably remain the same. The procedure to induce hardness was an accelerated one according to Varriano-Marston and Jackson (1981). The hardness induced shows properties of HTC which, according to the literature, were obtained by longer storage at high humidity but at a lower temperature, 30-35°C. However, all normal beans softened during 30 min of cooking.

M.A. Uebersax: What structural changes may have occurred during the initial drying process of the seed which could influence the observed results?
Authors: The initial drying process was not studied by us.

M.A. Uebersax: Do other studies exist to address these changes?
Authors: Other studies dealing with these changes are mentioned in the manuscript. However, these studies have not identified ultrastructural details as revealed by TEM in the present study.

M.A. Uebersax: Can the authors better describe the textural characteristics of these beans to enable better interpretation of the results and provide improved understanding of the extent or condition of hardening present in these beans.
Authors: The present study did not deal with physical measurements of texture. From our point of view it was important to determine whether the beans were soft or hard. The differences between HTC and normal beans were so obvious that the simple assay specified in the experimental section distinguished between them distinctly.

Reviewer III: Did the authors find any evidence for membrane disruption? No consistent trend has been shown in the literature regarding water absorption by hard and soft beans. The difference in water uptake between soft and hard beans however, was even more pronounced following 30 min cooking even though the cooking process disrupted plasma membranes to an even greater extent than storage at adverse conditions. This is supported by the increasing losses of soluble solids to the cooking water reported by the authors and would indicate that a factor other than membrane semipermeability may play an important role in the differences in water uptake between soft and hard beans. This factor may be related to the increased rigidity of cell walls and restricted swelling of hard-to-cook beans during soaking and cooking compared to nondefective samples.
Authors: Leakage of intracellular low molecular weight constituents from HTC beans into the soak water is an indication for damage to the plasma membrane. During cooking, the greater extent of leakage from normal beans compared to the HTC ones, indicates destruction of the plasmalemma of normal beans (the low molecular weight constituents having already leaked out from the HTC beans during the soaking before cooking). The inconsistent trend in the literature with respect to the extent of water imbibition of HTC beans is probably also due to the different ways it is reported. Not always are all the data necessary to correlate among various presentations reported unambiguously. Reduced water uptake by cooked HTC beans may also be the result of changes affecting the hydration capacity of the insoluble matrix of the bean tissue.

Reviewer III: What does the difference in staining ability mean?
Authors: A mixture of toluidine blue and basic fuchsin is known to be a multistain adsorbed by various cell components. The staining differences between the treatments indicate changes in the adsorption properties of some cell constituents, as can be seen in the light micrographs. For example, starch stained mainly after cooking, and this probably indicates adsorption of dye as a result of partial gelatinization and swelling. The secondary cell wall was stained intensively in HTC beans, and its ultrastructure was also distinctly different from that of normal beans. This indicates chemical and structural changes of these cellular components.

Reviewer III: What is the role of changes in secondary cell walls on the development and manifestation of the hard-to-cook defect?
Authors: We don't know. This has to be studied, as well as other aspects which can be elucidated by anatomical and ultrastructural work.

Reviewer III: It is difficult to agree with the identification of the middle lamella being as thin as claimed. The microscopic procedures used are well known to impart artifacts which could explain some of these results.
Authors: From the ultrastructural photomicrographs it can be seen that distinct differences exist in the middle lamellar zone after (rather than before) cooking between HTC and normal (control) beans. Furthermore, variable thicknesses have been observed along the middle lamella in the contact zones of adjacent cells.

Figures 21-26. Ultrathin sections of the cotyledon of a cooked hard-to-cook bean. Fig. 21 - The primary (W) and secondary (CS) cell walls are seen beside dark cytoplasm (Cy) and starch (S), where the middle lamella (ML) is seen undegraded in the adhesion zone between adjacent cells. Weakly stained locations (DM) indicate a partially dissolved cell wall matrix; bar=1 µm. Figs. 22, 23 - high magnification of secondary cell wall beside the primary cell wall (W) and the cytoplasm (Cy); bar=0.1 µm. Figs. 24-26 - High magnification of the middle lamella (ML) in several thicknesses between primary walls (W) of adjacent cells. While the middle lamella is seen undamaged, weakly stained locations appear in the primary wall matrix (Fig. 24 bar=0.1 µm; Fig. 25 bar=0.5 µm; Fig. 26 bar=0.5 µm).

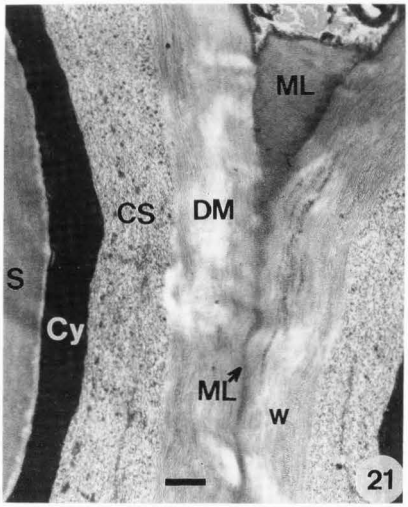
ML
CS
DM
S
Cy
ML
W
21

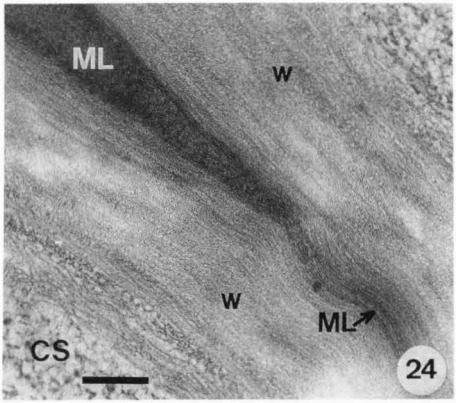
ML
W
W
ML
CS
24

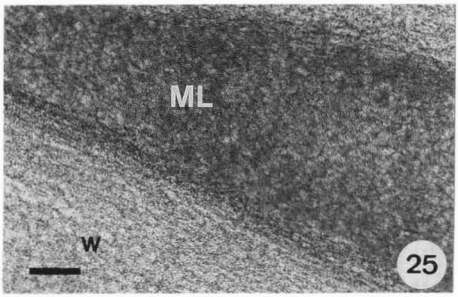
ML
W
25

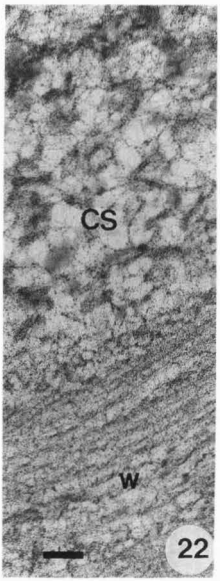
CS
W
22

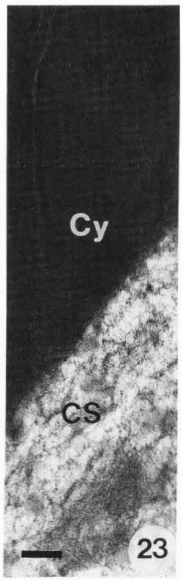
Cy
CS
23

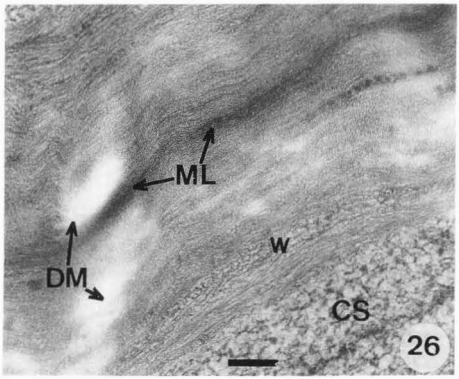
ML
W
DM
CS
26

FOOD STRUCTURE, Vol. 9 (1990), pp. 151-154
Scanning Microscopy International, Chicago (AMF O'Hare), IL 60666 USA

1046-705X/90$3.00+.00

TECHNICAL NOTE

ENCAPSULATION OF VISCOUS HIGH-FAT FOODS IN CALCIUM ALGINATE GEL TUBES AT AMBIENT TEMPERATURE

Ivan A. Veliky and Miloslav Kalâb *

Division of Biology, National Research Council of Canada
Ottawa, Ontario, Canada K1A OR6, and
*Food Research Centre, Research Branch, Agriculture Canada, Ottawa, Ontario, Canada K1A OC6

Abstract

Viscous high-fat foods such as cream, egg yolk, or mayonnaise are co-extruded with a 3% sodium alginate solution from a syringe into a 50 mM calcium chloride solution. The food sample passes through the inner tube of a double needle assembly while the alginate solution is simultaneously extruded through a mantle surrounding the inner needle. As the sodium alginate solution forms a gel on contact with calcium ions, the food sample becomes encapsulated in the calcium alginate gel formed on the surface of the food sample. The encapsulation procedure may be carried out within a temperature range between 0°C and 25°C. Samples may be prepared for scanning electron microscopy or for transmission electron microscopy by selecting either wide or narrow bore needles, respectively.

Initial paper received April 6, 1990
Manuscript received June 15, 1990
Direct inquiries to M. Kalab
Telephone number: 613 995 3722 ext. 7707

Key Words: Alginate, Coating, Electron microscopy, Encapsulation, Gel tubes, High-fat foods.

Introduction

The original procedure for the encapsulation of suspensions and dispersions of biological origin in agar gel tubes designed by Salyaev [7] has been modified by several authors for use with foods [3-6]. In a recent modification [6], the sample is aspirated into a glass Pasteur pipette, the lower end of the pipette is sealed with agar gel, and the pipette is repeatedly dipped into a warm (40°C) agar sol to form a sleeve around the Pasteur pipette. The sample is then transferred into the agar gel tube by pulling the Pasteur pipette out. In the *Discussion with Reviewers* in paper [6] Dylewski noted that the microstructure of some heat-sensitive high-fat foods may be affected by repeatedly dipping the food in the pipette into the warm agar sol. In order to reduce the exposure to heat, Goff (personal communication) has been using low-temperature gelling agarose for this purpose. Viscous foods may also be aspirated into agar gel tubes made around glass or metal rods [5] using the rod as a piston, and, thus, avoiding the exposure of the foods to heat, but this procedure is more difficult to perform than the former procedure [6]. In particular, it is difficult to properly seal both ends of the agar gel tubes following their contamination with fat.

A different approach is possible by using a sodium alginate solution which forms a gel on contact with calcium ions. This reaction makes it possible to instantly encapsulate viscous food samples at any temperature between 0°C and room temperature (~25°C) and is the subject of this technical note.

Materials and Methods

Sodium alginate (BDH Chemicals, Ltd., Poole, England) was dissolved in distilled water to form 2 to 4% solutions. Calcium chloride, 0.1 to 1.0 M solution, was mixed with a 2.5% glutaraldehyde solution (1:9, v/v) and the pH was adjusted to 6.5 using 0.2N NaOH.

High-fat food (egg yolk, cream, or mayonnaise) destined for examination by scanning electron microscopy (SEM)

was placed in a 5-mL syringe and a double needle assembly was attached to it. The double needle assembly consisted of an inner needle (~1 mm inner diameter) concentrically positioned inside an outer stainless steel tube (mantel) with a 0.3-mm gap between both tubes (Fig. 1). Three ribs, each 3 mm long, were soldered on the inner tube, 5 mm from the tube end, as spacers in order to maintain concentric position of both needles. Another 5-mL syringe filled with the sodium alginate solution was attached to the outer needle (Figs. 1 and 2). Both the food and the alginate solution were manually simultaneously extruded into the calcium chloride solution.

The long column of the encapsulated food (Fig. 3) was examined under a dissecting microscope and the best parts were cut into 10-15 mm sections as soon as the calcium alginate tubes were firm enough to be handled, *i.e.*, within 1-2 min. The food-containing gel tube was compressed with a pair of fine tweezers and cut at that location with a scalpel. The wet cut surface was blotted with paper tissue, covered with a droplet of the sodium alginate solution, and this droplet was gelled using a droplet of the calcium chloride solution, thus sealing the food inside the cut gel tube. These shorter sections were washed with a 50 mM calcium chloride solution, pH 6.5, and postfixed for 24 h at 6°C with a 2% osmium tetroxide solution made up in a combined imidazole and veronal-acetate buffer [1] in order to retain fat. The samples were then dehydrated in a graded ethanol series and freeze-fractured [1]. The fragments were immediately critical-point dried from carbon dioxide in a Samdri 3PVT apparatus; the heater of this apparatus was switched off at 35°C in the final step of drying. The dried sample fragments were mounted on aluminum stubs using a silver-based cement, coated with gold in a Technics Hummer II sputter coater, and examined at 20 kV in an ISI DS-130 scanning electron microscope equipped with an external oscilloscope [2]. Micrographs were taken on 35-mm 100 ASA film.

For transmission electron microscopy (TEM), the foods were prepared in two ways. Provided that fixation and dehydration sufficiently hardened the samples, they were cut into smaller (< 1 mm3) particles for embedding in a Spurr's low-viscosity medium (J.B. EM Service, Inc., Pointe Claire-Dorval, Quebec, Canada). Otherwise, a similar encapsulating apparatus was used but the diameter of the inner needle was reduced to <0.5 mm and the diameter of the outer needle was adjusted accordingly. Pulsed extrusion resulted in small encapsulated beads rather than tubes. The beads were better suited for TEM and were postfixed, dehydrated, and embedded in the same way as other solid samples [1].

Results and Discussion

Co-extrusion of high-fat food and a sodium alginate solution through concentric needles into a calcium chloride solution, which contained glutaraldehyde as a fixative, resulted in the encapsulation of a long column of the food under study in a calcium alginate gel (Fig. 3). The end of the double concentric needle assembly should be about 5 mm above the calcium chloride solution; if it is too low, the gel may form at the needle outlet and clog the needle. The diameter of the food column and the thickness of the calcium alginate coating depend on the diameters of the needles and the rates at which each of the two components are extruded: rapid extrusion of the alginate solution and slow extrusion of the viscous food produce a thick gel coating on a relatively thin food column. If the extrusion rates are reversed, an uneven gel coating may develop on the food column and the column may disintegrate in the calcium chloride solution. The optimum conditions founds were a 3% sodium alginate and 0.05 M calcium chloride solutions. The rate of extrusion varies with the consistency of the food under study and should be established experimentally.

The need to seal the food under study following the division of the long column into shorter segments is easy to meet. Compared to an agar gel coating, which is brittle, the calcium alginate coating is elastic; the cut may be sealed with a droplet of the sodium alginate solution by gelation.

Freeze-fractured cream samples which had been encapsulated for SEM, postfixed with a 2% osmium tetroxide solution in a buffered imidazole solution are shown in Fig. 4. The calcium alginate gel adhered to the samples through all treatment steps. In comparison with the *dipping* procedure using agar for encapsulation [6], no difference could be found between samples encapsulated according to this procedure and samples encapsulated in calcium alginate gels. The co-extrusion method, however, has been developed to provide an alternative to the agar gel encapsulation and to prevent exposure of heat-sensitive food samples to an elevated temperature before fixation.

Acknowledgments

Skillful technical assistance provided by Miss Gisèle Larocque is acknowledged. The authors thank Mrs. Paula Allan-Wojtas and Dr. D. N. Holcomb for useful suggestions. Electron Microscope Unit, Research Branch, Agriculture Canada in Ottawa provided facilities. Contribution NRCC No. 31643 from the National Research Council of Canada and Contribution 857 from the Food Research Centre.

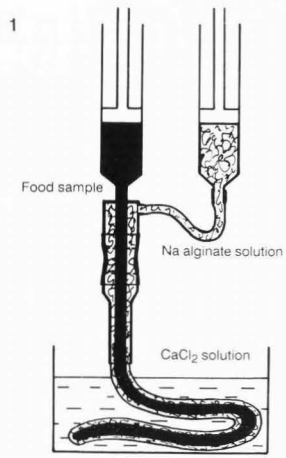

Fig. 1. Diagram of the apparatus for the encapsulation of viscous food samples in calcium alginate gel tubes by co-extruding the food samples with a 3% sodium alginate solution into a 50 mM calcium chloride solution.

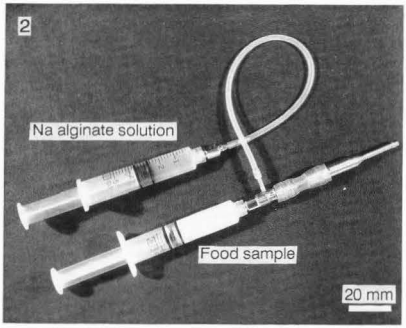

Fig. 2. A photograph of the encapsulation apparatus.

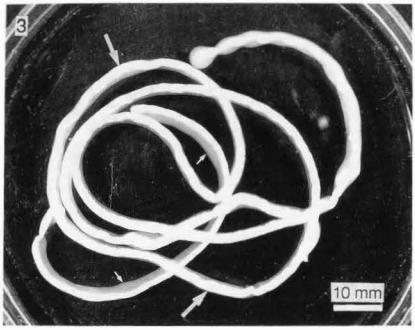

Fig. 3. Cream (large arrows) encapsulated an calcium alginate gel (small arrows). The long and curled encapsulated column will be cut into shorter sections for freeze-fracturing.

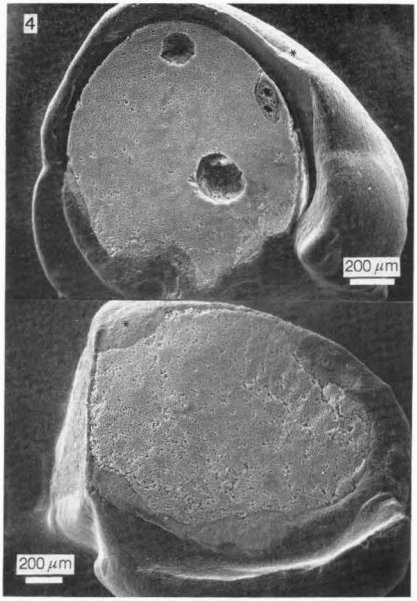

Fig. 4. SEM of 2 freeze-fractured cream samples shows smooth fracture planes and adherence of the alginate gel (*) capsules to the samples.

References

1. Allan-Wojtas P, Kaláb M. (1984). Milk gel structure. XIV. Fixation of fat globules in whole-milk yoghurt for electron microscopy. Milchwissenschaft **39**(6), 323-327.
2. Bond EF, Kaláb M. (1988). An external oscilloscope improves photography with the ISI DS-130 scanning electron microscope. Electron Microsc. Soc. Am. Bull. **18**(1), 90-91.
3. Henstra S, Schmidt DG. (1970). The microcapsule technique. An embedding procedure for the study of suspensions and emulsions. LKB Application Note No. 150.
4. Jewell GG. (1981). The microstructure of orange juice. Scanning Electron Microsc. **1981**;III:593-598.
5. Kaláb M. (1987). Encapsulation of viscous suspensions in agar gel tubes for electron microscopy. Electron Microsc. Soc. Am. Bull. **17**(1), 88-89.
6. Kaláb M. (1988). Encapsulation of viscous foods in agar gel tubes for electron microscopy. Food Microstruc. **7**(2), 213-214.
7. Salyaev RK. (1968). A method of fixation and embedding of liquid and fragile materials in agar microcapsulae. Proc. 4th Europ. Reg. Conf. Electron Microsc. Rome, Tipografia Poliglotta Vaticana, Rome, Italy, **II**, 37-38.

Discussion with Reviewers

Reviewer 1: What effect could calcium ions have on the food under study?

Authors: With milk products, calcium has been recommended as an ingredient in buffered fixatives by several authors [9, 12, 13] in order to maintain the integrity of the casein micelles. The concentration of calcium ions penetrating the food sample may be reduced by transferring the encapsulated food column into a glutaraldehyde solution containing 5 mM $CaCl_2$.

Reviewer 1: May any liquid food sample be examined by electron microscopy using the encapsulation technique described?

Authors: There are reports in the literature that this is possible [10, 11], but other authors mentioned problems encountered with milk [8]. Although milk may be encapsulated, the distribution of the casein micelles is affected by fixation with glutaraldehyde and the removal of the soluble components of the milk serum. When the serum is replaced with ethanol during dehydration, the fixed casein micelles sediment in the capsules irrespective whether they consist of agar or calcium alginate gels.

Additional References

8. Carroll RJ, Basch JJ, Phillips JG, Farrell HM Jr. (1985). Ultrastructural and biochemical investigations of mature human milk. Food Microstruc. **4**(2), 323-331.
9. Harwalkar VR, Allan-Wojtas P, Kaláb M. (1989). Effect of heating to 200°C on casein micelles in milk: A metal shadowing and negative staining electron microscope study. Food Microstruc. **8**(2), 217-224.
10. Henstra S, Schmidt DG. (1974). Ultradünnschnitte aus Milch mit Hilfe der Mikrokapselmethode [Ultrathin sections of milk by means of the microcapsulation method]. Naturwissenschaften **57**(5), 247 (in German).
11. Kaláb M. (1983). Electron microscopy of foods. In: Physical Properties of Foods. M Peleg and EB Bagley (eds), AVI Publishing Co., Inc., Westport, CT, USA, 43-104.
12. Nitschmann H. (1949). Elektronenmikroskopische Grössenbestimmung der Calciumcaseinatteilchen in Kuhmilch [Electron microscopic determination of calcium caseinate particles in bovine milk]. Helv. Chim. Acta **32**, 1258-1264 (in German).
13. Rose D, Colvin JR. (1966). Appearance and size of micelles from bovine milk. J. Dairy Sci. **49**, 1091-1097.

FOOD STRUCTURE, Vol. 9 (1990), pp. 155-173
Scanning Microscopy International, Chicago (AMF O'Hare), IL 60666 USA

1046-705X/90$3.00+.00

FOOD MICROSTRUCTURE --CUMULATIVE INDEX

D. N. Holcomb

Kraft General Foods Technology Center,
801 Waukegan Road,
Glenview, IL, USA 60025
Telephone: 708 998 3724

Introduction

Papers dealing with food microstructure have been published by Scanning Microscopy International (previously Scanning Electron Microscopy, Inc.-SEM, Inc.) for the past eleven years. For the years 1979, 1980 and 1981, the papers were initially published in the journal, Scanning Electron Microscopy. Those papers were also collected in the volume, "Studies of Food Microstructure", published by Scanning Electon Microscopy, Inc. in 1981. Beginning in 1982 and continuing through 1989, the papers were published in the biannual journal, Food Microstructure. In 1990, this journal's title has been changed to Food Structure and it is now published quarterly. At the time of this change, it seems appropriate to publish a cumulative bibliography of these food microstructure papers which have been published over the past eleven years to help readers to access that information.

The 243 references are listed first alphabetically by the first authors' last names. For each paper, the authors' names and year of publication are followed by the paper title; then by the journal citation. Finally, the "key words", which were used in making the subject index, are listed. The title and list of key words will help the reader determine the content of a paper. This list of names is followed by an author index and finally by the subject index. In the subject index, key words are listed alphabetically along with the numbers of the references which include those key words. Many of the key words were provided by the authors in their papers; additional subjects have been added for this bibliography. The reader should not assume that all appropriate key words from all papers have been included here; we have tried to be comprehensive, but have probably made some omissions.

Initial paper received May 15, 1990
Manuscript received June 15, 1990
Direct inquiries to D.N. Holcomb
Telephone number: 708 998 3724

KEY WORDS: Adulteration, carbohydrates, dairy products, fats, fluorescence microscopy, index, light microscopy, meat products, packaging, plant products, scanning electron microscopy, subject listing, transmission electron microscopy, X-ray microanalysis.

Abbreviations used

Abbreviation	Definition
LFRA	Leatherhead Food Research Association
LM	Light microscopy
SEM	Scanning electron microscopy
TEM	Transmission electron microscopy
XRD	X-ray diffraction
NMR	Nuclear magnetic resonance
ESR	Electron spin resonance

References

1. Agbo GN, Hosfield GL, Uebersax MA, Klomparens K. (1987). Seed microstructure and its relationship to water uptake in isogenic lines and a cultivar of dry beans (Phaseolus vulgaris L.). **Food Microstruc. 6,** 91-102. Bean, cell wall, cotyledon, cultivar, hilum, micropyle, seed coat, seed, water uptake, SEM.

2. Akin DE, Rigsby LL, Barton FE, II, Gelfand P, Himmelsbach DS, Windham WR. (1987). Influence of delignifying agents on tissue structure in Bermudagrass stems. **Food Microstruc. 6,** 103-113. Bermudagrass, dioxane, epidermis, lignin, permanganate, peroxide, ozone, SEM.

3. Allan-Wojtas P. (1984). Technical Note: Transportation of fragile food specimens such as milk gels destined for electron microscopy. **Food Microstruc. 3,** 93. Agar, gel, milk, SEM, TEM.

4. Allan-Wojtas P, Kalab M. (1984). Technical Tip: A simple procedure for the preparation of stirred yoghurt for scanning electron microscopy. **Food Microstruc. 3,** 197-198. Agar, gel, encapsulation, freeze-fracturing, yoghurt, SEM.

5. Allen RD, Arnott HJ. (1981). Effects of exogenous enzymes on oilseed protein bodies. **Scanning Electron Microsc. 1981; III: 561-570 (Studies of Food Microstructure, p.283-292, 1981).** Enzyme, germination, oilseed, protein body, SEM.

6. Allen RD, Arnott HJ. (1982). Protein bodies in dormant, imbibed and germinated sunflower cotyledons. **Food Microstruc. 1, 63-73.** Cotyledon, protein, protein body, sunflower, SEM, TEM.

7. Al Saleh A, Bouchet B, Gallant DJ. (1984). Mineral migration in the wheat kernel during mill conditioning. **Food Microstruc. 3, 149-158.** Kernel, milling, mineral, water content, wheat, X-ray mapping, X-ray microanalysis, SEM.

8. Al Saleh A, Gallant DJ. (1985). Rheological and ultrastructural studies of wheat kernel behaviour

under compression as a function of water content. **Food Microstruc. 4,** 199-211. Cell wall, compression, elasticity, endosperm, image analysis, Instron, kernel, rheology, seed, water content, wheat, SEM.

9. Al Saleh A, Marion D, Gallant DJ. (1986). Microstructure of mealy and vitreous wheat endosperms (Triticum durum L.) with special emphasis on location and polymorphic behaviour of lipids. **Food Microstruc. 5,** 131-140. Cell wall, durum, endosperm, freeze fracture, lamella, lipid, protein, starch, vitreosity, wheat, SEM, TEM.

10. Basgall EJ, Bechtel PJ, McKeith FK. (1983). An alternative to critical point drying for preparing meat emulsions for scanning electron microscopy. **Food Microstruc. 2,** 23-26. Critical point drying, cryofracturing, emulsion, fat, meat, protein, X-ray microanalysis, SEM.

11. Basrur PK, Frombach S, McDonell WN, Geissinger HD. (1983). Myofibrillar characteristics of porcine stress syndrome. **Food Microstruc. 2,** 111-118. Muscle, myofibril, pork, PSE pork, Z-line, SEM, TEM.

12. Bechtel DB. (1985). The microstructure of wheat: Its development and conversion into bread. **Food Microstruc. 4,** 125-133. Bread, dough, endoplasmic reticulum, endosperm, freeze-fracturing, Golgi apparatus, protein, starch, wheat, TEM.

13. Bechtel DB, Frend A, Kaleikau LA, Wilson JD, Shewry PR. (1989). Vacuole formation in wheat starchy endosperm. **Food Microstruc. 8,** 183-190. Acid phosphatase, autophagy, cytoplasm, endosperm, starch, vacuole, wheat, LM, TEM.

14. Bee RD, Izzard MJ, Harbron RS, Stubbs JM. (1987). The morphology of black tea cream. **Food Microstruc. 6,** 47-56. Black tea cream, coacervate, freeze etching, shadowing, LM, SEM, TEM.

15. Berendsen PB. (1982). Ultrastructural studies of milk digestion in the suckling rat. **Food Microstruc. 1,** 83-90. Casein, duodenum, fat, lipase, milk, rat, SEM, TEM.

16. Beveridge T, Jones L, Tung MA. (1983). Stranded structure development in thermally produced whey protein concentrate gel. **Food Microstruc. 2,** 161-163. Bubble, gel, protein, whey, SEM.

17. Brach EJ. (1983). Field spectroscopy in the food production chain. **Food Microstruc. 2,** 67-80. Avocado, corn, cotton, hologram, protein, radiometry, reflectance spectroscopy, remote sensing, wheat, LM, SEM.

18. Brooker BE. (1985). Observations on the air-serum interface of milk foams. **Food Microstruc. 4,** 289-296. Bubble, casein, chromatography, foam, interface, interfacial membrane, micelle, milk, plasma, protein, TEM.

19. Brooker BE. (1987). The crystallization of calcium phosphate at the surface of mould-ripened cheeses. **Food Microstruc. 6,** 25-33. Ammonia, Brie cheese, calcium phosphate, Camembert cheese, casein, Coulommier cheese, crystal, Lymeswold cheese, mold, X-ray microanalysis, SEM, TEM.

20. Brooker BE, Anderson M, Andrews AT. (1986). The development of structure in whipped cream. **Food Microstruc. 5,** 277-285. Bubble, casein, cream, cryo-SEM, electrophoresis, fat, foam, freeze fracturing, SEM, protein, whey, whipped cream, SEM, TEM.

21. Buchheim W. (1981). A comparison of the microstructure of dried milk products by freeze fracturing powder suspensions in non-aqueous media. **Scanning Electron Microsc. 1981;III: 493-502 (Studies of Food Microstructure, p.193-202, 1981).** Buttermilk powder, casein, cream powder, freeze fracture, milk, milk powder, quarg, replica, skim milk powder, whey, yoghurt, TEM.

22. Buchheim W. (1982a). Aspects of sample preparation for freeze-fracture/freeze-etch studies of proteins and lipids in food systems. A review. **Food Microstruc. 1,** 189-208. Butter, casein, fat globule, freeze-etch, freeze-fracture, gel, lipid, margarine, milk, micelle, protein, rennet coagulation, TEM.

23. Buchheim W. (1982b). Electron microscopic localization of solvent-extractable fat in agglomerated spray-dried whole milk powder particles. **Food Microstruc. 1,** 233-238. Fat, freeze-fracture, milk, milk powder, TEM.

24. Buchheim W, Barfod NM, Krog N. (1985). Relation between microstructure, destabilization phenomena and rheological properties of whippable emulsions. **Food Microstruc. 4,** 221-232. Cream, crystallization, emulsion, freeze fracturing, lipids, NMR, nuclear magnetic resonance, rheology, surfactant, viscosity, whippable emulsion, TEM.

25. Buchheim W, Falk G, Hinz A. (1986). Ultrastructural aspects and physico-chemical properties of ultra-high-temperature (UHT) treated coffee cream. **Food Microstruc. 5,** 181-192. Coffee cream, cream, fat, feathering, freeze fracturing, pH, protein, viscosity, TEM.

26. Cardello AV, Segars RA, Secrist J, Smith J, Cohen SH, Rosenkrans R. (1983). Sensory and instrumental texture properties of flaked and formed beef. **Food Microstruc. 2,** 119-133. Beef, flaked and formed, meat, soy isolate, sensory, texture, SEM.

27. Caric M, Gantar M, Kalab M. (1985). Effects of emulsifying agents on the microstructure and other characteristics of process cheese - a review. **Food Microstruc. 4,** 297-312. Cheddar cheese, citrates, crystal, curd, curd granule junction, emulsifying salt, fat, Feta cheese, Gouda cheese, Kachkaval cheese, phosphate, process cheese, process cheese food, process cheese spread, protein, LM, SEM, TEM.

28. Caric M, Kalab M. (1987). Effects of drying techniques on milk powders quality and microstructure: A review. **Food Microstruc. 6,** 171-180. Buttermilk, casein, crystal, fat, freeze fracturing, lactose, micelles, milk, milk powder, skim milk, whey, SEM, TEM.

29. Carroll RJ, Basch JJ, Phillips JG, Farrell HM, Jr. (1985). Ultrastructural and biochemical investigations of mature human milk. **Food Microstruc. 4,** 323-331. Agar, casein, electrophoresis, fat, human milk, lactation, micelle, microencapsulation, milk, staining, TEM.

30. Carroll RJ, Jones SB. (1979). Some examples of scanning electron microscopy in food science. **Scanning Electron Microsc. 1979;III: 253-259 (Studies of Food Microstructure, p.1-7, 1981).** Potato, cherry cracking, ethyl oleate, meat, tensile stress, connective tissue, tenderness, muscle, SEM, LM.

31. Carroll RJ, Lee CM. (1981). Meat emulsions-fine structure relationships and stability. **Scanning Electron Microsc. 1981;III: 447-452 (Studies of Food Microstructure, p.105-110, 1981).** Fat, frankfurter, meat emulsion, protein, SEM, TEM.

32. Cassens RG, Carpenter CE, Eddinger TJ. (1984). An analysis of microstructural factors which influence the use of muscle as a food. **Food Microstruc. 3,** 1-7. Connective tissue, fiber, meat, muscle.

33. Cassens RG, Eddinger TJ, Moss RL. (1986).

analysis to predict milling extraction rates of wheats. **Food Microstruc. 8,** 191-199. Cultivar, embryo, flour, grain, image analysis, milling, wheat.

59. Farah Z, Ruegg MW. (1989). The size distribution of casein micelles in camel milk. **Food Microstruc. 8,** 211-216. Amino acid, camel milk, casein, freeze fracturing, micelles, milk, TEM.

60. Fleming K, Jenness R, Morris HA, Schmidt R. (1985). Properties of calcium caseinates with disparate performance in imitation cheese. **Food Microstruc. 4,** 313-321. Calcium caseinate, casein, chromatography, electrophoresis, imitation cheese, SEM.

61. Flint FO. (1982). Light microscopy preparation techniques for starch and lipid containing snack foods. **Food Microstruc. 1,** 145-150. Cryosectioning, lipid, potato chip, snack food, staining, starch, LM.

62. Fulcher RG. (1982). Fluorescence microscopy of cereals. **Food Microstruc. 1,** 167-175. Aleurone layer, barley, cereal, fluorescence microscopy, lipid, niacin, phytin, oat, pericarp, phenolic, protein, fluorochrome, staining, wheat, LM.

63. Gallant DJ, Bouchet B. (1986). Ultrastructure of maize starch granules. A review. **Food Microstruc. 5,** 141-155. Amylomaize, corn, endosperm, lectin, maize, starch, waxy maize, zein body, SEM, TEM.

64. Gallant DJ, Bouchet B, Culioli J. (1984). Ultrastructural aspects of spun pea and fababean proteins. **Food Microstruc. 3,** 175-183. Fababean, fibers, isolate, pea, protein, spun protein, SEM, TEM.

65. Gavaric DD, Caric M, Kalab M. (1989). Effects of protein concentration in ultrafiltration milk retentates and the type of protease used for coagulation on the microstructure of resulting gels. **Food Microstruc. 8,** 53-66. Casein, coagulation, enzyme, fat, gel, gelation, Hoppler consistometer, micelle, milk, protease, protein, rennet, retentate, texture, ultrafiltration, SEM, TEM.

66. Geissinger HD, Stanley DW. (1981). Preparation of muscle samples for electron microscopy. **Scanning Electron Microsc. 1981;III: 415-426, 414 (Studies of Food Microstructure, p.61-72, 60, 1981).** Cardiac and skeletal muscle, freeze-fracture, meat, myofibril, SEM, TEM.

67. Glennie CW, Liebenberg NvdW, van Tonder HJ. (1984). Morphological development in sorghum grain. **Food Microstruc. 3,** 141-148. Aleurone, cell wall, endosperm, grain, pericarp, sorghum, starch, SEM, TEM.

68. Goebel NK, Grider J, Davis EA, Gordon J. (1984). The effects of microwave energy and convection heating on wheat starch granule transformations. **Food Microstruc. 3, 73-82.** Convective heating, gel, heat transport, microwave heating, starch, wheat, water transport, LM, SEM.

69. Goff HD, Liboff M, Jordan WK, Kinsella JE. (1987). The effects of Polysorbate 80 on the fat emulsion in ice cream mix: evidence from transmission electron microscopy studies. **Food Microstruc. 6,** 193-198. Agarose, casein, emulsifier, fat, ice cream, micelle, milk, Polysorbate 80, Tween 80, TEM.

70. Gordon A, Barbut S. (1989). The effect of chloride salts on the texture, microstructure and stability of meat batters. **Food Microstruc. 8, 271-283.** Batter, chloride salt, emulsion, fat, Instron, meat, pH, protein, salts, texture, SEM, TEM.

71. Green ML, Langley KR, Marshall RJ, Brooker BE, Willis A, Vincent JFV. (1986). Mechanical properties of cheese, cheese analogues and protein gels in relation to composition and microstructure. **Food Microstruc. 5, 169-180.** Casein, Cheddar cheese, cheese analogue, gel, Instron, protein, rheology, texture, whey, LM, TEM.

72. Grider J, Davis EA, Gordon J. (1983). Evaluation of selected properties of chlorinated wheat flours in a lean cake formulation. **Food Microstruc. 2, 153-160.** Batter, cake, chlorinated flour, particle size distribution, water transport, SEM.

73. Grote M, Fromme HG. (1984a). Determination of element concentrations in fresh and processed vegetables by quantitative X-ray microanalysis. **Food Microstruc. 3, 49-54.** Bean, carrot, vegetable, X-ray microanalysis.

74. Grote M, Fromme HG. (1984b). Electron microscopic investigations of the cell structure in fresh and processed vegetables (carrots and green bean pods). **Food Microstruc. 3, 55-64.** Bean, carrot, cell structure, pod, vegetable, SEM, TEM.

75. Gwiazda S, Noguchi A, Saio K. (1987). Microstructural studies of texturized vegetable protein products: effects of oil addition and transformation of raw materials in various sections of a twin screw extruder. **Food Microstruc. 6, 57-61.** Barrel, extrusion, flour, oil, protein, soybean, texturized vegetable protein, twin screw, LM, TEM.

76. Hachiya I, Koyano T, Sato K. (1989). Observation of seeding effects on fat bloom of dark chocolate. **Food Microstruc. 8, 257-261.** Bloom, chocolate, cocoa butter, cryo-SEM, fat, polymorphism, SEM.

77. Hamilton RMG. (1986). The microstructure of the hen's egg shell - a short review. **Food Microstruc. 5, 99-110.** Crystal, cuticle, egg shell, fiber, hen, mammillary knob, palisade/matrix, pore, SEM.

78. Harbers LH. (1985). Ultrastructural utilization of plants by herbivores. **Food Microstruc. 4, 357-364.** Bluestem, corn, digestion, fescue, forage, grass, herbivore, legume, plant, ruminant, silica, sorghum, vascular tissue, SEM.

79. Harwalkar VR, Allan-Wojtas P, Kalab M. (1989). Effect of heating to 200°C on casein micelles in milk: A metal shadowing and negative staining electron microscope study. **Food Microstruc. 8, 217-224.** Casein, micelle, milk, protein, shadowing, staining, TEM.

80. Harwalkar VR, Kalab M. (1981). Effect of acidulants and temperature on microstructure, firmness, and susceptibility to syneresis of skim milk gels. **Scanning Electron Microsc. 1981;III: 503-513 (Studies of Food Microstructure, p.211-221, 1981).** Acidulated milk gels, core-and-lining structure, gel firmness, rheology, skim milk gels, syneresis, SEM, TEM.

81. Harwalkar VR, Kalab M. (1986). Relationship between microstructure and susceptibility to syneresis in yoghurt made from reconstituted nonfat dry milk. **Food Microstruc. 5, 287-294.** Casein, centrifugation, lactose, milk, nonfat dry milk, protein, syneresis, yoghurt, SEM, TEM.

82. Harwalkar VR, Kalab M. (1988). The role of beta-lactoglobulin in the development of the core-and-lining structure of casein particles in acid-heat-induced milk gels. **Food Microstruc. 7, 173-179.** Acid-heat-induced milk gel, casein, core-and-lining structure, gel, gelation, lactoglobulin, micelle, milk, TEM.

83. Heathcock JF. (1985). Characterisation of milk proteins in confectionery products. **Food**

TEM.

110. **Kalab M, Allan-Wojtas P, Phipps-Todd BE. (1983).** Development of microstructure in set-style nonfat yoghurt - a review. **Food Microstruc. 2,** 51-66. Casein, gelation, micelle, milk, mucogenic bacteria, protein, whey, yoghurt, SEM, TEM.

111. **Kalab M, Allan-Wojtas P, Yang AF. (1988).** Sample holders for solid and viscous foods compatible with the Hexland Cryotrans CT 1000 assembly. **Food Microstruc. 7,** 115-120. Cold stage SEM, cream, Hexland, yoghurt, whipping cream, SEM.

112. **Kalab M, Caric M, Zaher M, Harwalkar VR. (1989).** Composition and some properties of spray-dried retentates obtained by the ultrafiltration of milk. **Food Microstruc. 8,** 225-233. Buttermilk, crystal, differential scanning calorimetry, DSC, lactose, milk, milk powder, retentate, spray drying, ultrafiltration, SEM.

113. **Kalab M, Comer F. (1982).** Detection of buttermilk solids in meat binders by electron microscopy. **Food Microstruc. 1,** 49-54. Buttermilk, meat, meat binder, micelle, nonfat dry milk, ultracentrifugation, TEM.

114. **Kalab M, Gupta SK, Desai HK, Patil GR. (1988).** Development of microstructure in raw, fried, and fried and cooked Paneer made from buffalo, cow, and mixed milks. **Food Microstruc. 7,** 83-91. Acidulated curd, buffalo milk, casein, core-and-lining structure, curd, Paneer, SEM, TEM.

115. **Kalab M, Modler HW. (1985).** Development of microstructure in a cream cheese based on Queso Blanco cheese. **Food Microstruc. 4,** 89-98. Casein, core-and-lining structure, cream cheese, curd, fat, Latin American white cheese, protein, Queso Blanco, SEM, TEM.

116. **Kalab M, Sargant AG, Froehlich DA. (1981).** Electron microscopy and sensory evaluation of commercial cream cheese. **Scanning Electron Microsc. 1981;III: 473-482, 514 (Studies of Food Microstructure, p.153-162, 152, 1981).** Cold stage SEM, cream cheese, flavour, freeze-fracture, rheology, SEM, TEM.

117. **Kalab M, Yun J, Yiu SH. (1987).** Textural properties and microstructure of process cheese food rework. **Food Microstruc. 6,** 181-192. Citrate, crystal, emulsifying salt, fat, melt, process cheese food, rework, texture, viscosity, LM, SEM.

118. **Kebary KMK, Morris HA. (1988).** Porosity, specific gravity and fat dispersion in blue cheeses. **Food Microstruc. 7,** 153-160. Blue cheese, fat, milk, porosity, specific gravity, LM.

119. **Kempton AG, Trupp S. (1983).** Image analysis of morphological changes in wiener batters during chopping and cooking. **Food Microstruc. 2,** 27-42. Batter, fat, image analysis, meat, staining, wiener, LM.

120. **Keresztes A, Boka K, Bacsy E, Kovacs E. (1989).** Ultrastructural effects of postharvest treatments on the vacuolar inclusions in pear (Pyrus communis L. cv. Hardenpont) peel. **Food Microstruc. 8, 75-79.** Calcium treatment, gamma irradiation, irradiation, pear, peel, vacuole, X-ray microanalysis, TEM.

121. **Keresztes A, Kovacs E. (1987).** Effect of ionizing irradiation and storage on mushroom ultrastructure II. The stipe and the upper part of the cap of Agaricus bisporus (LGE. Imbach). **Food Microstruc. 6, 75-79.** Cap, cells, cytoplasm, irradiation, mushroom, stipe, TEM.

122. **Keresztes A, Kovacs J, Kovacs E. (1985).** Effect of ionizing irradiation and storage on mushroom ultrastructure. I. The gills of Agaricus bisporus (LGE.) Imbach and Pleurotus ostreatus (Jacq.ex Fr.) Kummer. **Food Microstruc. 4, 349-355.** Hymenium, irradiation, mushroom, Pleurotus ostreatus, ripening, spore, SEM, TEM.

123. **Kerley MS, Fahey GC Jr, Gould JM, Iannotti EL. (1988).** Effects of lignification, cellulose crystallinity and enzyme accessible space on the digestibility of plant cell wall carbohydrates by the ruminant. **Food Microstruc. 7,** 59-65. Carbohydrate, cell, cell wall, cellulose, crystal, digestibility, enzymes, lignin, plant, phenolic acid, ruminant, SEM.

124. **Kim JM, Lee CM, Hufnagel LA. (1987).** Textural properties and structure of starch-reinforced surimi gels as affected by heat-setting. **Food Microstruc. 6,** 81-89. Gels, heat-setting, potato, rheology, starch, surimi, LM, TEM.

125. **Kirst E. (1986).** Lipolytic changes in the milk fat of raw milk and their effects on the quality of milk products. **Food Microstruc. 5,** 265-275. Butter, cream, fat, fatty acid, lipolysis, milk.

126. **Koolmees PA, Korteknie F, Smulders FJM. (1986).** Accuracy and utility of sarcomere length assessment by laser diffraction. **Food Microstruc. 5,** 71-76. Beef, laser diffraction, muscle, sarcomere, LM.

127. **Koolmees PA, Moerman PC, Zijderveld MHG. (1989).** Image analysis of the fat dispersion in a comminuted meat system. **Food Microstruc. 8,** 81-90. Batter, comminuted meat, fat, image analysis, meat, polyphosphate, water, LM.

128. **Kovacs E, Keresztes A. (1989).** The effect of irradiation on starch content in Golden Delicious apples. **Food Microstruc. 8,** 67-74. Amyloplast, apple, chloroplast, irradiation, plastid, staining, starch, sugar, TEM.

129. **Kovacs E, Keresztes A, Kovacs J. (1988).** The effects of gamma irradiation and calcium treatment on the ultrastructure of apples and pears. **Food Microstruc. 7,** 1-14. Apple, calcium, cell wall, epidermis, irradiation, pear, plastid, SEM, TEM.

130. **Lampila LE, Brown WD. (1986).** Changes in the microstructure of skipjack tuna during frozen storage and heat treatment. **Food Microstruc. 5,** 25-31. Collagen, connective tissue, fiber, fish, muscle, sarcomere, seafood, tuna, Z-lines, SEM.

131. **Lampila LE, Mohr V, Reid DS. (1985).** Scanning electron microscopic study of rockfish preserved at either ambient temperature or by isothermal freeze-fixation. **Food Microstruc. 4,** 11-16. Fish, freeze fixation, muscle, rockfish, seafood, Z-disc, SEM, TEM.

132. **Langton M, Hermansson A-M. (1989).** Microstructural changes in wheat starch dispersions during heating and cooling. **Food Microstruc. 8,** 29-39. Amylopectin, amylose, cryosectioning, dispersion, gel, staining, starch, wheat, LM, SEM.

133. **Larsson K. (1982).** Some effects of lipids on the structure of foods. **Food Microstruc. 1,** 55-62. Baking, bread, crystal, fat, lipid, polymorphism, staling, starch, triglyceride, LM.

134. **Lawrence RA, Jelen P. (1982).** Freeze induced fibre formation in protein extracts from residues of mechanically separated poultry. **Food Microstruc. 1,** 91-97. Alkaline extraction, chicken, macrophotography, mechanical deboning, poultry protein, SEM.

135. **Lee CM. (1985).** Microstructure of meat emulsions in relation to fat stabilization. **Food Microstruc. 4,** 63-72. Comminution, emulsion, fat,

Cantonese, and instant noodles. **Food Microstruc. 6,** 63-74. Bread, Cantonese noodle, dough, flour, Hokkien noodle, instant noodle, Kan Swi, noodle, protein, LM, SEM.

161. **Moss R, Stenvert NL, Kingswood K, Pointing G. (1980).** The relationship between wheat microstructure and flourmilling. **Scanning Electron Microsc. 1980;III: 613-620 (Studies of Food Microstructure, p.305-312, 1981).** Aleurone layer, bran, endosperm, flour, milling, wheat, SEM.

162. **Nakai S, Li-Chan E. (1987).** Effect of clotting in stomachs of infants on protein digestibility of milk. **Food Microstruc. 6,** 161-170. Bovine, casein, clotting, digestibility, electrophoresis, infant, milk, pepsin, pH, rennet, LM, SEM.

163. **Nakamura M, Muguruma M, Fukazawa T, Yamaguchi M. (1988).** The retention of contractility of rabbit myofibrils during storage at 25°C. **Food Microstruc. 7,** 47-52. Contractility, electrophoresis, myofibril, myosin, muscle, rabbit, Z-line, TEM.

164. **Offer G, Knight P, Jeacocke R, Almond R, Cousins T, Elsey J, Parsons N, Sharp A, Starr R, Purslow P. (1989).** The structural basis of the water-holding, appearance and toughness of meat and meat products. **Food Microstruc. 8,** 151-170. Confocal microscopy, fluorescence microscopy, meat, muscle, myofibril, rabbit, texture, water-holding, LM, SEM, TEM.

165. **Omar MM, Buchheim W. (1983).** Composition and microstructure of soft brine cheese made from instant whole milk powder. **Food Microstruc. 2, 43-50.** Brine cheeses, casein, freeze-fracturing, milk, whole milk powder, TEM.

166. **Orcutt MW, Dutson TR, Wu FY, Smith SB. (1986).** The fine structure of the endomysium, perimysium, and intermyofibrillar connections in muscle. **Food Microstruc. 5,** 41-51. Bovine, collagen, endomysium, fiber, intermyofibrillar connection, muscle, myofibril, perimysium, rabbit, recticular fiber, Z-line, SEM, TEM.

167. **Pagani MA, Gallant DJ, Bouchet B, Resmini P. (1986).** Ultrastructure of cooked spaghetti. **Food Microstruc. 5,** 111-129. Flour, freeze fracturing, lipid, pasta, protein, spaghetti, staining, starch, wheat, SEM, TEM.

168. **Pagani MA, Resmini P, Dalbon G. (1989).** Influence of the extrusion process on characteristics and structure of pasta. **Food Microstruc. 8,** 173-182. Dough, extrusion, fibril, freeze fracturing, pasta, protein, rheology, spaghetti, starch, wheat, SEM, TEM.

169. **Parnell-Clunies EM, Kakuda Y, Humphrey R. (1986).** Electron dense granules in yoghurt: characterization by X-ray microanalysis. **Food Microstruc. 5,** 295-302. Artefact, casein, fat, yoghurt, X-ray microanalysis, TEM, STEM.

170. **Paquet A, Kalab M. (1988).** Amino acid composition and structure of cheese baked as a pizza ingredient in conventional and microwave ovens. **Food Microstruc. 7,** 93-103. Amino acid composition, Cheddar cheese, chromatography, curd granule junction, fat, microwave, Mozzarella cheese, process cheese, protein, SEM, TEM.

171. **Patton JS, Vetter RD, Hamosh M, Borgstrom B, Lindstrom M, Carey MC. (1985).** The light microscopy of triglyceride digestion. **Food Microstruc. 4,** 29-41. Biosalt, colipase, digestion, fat, lipase, liquid crystal, triglyceride, LM.

172. **Paulson AT, Tung MA. (1989).** Microstructure and texture of meat emulsions supplemented with plant proteins. **Food Microstruc. 8,** 41-51. Canola protein, emulsion, meat, plant, protein, soy protein, texture, LM, SEM.

173. **Pearce LE, Davis EA, Gordon J, Miller WG. (1987).** An electron spin resonance study of stearic acid interactions in model wheat starch and gluten systems. **Food Microstruc. 6,** 121-126. Electron spin resonance, ESR, gluten, stearic acid, starch, wheat.

174. **Pearce LE, Davis EA, Gordon J, Miller WG. (1985).** Application of electron spin resonance techniques to model starch systems. **Food Microstruc. 4,** 83-88. Electron spin resonance, ESR, starch, water.

175. **Pomeranz Y. (1982).** Grain structure and end-use properties. **Food Microstruc. 1,** 107-124. Aleurone layer, bran, cereal, germ, germination, grain, hull, malting, starch, wheat, SEM, TEM.

176. **Pomeranz Y, Czuchajowska Z. (1985).** Structure of coarse and fine fractions of corn samples ground on the Stenvert hardness tester. **Food Microstruc. 4,** 213-219. Cell wall, corn, dent, endosperm, flint corn, staining, Stenvert hardness tester, LM, SEM.

177. **Pomeranz Y, Meyer D. (1984).** Light and scanning electron microscopy of wheat- and rye-bread crumb. Interpretation of specimens prepared by various methods. **Food Microstruc. 3,** 159-164. Bread, crumb, rye, wheat, LM, SEM.

178. **Rao MV, Gault NFS, Kennedy S. (1989).** Changes in the ultrastructure of beef muscle as influenced by acidic conditions below the ultimate pH. **Food Microstruc. 8,** 115-124. Beef, fiber, meat, muscle, myofibril, sarcomere, Z-line, TEM.

179. **Ray FK, Miller BG, Van Sickle DC, Aberle ED, Forrest JC, Judge MD. (1979).** Identification of fat and protein components in meat emulsions using SEM and light microscopy. **Scanning Electron Microsc. 1979;III: 473-478 (Studies of Food Microstructure, p.99-104, 1981).** Fat, liver sausage, meat, meat emulsion, protein, stain, wiener, LM, SEM.

180. **Rayan AA, Kalab M, Ernstrom CA. (1980).** Microstructure and rheology of process cheese. **Scanning Electron Microsc. 1980;III: 635-643 (Studies of Food Microstructure, p.143-151, 1981).** citrate crystal, fat, meltability, phosphate crystal, process cheese, rheology, SEM, TEM.

181. **Reeve M, Sherman P. (1986).** Rheological and particle size changes in corn oil-in-water emulsions stabilized by 7S soybean proteins. **Food Microstruc. 5,** 163-168. Corn, disc centrifuge photosedimentometer, emulsion, oil-in-water, pH, protein, rheology, soybean.

182. **Resmini P, Pagani MA. (1983).** Ultrastructure studies of pasta. A review. **Food Microstruc. 2,** 1-12. Cereal, dough, Durum wheat, freeze fracture, flour, pasta, protein, rice, semolina, spaghetti, starch, wheat, TEM.

183. **Rosenberg M, Talmon Y, Kopelman IJ. (1988).** The microstructure of spray-dried microcapsules. **Food Microstruc. 7,** 15-23. Encapsulation, gum Arabic, microcapsule, SEM.

184. **Rousseau M. (1988).** Changes in the microstructure of Saint Paulin cheese during manufacture studied by scanning electron microscopy. **Food Microstruc. 7,** 105-113. Casein, cold-stage SEM, curd, fat, Saint Paulin cheese, SEM.

185. **Ruegg M, Blanc B. (1982).** Structure and properties of the particulate constituents of human milk. A review. **Food Microstruc. 1,** 25-47. Casein,

curd, fat, fatty acid distribution, freeze-fracture, human milk, lactation, micelle, milk, SEM, TEM.

186. Ruegg M, Moor U. (1987). The size distribution and shape of curd granules in traditional Swiss hard and semi-hard cheeses. **Food Microstruc. 6, 35-46.** Appenzeller cheese, curd, curd granule junction, Emmentaler cheese, Gruyere cheese, image analysis, Raclette cheese, Sbrinz cheese, Tilsiter cheese, LM.

187. Saio K. (1981). Microstructure of traditional Japanese soybean foods. **Scanning Electron Microsc. 1981;III: 553-559 (Studies of Food Microstructure, p.275-281, 1981).** Cryomicroscopy, kori-tofu, seed coat, soybean, texture, tofu, LM, SEM, TEM.

188. Saio K, Kondo K, Sugimoto T. (1985). Changes in typical organelles in developing cotyledons of soybean. **Food Microstruc. 4, 191-198.** Cell, cotyledon, endoplasmic reticulum, lipid, organelle, protein, soybean, starch, LM, TEM.

189. Saio K, Nakano Y, Uemoto S. (1983). Microstructure of winged beans. **Food Microstruc. 2, 175-181.** Bean, cell wall, cotyledonary cell, lipid, plasmodesmata, protein, starch, winged bean, LM, SEM.

190. Saio K, Suzuki H, Kobayashi T, Namikawa M. (1984). Microstructural changes in winged bean and soybean during fermentation into miso. **Food Microstruc. 3, 65-71.** Bean, cell wall, fermentation, lipid, miso, protein, soybean, LM, TEM.

191. Saito Z. (1988). Lactose crystallization in commercial whey powders and in spray-dried lactose. **Food Microstruc. 7, 75-81.** Crystal, lactose, whey, X-ray diffraction, SEM.

192. Saito Z. (1985). Particle structure in spray-dried whole milk and in instant skim milk powder as related to lactose crystallization. **Food Microstruc. 4, 333-340.** Crystallization, lactose, milk, skim milk, skim milk powder, X-ray diffraction, LM, SEM.

193. Salgo A, Torok S, Sandor S. (1989). Microstructure of extruded mixtures of cereals and oil seed processing residues. **Food Microstruc. 8, 245-252.** Amino acid, cereal, extrusion, maize, oil, protein, pumpkin, rice, sunflower, wheat, oilseed, seed, SEM.

194. Saltmarch M, Labuza TP. (1980). SEM investigation of the effect of lactose crystallization on the storage properties of spray dried whey. **Scanning Electron Microsc. 1980;III: 659-665 (Studies of Food Microstructure, p.203-209, 1981).** Browning, crystal, lactose, Maillard reaction, sorption isotherm, water activity, whey powder, SEM.

195. Sargent JA. (1988). The application of cold stage scanning electron microscopy to food research. **Food Microstruc. 7, 123-135.** Barley, bread, bubble, chocolate, cocoa, cold stage SEM, cotyledon, cream, cress, dough, emulsion, endosperm, fat, foam, ice cream, mayonnaise, meat, meringue, milk, muscle, myofibril, peanut, pizza, potato, salad dressing, seed, spoilage organism, starch, sugar, wheat, SEM.

196. Sato K. (1987). Physical and molecular properties of lipid polymorphs - a review. **Food Microstruc. 6, 151-159.** Cocoa butter, differential scanning calorimetry, DSC, fat, lipid, oleic acid, polymorphism, stearic acid, triglyceride, X-ray diffraction.

197. Schellhaass SM, Morris HA. (1985). Rheological and scanning electron microscopic examination of skim milk gels obtained by fermenting with ropy and non-ropy strains of lactic acid bacteria. **Food Microstruc. 4, 279-287.** Centrifugation, flow curve, gel, Haake Rotovisco viscometer, lactic acid bacteria, milk, rheology, ropy strain, shear-thinning, skim milk, syneresis, viscosity, water activity, SEM.

198. Schmidt DG. (1982). Electron microscopy of milk and milk products: problems and possibilities. **Food Microstruc. 1, 151-165.** Auger electron spectrometry, calcium tyrosinate, casein, crystal, freeze-etch, freeze-fracture, Gouda cheese, micelles, milk, shadowing, skim milk, whipped cream, X-ray microanalysis, SEM, TEM.

199. Schmidt DG, van Hooydonk ACM. (1980). A scanning electron microscopical investigation of the whipping of cream. **Scanning Electron Microsc. 1980; III: 653-658, 644 (Studies of Food Microstructure, p. 187-192, 210, 1981).** Cream, cryomicroscopy, fat, freeze etch, whipping, SEM.

200. Schmidt GR. (1984). Processing effects on meat product microstructure. **Food Microstruc. 3, 33-39.** Emulsion, fat, meat, protein, LM, SEM.

201. Sealy L, Renaudin S, Gallant DJ, Bouchet B, Brillouet JM. (1985). Ultrastructural study of yam tuber as related to postharvest hardness. **Food Microstruc. 4, 173-181.** Autoradiography, cell, lamella, lignification, parenchyma cell, staining, tuber, yam, SEM, TEM.

202. Seideman SC, Cohen SH, Schollmeyer JV. (1984). Some factors influencing ante-mortem changes in muscle: a brief review. **Food Microstruc. 3, 127-132.** Enzyme, fiber, muscle, Z-lines, TEM.

203. Shomer I, Weinberg ZG, Vasiliver R. (1987). Structural binding properties of silvercarp (Hypophtalmichthys molitrix) muscle affected by NaCl and $CaCl_2$ treatments. **Food Microstruc. 6, 199-207.** Carp, fish, muscle, myofibril, salt treatment, sarcomere, silvercarp, Z-line, TEM.

204. Siddiqui IR, Yiu SH, Jones JD, Kalab M. (1986). Mucilage in yellow mustard (Brassica hirta) seeds. **Food Microstruc. 5, 157-162.** Brassica hirta, carbohydrate, chromatography, electrophoresis, hull, mucilage, mustard, polysaccharide, seed coat, seed, staining, LM, SEM.

205. Smith LB. (1981). An SEM study of the effects of avian digestion on the seed coats of three common angiosperms. **Scanning Electron Microsc. 1981; III: 545-552 (Studies of Food Microstructure, p. 267-274, 1981).** Angiosperm, avian digestion, digestion, germination, seed, seed coat, SEM.

206. Sosnicki A, Cassens RG, McIntyre DR, Vimini RJ, Greaser ML. (1988). Characterization of hypercontracted fibers in skeletal muscle of domestic turkey (Meleagris gallopavo). **Food Microstruc. 7, 147-152.** Cell, fat, fiber, Meleagris gallopavo, muscle, skeletal muscle, turkey, TEM.

207. Spaeth SC, Debouck DG, Tohme J, Van Beem J. (1989). Microstructure of Nunas: Andean popping beans (Phaseolus vulgaris L.). **Food Microstruc. 8, 263-269.** Bean, cell wall, cotyledon, hilum, microwave, nunas, popping bean, starch, SEM.

208. Spaeth SC, Hughes JS. (1987). Cellular rupture and release of protoplasm and protein bodies from bean and pea cotyledons during imbibition. **Food Microstruc. 6, 127-134.** Bean, cell, cotyledon, pea, Phaseolus vulgaris, Pisum sativum, SEM.

209. Stanley DW. (1983). A review of the muscle cell cytoskeleton and its possible relation to meat texture and sarcolemma emptying. **Food Microstruc. 2, 99-109.** Cell, cytoskeleton, desmin, immunofluorescence, interference light microscopy, muscle, sarcolemma, texture, Z-line, LM, SEM, TEM.

210. Stasny JT, Albright FR, Graham R. (1981). Identification of foreign matter in foods. **Scanning Electron Microsc. 1981; III: 599-610, 560 (Studies of Food Microstructure, p.39-50, 24, 1981).** Asbestos, glass, lead, paint, pest fragments, X-ray microanalysis, SEM, XRD.

211. Swanson BG, Hughes JS, Rasmussen HP. (1985). Seed microstructure: Review of water imbibition in legumes. **Food Microstruc. 4,** 115-124. Bean, cowpea, lamella, legume, protein, seed, soybean, water imbibition, SEM.

212. Swatland HJ. (1985). Early research on the fibrous microstructure of meat. **Food Microstruc. 4,** 73-82. Cytoskeleton, fiber, meat, myofibril, sarcomere, LM.

213. Swatland HJ. (1984). Studies on the microdistribution of aerobic enzymes and myoglobin in pork. **Food Microstruc. 3,** 9-15. Color, enzyme, fiber optics, meat, myoglobin, pork, staining, succinate dehydrogenase, LM.

214. Swatland HJ. (1983). Morphometry of meat by scanning light microscopy. **Food Microstruc. 2,** 135-141. Enzyme, meat, morphometry, pork, stereology, succinate dehydrogenase, LM.

215. Tamime AY, Kalab M, Davies G. (1989). Rheology and microstructure of strained yoghurt (Labneh) made from cow's milk by three different methods. **Food Microstruc. 8,** 125-135. Casein, consistency, Labneh, LFRA texture analyzer, micelle, milk, retentate, rheology, texture, ultrafiltration, yoghurt, SEM, TEM.

216. Tamime AY, Kalab M, Davies G. (1984). Microstructure of set-style yoghurt manufactured from cow's milk fortified by various methods. **Food Microstruc. 3,** 83-92. Casein, micelle, milk, mucogenic bacteria, void space, yoghurt, SEM, TEM.

217. Taranto MV, Wan PJ, Chen SL, Rhee KC. (1979). Morphological, ultrastructural and rheological characterization of Cheddar and Mozzarella cheese. **Scanning Electron Microsc. 1979;III: 273-278 (Studies of Food Microstructure, p.163-168, 1981).** Cheddar cheese, fat, Mozzarella cheese, protein, rheology, LM, SEM, TEM.

218. Taranto MV, Yang CST. (1981). Morphological and textural characterization of soybean Mozzarella cheese analogs. **Scanning Electron Microsc. 1981;III: 483-492 (Studies of Food Microstructure, p. 169-178, 1981).** Mozzarella cheese, rheology, soybean, texture profile analysis, SEM.

219. Trakoontivakorn G, Patterson ME, Swanson BG. (1988). Scanning electron microscopy of cellular structure of Granny Smith and Red Delicious apples. **Food Microstruc. 7,** 205-212. Apple, cell, core, skin, SEM.

220. Tung MA, Jones LJ. (1981). Microstructure of mayonnaise and salad dressing. **Scanning Electron Microsc. 1981;III: 523-530 (Studies of Food Microstructure, p.231-238, 1981).** Mayonnaise, salad dressing, LM, SEM, TEM.

221. Unklesbay K, Unklesbay N, Keller J. (1986). Determination of internal color of beef ribeye steaks using digital image analysis. **Food Microstruc. 5,** 227-231. Beef, color, image analysis, meat, ribeye, steak.

222. Varriano-Marston E, DeFrancisco A. (1984). Ultrastructure of quinoa fruit (Chenopodium quinoa Willd). **Food Microstruc. 3,** 165-173. Fruit, germination, pericarp, quinoa, seed, starch, X-ray microanalysis, SEM, TEM.

223. Vaughan JG. (1981). Light microscopy of plant constituents in animal feeds. **Scanning Electron Microsc. 1981;III: 577-582 (Studies of Food Microstructure, p.299-304, 1981).** Adulteration, animal feed, flavor, mustard, olive, orange, rape, sunflower, tannin, toxicity, wheat, LM.

224. Voyle CA. (1981a). Scanning electron microscopy in meat science. **Scanning Electron Microsc. 1981;III: 405-413 (Studies of Food Microstructure, p. 51-59, 1981).** Bovine, meat, muscle, myofibril, sarcomere, SEM, TEM.

225. Voyle CA. (1981b). Microscopical observations on electrically stimulated bovine muscle. **Scanning Electron Microsc. 1981;III: 427-434 (Studies of Food Microstructure, p.79-86, 1981).** Bovine, electrical stimulation, meat, muscle, myofibril, sarcomere, LM, SEM, TEM.

226. Voyle CA, Jolley PD, Offer GW. (1986). Microscopical observations on the structure of bacon. **Food Microstruc. 5, 63-70.** Bacon, meat, muscle, myofibril, polyphosphate, TEM.

227. Voyle CA, Jolley PD, Offer GW. (1984). The effect of salt and pyrophosphate on the structure of meat. **Food Microstruc. 3,** 113-126. Fibrils, meat, muscle, myofibril, myosin, polyphosphate, pyrophosphate, salt, Z-lines, TEM.

228. Walter WM, Jr., Fleming HP, Trigiano RN. (1985). Comparison of the microstructure of firm and stem-end softened cucumber pickles preserved by brine fermentation. **Food Microstruc. 4,** 165-172. Cell wall, cucumber, enzyme, fermentation, hyphae, lamella, microfibril, paraffin, pectin, pickle, LM, SEM, TEM.

229. Williams CS, Williams JW, Chung RA. (1986). Comparative microscopy and morphometry of skeletal muscle fibers in poultry. **Food Microstruc. 5,** 207-217. Chicken, microwave, muscle, poultry, sarcomere, skeletal muscle, texture, Z-line, LM, TEM.

230. Wolf WJ, Baker FL. (1980). Scanning electron microscopy of soybeans and soybean protein products. **Scanning Electron Microsc. 1980;III: 621-634 (Studies of Food Microstructure, p.239-252, 1981).** Cotyledon, flour, protein, soybean, seed coat, SEM.

231. Wolf WJ, Baker FL, Bernard RL. (1981). Soybean seed coat structural features: pits, deposits and cracks. **Scanning Electron Microsc. 1981;III: 531-544 (Studies of Food Microstructure, p.253-266, 1981).** Cultivar, seed, seed coat, seed crack, seed deposit, seed pit, soybean, SEM.

232. Wood DA, Craig GD, Atkey PT, Newsam RJ, Gull K (1985). Ultrastructural studies on the cultivation processes and growth and development of the cultivated mushroom Agaricus bisporus. **Food Microstruc. 4,** 143-164. Autoradiography, cell, cell division, compost, cultivation, fungal spore, glycocalyx, mushroom, staining, stipe, straw cell, LM, SEM, TEM.

233. Yamaguchi M, Kamisoyama H, Nada S, Yamano S, Izumimoto M, Hirai Y, Cassens RG, Nasu H, Muguruma M, Fukazawa T. (1986). Current concepts of muscle ultrastructure with emphasis on Z-line architecture. **Food Microstruc. 5,** 197-205. Dog, fish, muscle, myofibril, protein, rod body, Z-line, TEM.

234. Yang CS, Taranto MV. (1982). Morphological and textural comparisons of soybean Mozzarella cheese analogs prepared with different hydrocolloids. **Food Microstruc. 1,** 223-231. Mozzarella cheese analog, hydrocolloid, soybean, texture profile analysis,

SEM.

235. Yang M, Grider J, Gordon J, Davis EA. (1985). Small angle X-ray scattering by hydrated wheat starch granules. **Food Microstruc. 4,** 107-114. Retrogradation, starch, wheat, X-ray scattering, SEM.

236. Yiu SH. (1989). Cereal structure and its relationship to nutritional quality. **Food Microstruc. 8,** 99-113. Bran, cell wall, cereal, fiber, fluorescence microscopy, nutrition, oat, phytate, rat, staining, starch, wheat, LM, SEM.

237. Yiu SH. (1986). Effects of processing and cooking on the structural and microchemical composition of oats. **Food Microstruc. 5,** 219-225. Aleurone layer, cell wall, fluorescence microscopy, oat, staining, LM.

238. Yiu SH. (1985). A fluorescence microscopic study of cheese. **Food Microstruc. 4,** 99-106. Blue cheese, Camembert cheese, casein, Cheddar cheese, crystals, fat, fluorescence microscopy, Mozzarella cheese, staining, LM.

239. Yiu SH, Altosaar I, Fulcher RG. (1983). The effects of commercial processing on the structure and microchemical organization of rapeseed. **Food Microstruc. 2,** 165-173. Cereal, flake, fluorescence microscopy, meal, press cake, rapeseed, seed, LM, SEM.

240. Yiu SH, Mongeau R. (1987). Fluorescence and light microscopic analysis of digested oat bran. **Food Microstruc. 6,** 143-150. Bran, digestion, fluorescence microscopy, oat, rat, staining, X-ray microanalysis, LM.

241. Yiu SH, Poon H, Fulcher RG, Altosaar I.(1982). The microscopic structure and chemistry of rapeseed and its products. **Food Microstruc. 1,** 135-143. Cereal, fluorescence microscopy, mucilage, phytin, phenolics, rapeseed, seed, testa, LM.

242. Young CT, Schadel WE. (1989). A method for light and scanning electron microscopy of drought-induced damage of resting peanut seed tissue. **Food Microstruc. 8,** 253-256. Arachis hypogaea, cytoplasm, peanut, seed, LM, SEM.

243. Young CT, Schadel WE. (1984). Effect of environment on the physical structure of the peanut (Arachis hypogaea L.). **Food Microstruc. 3,** 185-190. Cotyledon, cytoplasm, peanut, SEM.

Author Index

Subject Index

Scanning Microscopy International
P.O. Box 66507
Chicago (AMF O'Hare), IL 60666
Phone: 708 529 6677 FAX: 708 980 6698

Food Structure (Previously Food Microstructure till 1989)

and

Special Offer on Past Issues

We pride ourselves in publishing a journal having such noteworthy features as prompt publication of full length peer-reviewed papers; high quality reproduction of micrographs including color illustrations; and **a unique feature, the Discussion with Reviewers** where the authors' answers to the questions raised by the reviewers are published at the end of each paper (most reviewers' names are disclosed to the authors and readers).

Starting in 1990 the journal has changed its name to **Food Structure** and is published as a quarterly. We invite your contributions, participation in our programs (as a contributor or attendee), and subscriptions. Instructions for authors are included in each issue of the journal and are available on request. The next **Food Structure meeting will be at the Hyatt Regency Hotel, Bethesda (outside of Washington DC), May 4 to 9, 1991**; a **Letter of Intent** form and other information is available on request.

A Special offer on Food Microstructure (expiring Jan. 1, 1991): All back issues of Food Microstructure, 1982-1989 (volumes 1 to 8, 207 papers in 16 issues in total) **AND** the hardbound book STUDIES OF FOOD MICROSTRUCTURE (with 36 food related papers from 1979-1981) for US$279 (for US delivery) or US$299 (for outside US delivery by surface mail). Compared with the regular prices of $479 (for US delivery) - this special offer provides **a saving of $200** (and even a larger saving of $223 for outside US delivery). The regular price for a subscription for any one year during 1982-1987 is $50 (for US delivery) or $55 (for outside US delivery); and for the year 1988-1990 is $65 (for US delivery) or $70 (for outside US delivery).

Please complete and return a mailing list form (available on request) to receive further information about our publications and programs as it is issued. Please contact Dr. Om Johari, Managing Editor, for any additional information.

In Canada, please contact our Editor-in-Chief: Dr. Milos Kalab, Agriculture Canada Food Research Center, Ottawa, Ont. K1A 0C6, Canada (phone: 613 995 3722 ext. 7707; FAX: 613 995 3845).

In Europe, please contact our European Editor: Dr. Isaac Heertje, Unilever Research Lab., Postbus 114, 3130 AC Vlaardingen Netherlands (Phone: 31-10-4605513; FAX: 31-10-460 5671).

6/29/90 Om Johari, Managing Editor, Food Structure

FOOD STRUCTURE
INSTRUCTIONS TO AUTHORS

Revised 12-89

Papers for publication in the international journal Food Structure are invited. Papers can cover all types of foods and feeds, including vegetables, fruits, grains, seafoods, meat, dairy products, fats and others. The theme of the Journal is structure of foods and feeds with special emphasis on relation between processing, molecular properties, microstructure and macroscopic behavior. Papers related to techniques to study feed structure and their applications are also welcome.

Papers for Food Structure (FS) may be offered at any time. Papers can be for publication only, or intended for oral presentation at the Annual Food Structure meeting generally in early spring. The latter papers are due two months prior to the start of the meeting; only papers acceptable for publication are allowed oral presentation. Oral presentation of a paper at some other meeting or publication as unreviewed abstract (e.g., in proceedings, etc.) does not preclude consideration of a paper by FS.

The letter accompanying the paper should contain names and complete addresses of at least **four persons competent to review the paper**. Suggested reviewers: **a.** must neither be from author's current or recent affiliations, nor coworkers; **b.** should preferably be active researchers in the field (e.g., whose work is being extensively referred to); and **c.** need not be personally known or contacted by the authors. The editors **will select** the most suitable reviewers irrespective of their location. Each paper will be intensely reviewed by at least three reviewers.

The **initial paper (hereafter referred to as "paper")** should conform to **these Instructions.** However, to be published after reviewing, **the final manuscript (hereafter referred to as "manuscript") should be either a. submitted on the model sheets conforming to the Manuscript Preparation Guidelines (mailed along with the reviewers' comments), or b. sent to Scanning Microscopy International (SMI) for preparation at a nominal cost (per details mailed with reviews).** In addition to all the text, the **manuscript** may have to contain the author's publishable responses to questions raised by the paper's reviewers (see the Discussion with Reviewers in papers published in Food Microstructure).

The following types of contributions can be offered. A length limit is not imposed on papers. Short, but complete, papers are welcome.

RESEARCH PAPER: Presents new unpublished findings.

REVIEW PAPER: Includes an extended literature review and complete bibliography, **emphasizes author's new unpublished findings** and in an extended discussion puts the topic in proper perspective.

TUTORIAL PAPER: Contains an **organized comprehensive review** of **ALL** relevant published material as for a teaching lecture.

TECHNICAL TIP: Paper should have no more than 1000 words.

LETTER TO THE EDITOR: Commenting on paper already published in Food Microstructure/Food Structure.

The author should indicate the type of paper and carefully adhere to the applicable definition, since the reviewers and editors judge the paper accordingly.

INSTRUCTIONS FOR SUBMISSION OF PAPERS

Type paper in **double-spaced** format on standard size paper.

The paper should include title page, abstract, all headings and text. On the **title page** include: **a. a short title** which accurately represents the contents of the paper; **b.** an **informative running head** consisting of no more than 50 characters; **c. names and affiliations** of all authors, **name and complete work and home addresses and phone numbers of the person to contact; d. 10 key words/phrases** suitable for subject index; and **e. for review papers, indicate page numbers containing new material** (e.g., "new material will be found on pages __.").

An **Abstract** (of 100-250 words) is required for all papers. The Abstract should be concise and include the purpose of the paper, major results obtained and conclusions. Phrases such as "will be described," "is discussed," "are presented" etc. should be avoided.

The **Introduction** of the paper **must** contain a clear, concise statement of the purpose of the paper and the relationship of this paper to what is already in the literature. As applicable, a **Materials and Methods** section with **complete specimen preparation** information must be included (even if already published elsewhere), so that the work can be duplicated by others.

Equations should be numbered consecutively, using arabic numerals. Each **symbol and abbreviation** should be defined when first used. **SI units must be used;** other metric units or U.S. customary units (English), if used, must be given in parentheses.

REFERENCES

Include all references relevant to paper which are either readily available published works or papers in press. Work in progress, manuscripts submitted or in preparation, unpublished findings, personal communications etc. must be excluded from the reference list but may be acknowledged in the text (in parentheses).

The reference list at the end of the paper must be organized in alphabetical order by the first authors' names. Names of all authors (last names and initials only, with a comma between names and no other punctuation), full titles of papers, appropriate bibliographic information (with standard abbreviations for journals, and editors and publishers for books and proceedings), and inclusive pagination must be included. Availability information must be included for all non-journal references.

When referencing **SMI publications**, use the following formats only:

Journals: Frederik PM, Busing WM, Persson A. (1984). Surface defects on thin cryosections. Scanning Electron Microsc. 1984; I:433-443.

Food Microstructure: Elgasim EA, Kennick WH. (1982). Effect of high hydrostatic pressure on meat microstructure. Food Microstruc. 1, 75-82.

In the **text, cite references** in one of the following two styles:

a. Cowley (1967) or (Cowley, 1967) or Crewe and Wall (1970). If there are three or more authors, use the form Venables et al. (1978). If more than one paper is published in the same year by the same author (or group of authors) use the form (Rose, 1974a), etc.

b. As long as there is consistency, either superscript[1] or full-size numerals in brackets [1] can be used. In this case, the numbering must be in sequence in the reference list, but the references will generally not appear in sequence in the text.

ILLUSTRATIONS AND TABLES

Number each figure and table with **an arabic numeral and refer to them in sequence in the text.** Several illustrations within a figure must be designated a, b, c, etc. Each table must have a title. ***Each figure must have a caption*** – either on its own page or all captions should be placed together on separate pages. **Very important: Use arrows or letters to identify features referred to, and so indicate in the caption.** Illustrate text with the fewest photographs possible. Indicate magnification on photos by a line of, e.g., 1 μm, 10 μm, 100 μm, or 1 mm length; identify either on the photo or in the caption. Use nm, μm, or mm; do not use μ, u or -X.

Quality of Illustrations. *Photos should be clear, clean, unscreened* (screened photos are not acceptable), *black and white glossy prints.* **Color photographs** can be published by prior arrangement between author and the managing editor, whereby the author will be asked to pay the additional cost.

Size. Illustrations should be of a size appropriate to content and be **clustered to make the best use of space.** Micrographs should be preferably one column wide (10.5 cm) or two column wide (22 cm) **or** be grouped to fill one column width (10.5 cm) or two column widths (22 cm). Line drawings and tables should preferably be one column wide only (10.5 cm). All letters and symbols on illustrations and tables must be larger than 2.0 mm. **THE ILLUSTRATIONS, TABLES AND LETTERING INCLUDED WITH THE PAPER MUST CONFORM TO THESE INSTRUCTIONS.** *Permission for unusually large illustrations and/or tables must be requested when the paper is submitted.*

SUBMISSIONS AND COMMUNICATIONS

Submit 4 copies of the paper. Each of the 4 copies must include its own set of illustrations and clear glossy prints of all photographs. (Retain the best set of prints for your manuscript, since illustrations sent with paper may not be returned.) Papers containing photocopies (Xerox, etc.) of photographs will not be processed for reviewing; manuscripts containing photocopies of tables and illustrations are not accepted. All illustrations must be organized in sequence (must not be mounted on cardboards) and placed in separate envelopes. Place each copy of the paper *(together with its envelope of illustrations) in a separate, unsealed, ready-to-mail envelope,* so that the paper can be sent directly to its reviewers.

For **submission** of papers and **inquiries** contact: one of the editors or **Dr. Om Johari**, Managing Editor, **(phone: 708-529-6677; Fax: 708-980-6698)**, P.O. Box 66507, AMF O'Hare, IL 60666 USA. (**Street address,** if needed, is: 1034 Alabama Dr., Elk Grove Village, IL 60007, USA).

OTHER IMPORTANT ITEMS

Reprints. 15 complimentary tear sheets are provided. Information for ordering additional reprints is sent with the proofs.

Copyright. Food Structure is a copyrighted publication. Letters granting permission to use other copyrighted material must accompany the **manuscript.**

Cover Photo: The thermotropic behavior of coconut oil during wheat dough mixing is studied in a paper by C. Le Roux et al (pages 123-131) showing evidence for a solid-liquid phase separation. The modifications in fat crystallization are mostly due to the mixing temperature of batter. This electron micrograph, by freeze-fracturing, shows small fat globules and irregular fat crystalline platelet areas.